1.0 INTRODUCTION

This report describes the Turkey Point Unit 3 containment dome, delamination of the dome concrete during post tensioning of tendons, the subsequent investigation and analysis of this phenomena, and the repair and test program. When about two thirds of the dome tendons had been tensioned, it was noted that concrete cracking and sheathing filler leakage was developing and that in some areas of the dome, the concrete felt springy when walked on. The dome was struck with a sledge hammer and, in some areas, it sounded as if it were hollow. The concrete was locally removed in some of these areas and shallow (approximately 1/2" to 4") delamination planes were found running almost parallel with the surface, but eventually intersecting it. A full investigation was begun to determine both the extent and cause of the delaminations, and to cover the following:

1. Construction Procedures
2. Core Sampling
3. Concrete Removal
4. Materials Properties
5. Analysis of Loads During Construction

As a result of the investigation, it has been determined that insufficient contact area in the southern portion of the meridional construction joint and around the ventilation blockouts, together with unbalanced post-tensioning loads, were the major causes of the delaminations. After the post-tensioning was complete, there was no evidence that the dome was not capable of indefinitely resisting the applied loads. From detensioning there was no detectable loss in the tendon forces due to the delaminations.

Concrete replacement procedures have been prepared and will include modifications to the original placement procedures shown to be desirable during the analysis of the delamination causes.

The completed dome will meet performance requirements and the adequacy will be demonstrated during structural tests.

The firm of T. Y. Lin, Kulka, Yang and Associate, the consultant in the design of the containment, has participated in the investigation program and the concrete replacement method selection.

2.0 DOME AND CONSTRUCTION DESCRIPTION

2.1 DOME DESCRIPTION

The containment is described in FSAR, Section 5.1.2 and shown in FSAR Figure 5.1-1 (2 sheets).

The dome design geometry and dimensions are shown in Figure 2-1.

2.2 CONSTRUCTION DESCRIPTION

Locations of construction joints and dates of concrete placement are shown on Figure 2-2. Concrete placed between October 21, 1969 and March 3, 1970 inclusive consists of the top portion of the dome and the construction blockouts. These locations are where delaminations (discussed later) were found. A work stoppage of seven weeks duration resulted in the time lapse between the two largest pours.

Expanded metal was used to form the construction joints. The concrete was placed with buckets and pumps and vibrated for consolidation. Some of the concrete was pumped through aluminum pipe, a practice subsequently discontinued although tests indicated no significant reduction in strength of this concrete.

A white pigmented concrete curing compound meeting ASTM C-309 was applied on all exposed surfaces. However, a rainstorm occurred shortly after coating the east half of the dome, placed October 21, 1969, and washed away most of the curing compound. A work stoppage the next day, October 22, 1969 and lasting seven weeks, prevented reapplication of a curing compound.

The dome post-tensioning tendons are composed of 3 groups oriented as shown on Figure 2-3. The tendons are arranged in five layers. The tendons in Group I are in a single layer and are spaced approximately 1'-8" from center to center, whereas the tendons in Groups 2 and 3

are in 2 layers for each group spaced approximately 3'-4" from center to center of tendons in a layer. Tensioning of tendons utilized conventional equipment and techniques. The tensioning sequence is given on Table 2-1 and discussed in Section 5.5. Sheathing filler pumps, with a pressure capability of between 200 and 250 psi, were used to inject the sheathing filler for tendon corrosion protection.

TABLE 2-1

TENDON TENSIONING SEQUENCE

May 27	1D50	1D46	2D32	2D28	3D50	3D46	1D54				
28	1D14	1D10	1D6	1D2	2D36	2D24	2D20	3D10	3D6		
June 1	1D30	1D26	1D22	1D18	2D16	2D12	2D8	3D26	3D22	3D18	3D14
2	1D42	1D38	1D34	2D48	2D4	3D30	1D53				
3	2D25	1D51	1D49	2D44	2D40	2D27	2D23	3D42	3D38	3D34	
4	2D21	2D17	3D53	1D47	1D45	1D43	1D41	1D39	1D37	2D19	2D15
	3D55	3D51	3D47	1D35							
5	2D13	1D33	1D31	1D29	2D11						
8	2D9	2D5	3D45	3D41	3D37	2D7	2D3	3D39	3D43		
9	2D1	3D33	3D29	3D25	2D55	2D53	3D35	3D31	3D27		
10	1D27	1D23	1D25	1D21	2D51	2D47	3D21	3D17	3D13	2D49	2D45
	3D23	3D19	3D15	3D11							
15	1D19	1D15	1D17	2D43	2D39	2D31	3D9	3D5	2D37	3D7	3D3 2D41
16	1D11										
17	1D7	1D9									
25	3D52	3D44									
26	3D40	3D36	3D32	3D28	3D24	3D20	3D16				
29	3D12	3D8	3D4								
30	1D3	2D30	1D5	2D26	2D22	2D18	2D14				
July 1	2D10	2D6	2D2	1D8	1D4						
2	2D42	2D38	2D34	1D13	1D24	1D20	1D16	1D12			
3	2D50	2D46									
6	1D32	2D54									
8	1D52	1D48	1D44	1D40	1D36	2D52					
13	1D1	3D2									
14	2D35	2D33									
21	3D54										
22	3D48	3D49									
Aug. 25	1D28	1D55									

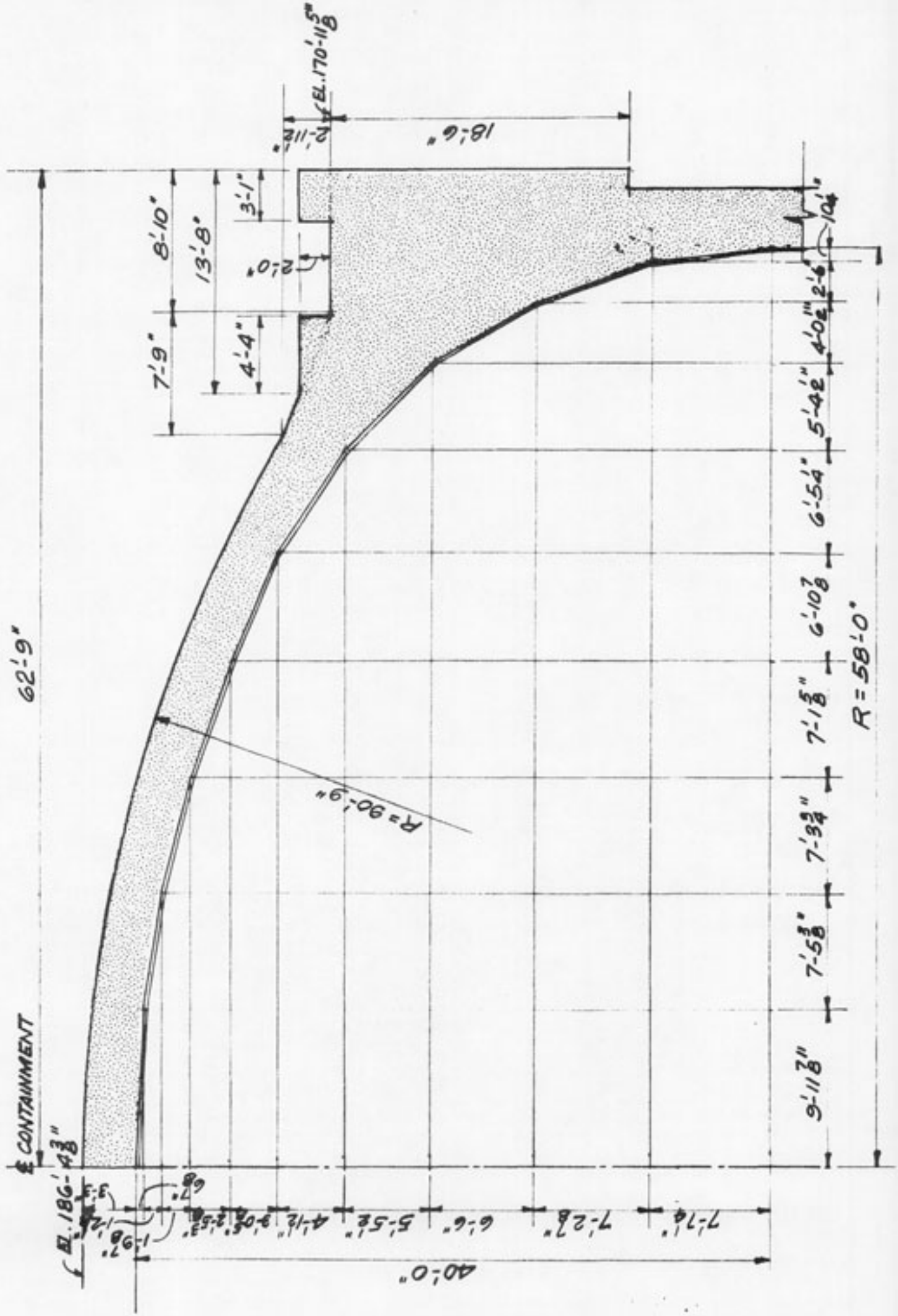

CONTAINMENT DOME GEOMETRY

FIG. 2-1

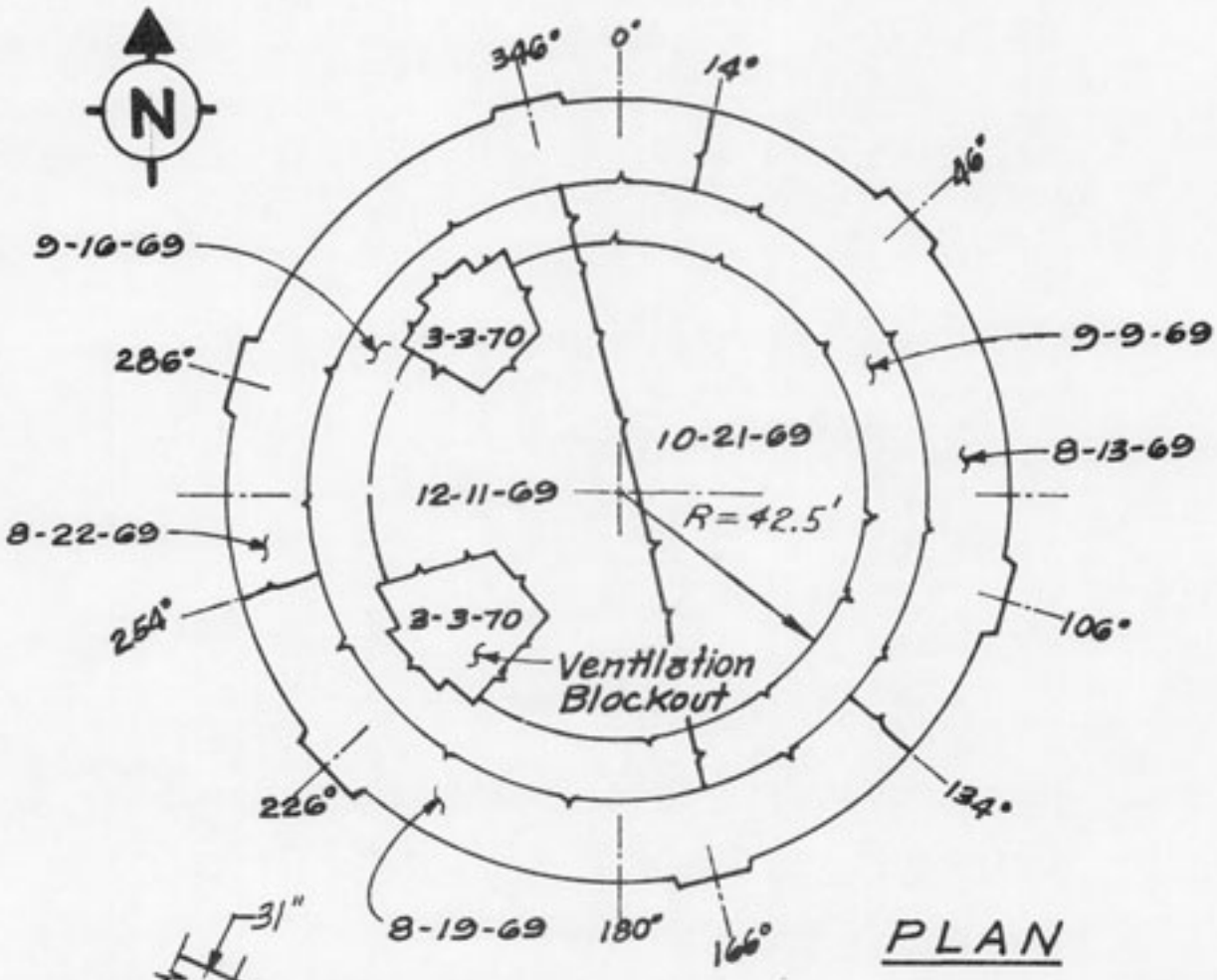

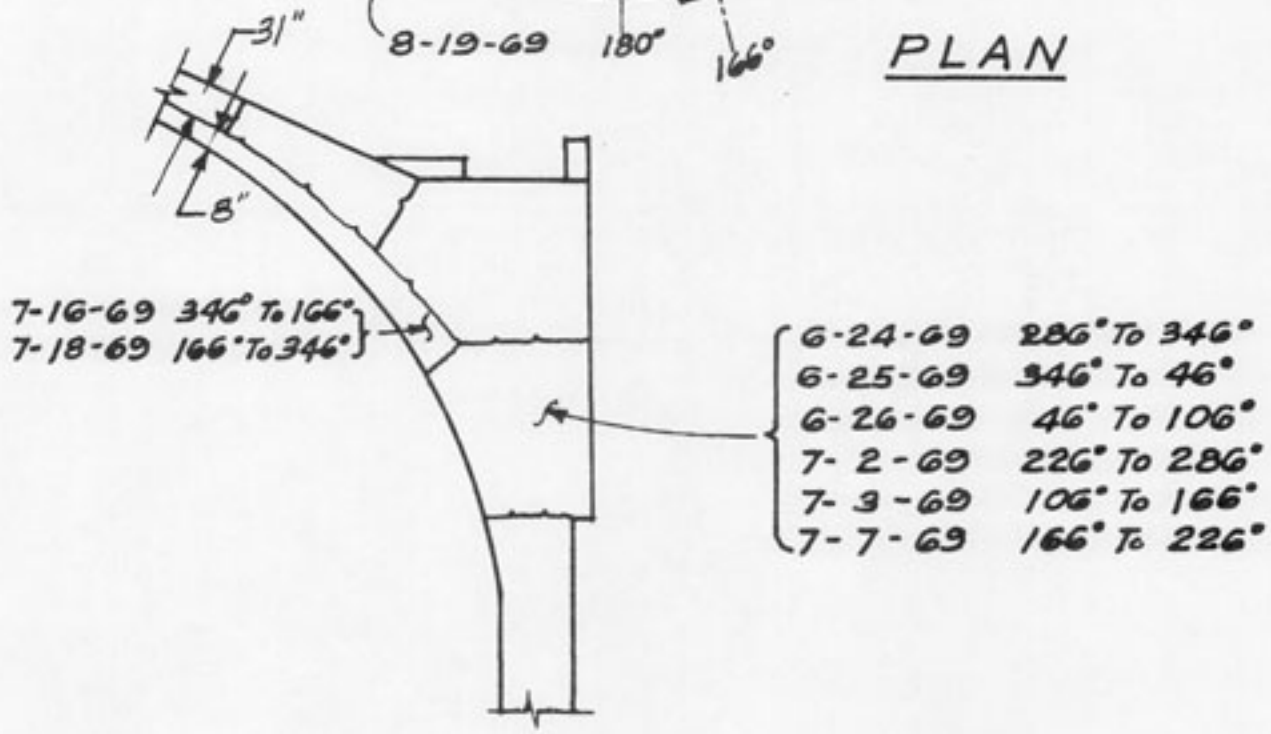

CONSTRUCTION SEQUENCE

FIG. 2-2

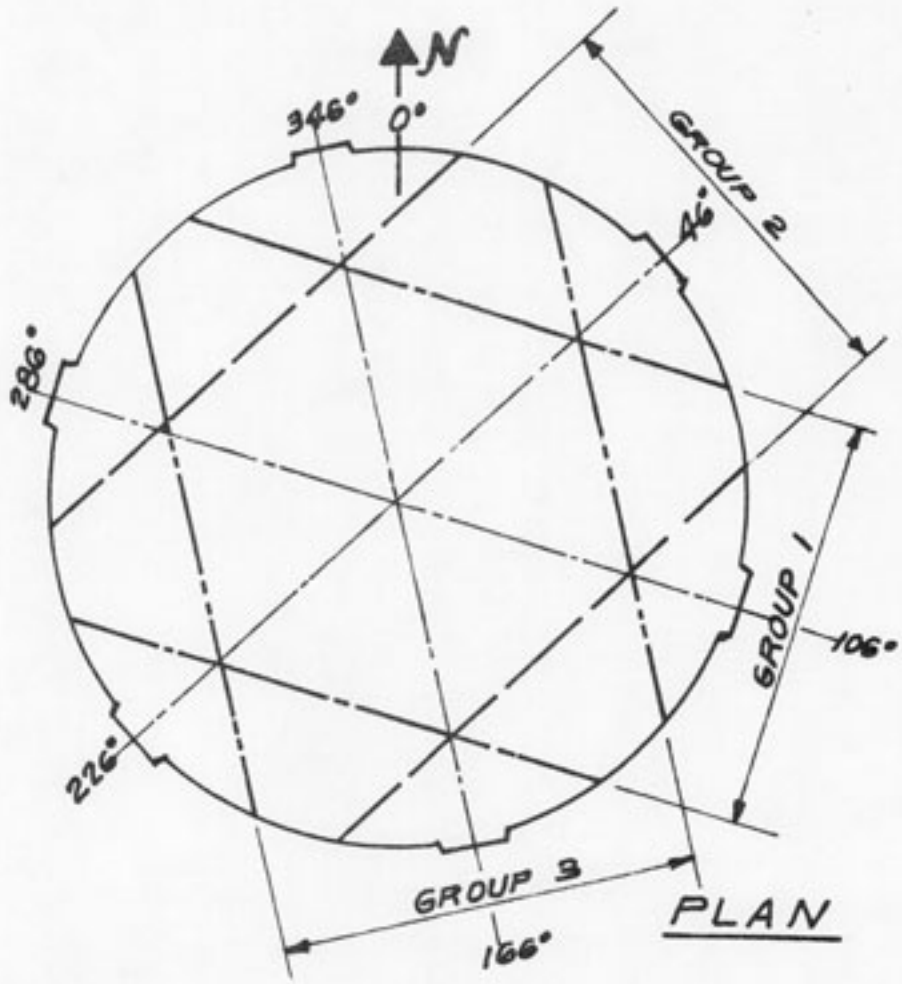

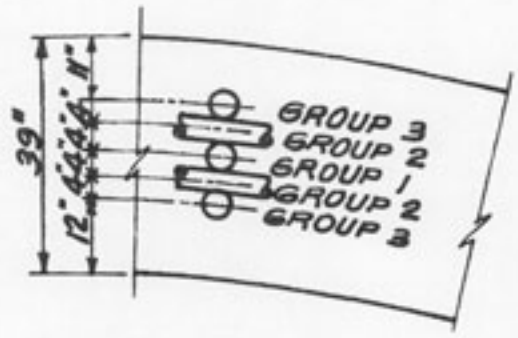

SECTION

TENDON LAYOUT

FIG. 2-3

3.0 FIELD OBSERVATIONS AND INVESTIGATION

3.1 INITIAL OBSERVATIONS

On June 17, 1970, when 110 out of 165 dome tendons had been tensioned, sheathing filler was observed leaking from a crack in the dome surface. Nine sheaths had been filled on June 16, 4 were filled on June 17, and this work was considered to be the source of the sheathing filler leak.

The leakage location was at azimuth 216 degrees and a radius of 35' from the dome center. A small amount of concrete was chipped away adjacent to the crack. A crack plane parallel to the surface (delamination) was found within an inch or so of the surface. There was evidence of sheathing filler flow on the surfaces created by the delamination.

On June 22, 1970, a small bulge in the dome surface was noticed at azimuth of 296 degrees and radius of 25 feet. The concrete was broken through in one small spot with a hammer and a delamination was discovered at about ½" depth. The exploratory chipping was expanded laterally and towards the center of the dome, revealing that the delamination became thicker as the dome center was approached. This stage of chipping was stopped at about 15 feet radius, at which point the separated layer was about 4" thick.

The initial investigation to determine the extent of the concrete separation below the surface was performed by soundings with a Swiss hammer and a steel sledge hammer. The steel hammer was found to be more effective in finding separations deeper into the concrete, and is considered reliable up to a depth of about 10 inches.

Sonic investigations with a V-scope were considered. The pulse velocity technique does not lend itself to a concrete mass with large numbers of embedded conduits and a liner plate on the underside of the dome.

Moreover, the presence of an intentional construction joint 8 inches from the liner plate further diminishes the reliability of the pulse velocity technique. The reflection method of ultrasonic examination used in metals has not been perfected for a heterogeneous mass such as concrete. A method of sonic induced vibratory resonance of concrete surfaces was tried but proved unsuccessful.

3.2 DOME CONCRETE CORING AND REMOVAL (BEFORE DETENSIONING)

In order, to estimate the depth and extent of the delaminations 65-4" diameter concrete cores were removed from the Unit 3 containment dome prior to destressing the tendons. The percentages of cores to various depths are as follows:

77% to the 1st layer of tendons
71% to the 2nd layer
22% to the 3rd layer
17% to the 4th layer
11% to the 5th layer

A summary of the information obtained from coring is given in Table 3-1. To help visualize the extent and depth of the delaminations inferred from coring, Figures 3-1 and 3-2 have been included. Figure 3-1 shows the core locations together with the depth to the delaminations and the core hole depth. Figure 3-2 is an estimate, from coring information, of the depth and area extent of the delaminations.

Concrete in an area approximately 7' x 7', with its northwest corner near core 23A, was removed to determine the condition of the meridional construction joint. The concrete was removed to a depth of from 12" to 15" so that the difficulty of concrete removal could also be determined.

The following is a summary of the information obtained from both coring and the 7' x 7' concrete removal area:

(1) The depth and extent of the delaminations has considerable symmetry about the meridional construction joint with major delaminations occurring on the south side of the dome.

(2) The delaminations appear to have originated at the meridional construction joint and then progressed away from the joint getting closer to the surface with eventual outcropping or termination at a circumferential construction joint.

(3) The adequacy of the meridional construction joint varied throughout the joint because of the small voids and other evidence of lack of proper consolidation found. Also sheathing filler was found on the joint to within about 6" of the concrete surface.

(4) Some of the core holes show multiple delaminations with gaps between delaminated surfaces of as great as 1".

(5) Many of the core holes had sheathing filler in them after coring, indicating that the delamination plane is continuous over areas other than those immediately around the sheath which was the source of sheathing filler.

3.3 DETENSIONING OF TENDONS

The tendons were detensioned to allow safe concrete removal from around them and so that the replaced concrete will assist the remaining concrete in resisting the prestressing forces.

All but two tendons, out of 165, were tensioned and therefore detensioned. The liftoff readings for tensioning and detensioning verify that the delaminated dome did indeed withstand the prestressing loads for over

two months without greater than the normally anticipated losses in tendon forces.

The predicted prestressing forces loss, with assumptions given in the FASR, but for the period that the dome was prestressed, is calculated to be approximately 13% of the minimum ultimate strength of the tendons. The average actual loss was found to be 7.1% based on the liftoff readings. The effective prestress at the time of detensioning was therefore equal or greater than calculated. Figure 3-3 shows the tendon force distribution based on the detensioning liftoff readings. The delaminations did not result in a detectable effect on the prestressing forces. Further, the full prestressing force did not result in continuing delamination attributable to the forces.

3.4 RESULTS OF INSTRUMENT READINGS DURING DETENSIONING

Strain, temperature and deformation measurements were made during tendon detensioning. Strain and temperature measurements were automatically recorded on the magnetic tape of a data acquisition system. The measurements were reduced and plotted by use of a digital computer. The deformation measurements were manually made using a level and level rod.

The measurement locations are on azimuth 256°. Figure 3-2 shows the azimuth location relative to the delaminated areas. Figure 3-4 shows the radial location of sensors on azimuth 256°.

The strain sensors are more completely described in the FSAR. They consist of electric resistance strain gages mounted and waterproofed on 3 foot long sections of No. 4 reinforcing steel. The sensors were installed before concrete placement with their measurement axes

perpendicular to dome radii. Circumferential sensors have measurement axes parallel to the base slab of the containment. Measurement axes for meridional sensors are in planes which pass through the dome axis and which are perpendicular to the measurement axes of the adjacent circumferential sensors.

Figures 3-5 to 3-16 show strain change measurements made prior to and during tendon detensioning. The measurements are related to time and the percentage of completion for detensioning is shown with the same time base. Strain change measurements prior to detensioning are shown to illustrate the stability of the measurements when environmental changes and small prestressing losses affected the structure. Sensor measurements are not available for situations where defective sensors were disconnected. Strain measurements at completion of detensioning were hand plotted in advance of periodic computer handling of the acquired data.

Figures 3-17 to 3-20 show temperature measurements from thermocouples installed and grouted in holes drilled after concrete placement. The time base for the Figures 3-17 to 3-20 is identical to that for Figures 3-5 to 3-16.

Temperature changes affected outside strain measurements to a greater degree than was the case for inside strain measurements. For example see Figures 3-5, 3-7, 3-17 and 3-18. The magnitude of strain change, on diurnal and other cyclic bases, can be seen for periods when detensioning was not being done. Diurnal strain changes are on the order of 20 microstrain (micro inches per inch) for outside sensors and 10 microstrain for inside gages.

The strain change from detensioning tendons may be determined by noting the strain change during a particular time period and the change in

percentage of completion of detensioning for the same period. The strain change in some instances was affected by the delamination planes nearby. For example sensor 21 (Figure 3-13) was located at a delamination plane and was exposed by chipping which started about day 335 (Dec. 1). At that time, compression strain again started to increase although detensioning work had been halted by a work stoppage.

The cause of the delaminations cannot be independently proven by the strain measurements. Symptoms of unusual strain patterns are shown. The symptoms include the nonuniformity of strain at radii 2.5 and 46 feet (Figures 3-5 to 3-7 and 3-10 to 3-12). The measurements show a general trend to circumferential strains that are larger than meridional strains. They also show nonuniform strain patterns that are indicative of nonuniform force distribution in planes that are parallel to the shell middle surface and/or bending perpendicular to the middle surface.

Elevations at the dome apex were measured before placement of concrete; after completion of dome tendon post-tensioning; and after completion of dome tendon detensioning. The dome apex moved downward 1-3/8"±1/8" as a result of dome tendon post-tensioning and concrete dead load, shrinkage, creep and temperature changes. The apex moved upward 7/8"±1/8" as a result of detensioning dome tendons, any creep recovery, and temperature changes. As expected, the upward movement of 7/8" was closest to 2/3" of movement predicted by calculations which assumed material elasticity and did not consider the effect of delaminations. Further, the small movements confirm that the effective prestress should be, as measured, within the range expected.

The small measurements and measurement differences, show that the cause of delaminations cannot be independently identified from the measurements. They further show that the delaminations did not contribute significantly to the dome deformation.

3.5 DOME CONCRETE REMOVAL

The delaminated concrete was removed using chipping guns and jack hammers. During concrete removal the construction joints were further examined for adequacy by concrete coring. The results of this coring program are shown in Table 3-2 and Figure 3-21. After the known delaminated concrete was removed additional concrete cores were taken to check for the existence of deep delaminations. The results of this program are shown in Table 3-3 and Figure 3-22. Figure 3-23 shows the depth and extent of the delaminations as indicated by concrete removal and coring. All delaminated concrete had been removed prior to producing Figure 3-23. Figures 3-24 and 3-25 are cross sections through the dome which show the variation in the delaminated planes. Figures 3-26 and 3-27 show the east and west sides of the dome during concrete removal. Figures 3-28 and 3-29 show detailed pictures of both the construction joints and delamination planes.

The following are observations made during and after concrete removal:

(1) Delamination planes - as shown by a comparison of Figures 3-2 and 3-23 the extent and depth of the delaminations were essentially the same as indicated by the initial coring program. Figures 3-24 and 3-25 show that the delamination pattern varied at various locations. In some locations the delaminations had a stepped pattern from tendon to tendon whereas in other locations a rather smooth plane intersected the surface or a construction joint.

(2) Extent of sheathing filler on delaminated planes - approximately 50% of the delaminated planes had a coating of sheathing filler present. This percentage was not an even distribution; some large areas did not have evidence of sheathing filler. However, only 20% of the delaminations at a depth of

of 15" to 19" showed evidence of sheathing filler. The maximum amount of sheathing filler was found on delaminated planes that intersected the center of the tendons.

(3) Construction joints - Figures 3-21, 3-28 and 3-29 show conditions found at construction joints during concrete coring and removal. At the south side of the meridional construction joint, grease was found on the vertical surfaces in a band varying from about 3" to 6" or more in width. The band started approximately 10' from the apex and was approximately 25 feet in length. A portion of the band is shown on Figure 3-28. Voids were found, with the worst voids located in the joints for the ventilation blockouts. There was evidence of lack of concrete consolidation in the northwest blockout.

3-1 (Sheet 1)
TURKEY POINT UNIT #3
CONTAINMENT STRUCTURE DOME
Coring Log Summary (Before Detensioning)

Hole No.	Azimuth	Radius	Depth to Delamination & Separation Distance (in.)	Depth of Hole (in.)	Sheathing Filler Present at Delamination	Examined with Boroscope	Photograph Taken	Comments
1	233°-00'	17'-10"	(8½,⅛) (9⅛,1/8) (10⅛,1/8) (13,⅛)	16	Yes	No	Yes	
2	70°-00'	36'-3"	(9,)	13	Yes	Yes	No	Hit Sheath
3								
4	354°-30'	30'-2"	None	16	-	No	No	
5	142°-00'	18'-8"	(11 3/4,⅛)	16	Yes	Yes	Yes	Hit Sheath
5A	158°-50'	13'-11"	(10, ⅛) (11⅛,⅛)	24	Yes	Yes	No	Hit Sheath, on C.J.
6	270°-00'	16'-10"	(6⅛, 3/4)	16	No	Yes	Yes	
7	83°-00'	15'-4"	(9,⅛)	16	Yes	No	No	
7A	91°-00'	10'-0"	(8,⅛)	10	No	Yes	Yes	Hit Sheath
8	227°-30'	39'-10"	None	15⅛	No	Yes	Yes	
9	243°-00'	8'-5"	(12,⅛)	27	Yes	Yes	No	
10	173°-30'	35'-3"	(10 3/4,)	10 3/4	Yes	No	No	Hit Sheath
10A	170°-03'	43'-10"	None	26 3/4	-	No	No	Hit Sheath
10B	163°-04'	43'-0"	None	5	-	No	No	On C.J.
10C	160°-19'	43'-0"	None	21⅛	-	Yes	No	Hit Sheath, on C.J.
11	29°-30'	9'-8"	None	17⅛	-	Yes	No	Hit Sheath
11A	98°-15'	5'-3"	None	29 3/4	-	No	No	
12	109°-30'	18'-0"	(11,⅛)	15⅛	Yes	Yes	Yes	
12A	116°-50'	20'-7"	(9,), (11,)	11	Yes	Yes	No	
13	322°-30'	41'-9"	None	15 3/4	-	No	No	
14	28°-30'	37'-0"	None	15⅛	-	Yes	No	
15	208°-00'	24'-10"	(11⅛, 1)	16⅛	Yes	Yes	Yes	
15A	215°-20'	26'-1"	(7⅛,1)	24	Yes	Yes	No	Hit Sheath, on C.J.

3-1 (Sheet 2)
TURKEY POINT UNIT #3
CONTAINMENT STRUCTURE DOME
Coring Log Summary (Before Detensioning)

Hole No.	Azimuth	Radius	Depth to Delamination & Separation Distance (in.)	Depth of Hole (in.)	Sheathing Filler Present at Delamination	Examined with Boroscope	Photograph Taken	Comments
16	83°-30'	25'-0"	(10¼,3/4) (12,¼)	15½	Yes	Yes	Yes	
17	90°-09'	35'-10"	(4,)	11½	Yes	Yes	No	
17A	78°-20'	36'-3"	None	9¼	-	No	No	Hit Sheath
18	106°-51'	30'-11"	(7½,3/4) (9¼,½)	9½	No	Yes	Yes	
19	121°-51'	36'-2"	(11½,)	11½	Yes	No	No	
19A	118°-00'	43'-0"	None	10½	-	Yes	No	On C.J.
20	127°-30'	26'-4"	(9 3/4, 3/4)	10½	Yes	No	No	
20A	122°-15'	23'-1"	(10 3/4, ½) (14, 1/8)	20	Yes	No	No	
21	114°-06'	8'-3"	(10 3/4, 1/8)	16	No	No	No	
22	147°-11'	30'-6"	(7,¼) (9½, 1)	10 3/4	No	Yes	Yes	
23	177°-15'	24'-6"	(14,) (15,)	29 3/4	Yes	Yes	Yes	
23A	161°-57'	24'-1"	None	10	-	No	No	On C.J.
23B	161°-37'	21'-10"	(11¼,1) (12¼,¼)	24	Yes	Yes	No	(2nd Delam. East Side on C.J.)
24	191°-15'	33'-8"	(14,)	14	Yes	No	No	
25								
26	210°-54'	35'-11"	(5¼,¼)	29 3/4	Yes	Yes	No	
27	230°-03'	30'-1"	(4½, 1/8) (6,3/4)	11	Yes	Yes	Yes	1st Delam. East Side
28	251°-42'	45'-11"	None	18	-	No	No	
29	243°-37'	36'-4"	(3½, ¼)	16	No	Yes	No	
30	254°-40'	25'-2"	(5 3/4,)	5 3/4	Yes	No	No	
31	264°-40'	34'-9"	(1 3/4, ¼)	14¼	Yes	Yes	No	Hit Sheath
32	284°-54'	25'-3"	(2, 1)	11½	No	Yes	Yes	
33	297°-06'	33'-7"	None	16	-	Yes	No	
34	326°-00'	12'-10"	None	29¼	-	No	No	

3-1 (Sheet 3)
TURKEY POINT UNIT #3
CONTAINMENT STRUCTURE DOME
Coring Log Summary (Before Detensioning)

Hole No.	Azimuth	Radius	Depth to Delamination & Separation Distance (in.)	Depth of Hole (in.)	Sheathing Filler Present at Delamination	Examined with Boroscope	Photograph Taken	Comments
35	317°-35'	32'-1"	None	16 3/4	-	Yes	No	
36	331°-00'	23'-8"	None	16	-	Yes	No	
37	338°-19'	35'-11"	None	17	-	No	No	
38	359°-13'	18'-10"	None	18½	-	No	No	Hit Sheath
38A	353°-40'	16'-4"	None	29½	-	Yes	No	Hit Sheath, on C.J.
39	18°-00'	28'-4"	None	15½	-	No	No	
40	10°-25'	40'-2"	None	18¼	-	No	No	
41	38°-30'	21'-6"	None	17	-	No	No	Hit Sheath
42	43°-40'	31'-9"	None	16	-	No	No	
43	61°-13'	38'-5"	None	16¼	-	No	No	
43A	49°-20'	43'-0"	None	29½	-	No	No	On C.J.
44	64°-08'	26'-4"	(4½, ½)	16	No	No	No	
45	77°-45'	40'-6"	None	17	-	No	No	
A	324°-00'	16'-5"	(5, ½)	18 3/4	No	Yes	-	
B	305°-18'	28'-6"	None	12	-	Yes	Yes	On C.J.
B'	310°-30'	27'-7"	None	19½	-	No	No	On C.J.
C	62°-50'	17'-0"	(5,)	15½	No	Yes	No	
D	233°-46'	29'-3"	(4¼,) (5½,)	15	No	Yes	No	
E	294°-21'	13'-4"	(6,)	16½	No	Yes	No	
F	27°-30'	20'-5"	None	16	-	No	No	

3-2 (Sheet 1)
TURKEY POINT UNIT #3
CONTAINMENT STRUCTURE DOME
Coring Log Summary

Hole No.	Azimuth	Radius	Depth to Delamination & Separation Distance (in.)	Depth of Hole (in.)	Sheathing Filler Present at Delamination	Examined with Boroscope	Photograph Taken	Comments
46	350°-07'	30'-5"	None	23	No	Yes	No	
47	332°-32'	28'-3"	None	30-1/4	No	Yes	No	Very Poor Bond Around Top Layer of Rebar Four Consolidation
48	347°-2'	42'-6"	None	20	No	Yes	No	
49	333°-18'	42'-11"	None	20	No	Yes	No	Large Void Around Top Layer Rebar
50	319°-52'	45'-6"	None	35	No	Yes	No	Hit Sheath at 9",23"&26"
51	301°-24'	42'11"	None	21-3/4	No	Yes	No	Very Poor Bond To a Depth of 7"
52	285°-27'	42'-9"	None	19	No	Yes	No	
53	269°-17'	42'-10"	None	21-3/4	No	Yes	No	Hit Sheath at 21"
53A	272°-18'	42'-7"	None	22				
53B	269°-56'	42'-9"	None	20				
54	255°-28'	42'-8"	None	20	No	Yes	No	Hit Sheath at 13"
55	237°-35'	43'-0"	None	20	No	Yes	No	
56	224°-12'	44'-10"	None	31-1/2	No	Yes	No	No. of Voids in Concrete, Hit Sheath at 9"
57	191°-10'	42'-3"	(15, 1/16)	32	Yes	Yes	No	Hit Sheath at 9"
58	145°-33'	42'-9"	(12, 1/16)	31	Yes	Yes	No	
59	90°-11'	42'-3"	None	34	No	Yes	No	Hit Sheath at 12". Large No. of Voids in Concrete.
60	74°-55'	42'-5"	None	20	No	Yes	No	Hit Sheath at 19"; Large Voids in Concrete.

3-2 (Sheet 2)
TURKEY POINT UNIT #3
CONTAINMENT STRUCTURE DOME
Coring Log Summary

Hole No.	Azimuth	Radius	Depth to Delamination & Separation Distance (in.)	Depth of Hole (in.)	Sheathing Filler Present at Delamination	Examined with Boroscope	Photograph Taken	Comments
61	45°-11'	42'-10"	None	32	No	Yes	No	Hit Sheath At 22".
62	30°-09'	43'-0"	None	20-1/4	No	Yes	No	
63	13°-06'	42'-9"	None	19-3/4	No	No	No	
64	358°-52'	42'-8"	None	31	No	No	No	
65	357°-43'	10'-0"	None	23	No	No	No	
66	124°-44'	2'-9"	None	23	No	No	No	

3-3 (Sheet 1)
TURKEY POINT UNIT #3
CONTAINMENT STRUCTURE DOME
Coring Log Summary
(Coring After Concrete Removal)

Hole No.	Azimuth	Radius	Depth to Delamination & Separation Distance (in.)	Depth to Top & Bot. of Hole (in.)*	Sheathing Filler Present at Delamination	Examined with Boroscope	Photograph Taken	Comments
67	126°-38'	24'-7½"	None	18, 26		Yes	No	Hit Sheath
68	197°-16'	18'-7½"	(17,0)	13, 17	No	Yes	No	
68A	191°-11'	19'-1"	(17,0)	13, 19	No	Yes	No	Hit Sheath
68B	190°-41'	18'-5"	(17,0)	13, 23	Yes	Yes	No	Chipped to Delamination
69	164°-54'	18'-9½"	(17,0)	13, 22	Yes	Yes	No	
70	226°-41'	26'-10"	None	11, 23		Yes	No	
71	191°-42'	9' - 7"	None	11, 23		Yes	No	
72	194°-20'	21'-11"	(19,0)	17, 29	No	Yes	No	
73	222°-58'	20'-5"	None	15, 22		Yes	No	
74	69°-04'	28'-5"	None	10, 21		Yes	No	
75	168°-04'	30'-6"	None	9, 27		Yes	No	
76	170°-38'	22'-2"	(15½,0)	12, 23	No	Yes	No	Chipped to Delamination
77	156°-18'	31'-2"	None	16, 32½		Yes	No	
78	175°-56'	15'-2"	None	19, 30½		Yes	No	
79	148°-27'	22'-4"	None	13, 30		Yes	No	
80	109°-29'	32'-2"	None	10½, 15		Yes	No	Hit Sheath
81	157°-40'	28'-0"	None	14, 18		Yes	No	
81A	152°-43'	29'-2½"	None	15, 32		Yes	No	
82	186°-27'	28'-5"	None	12, 30		Yes	No	
83	107°-52'	32'-2"	None	10, 29		Yes	No	
84	147°-00'	14'-9"	None	15, 31		Yes	No	
85	126°-16'	12'-3"	None	10, 20		Yes	No	
86	67°-27'	27'-9"	None	10, 26		Yes	No	Hit Sheath
87	74°-07'	28'-5"	None	10, 17		Yes	No	Hit Sheath
87A	76°-13'	28'-10"	None	11, 30		Yes	No	

*These holes were cored after concrete removal. Top and bottom of hole are relative to the original concrete surface.

3-3 (Sheet 2)
TURKEY POINT UNIT #3
CONTAINMENT STRUCTURE DOME
Coring Log Summary
(Coring After Concrete Removing)

Hole No.	Azimuth	Radius	Depth to Delamination & Separation Distance (in.)	Depth to Top & Bot. of Hole (in.)*	Sheathing Filler Present at Delamination	Examined with Boroscope	Photograph Taken	Comments
88	219°-38'	9'-9"	None	12, 31		Yes	No	Good Bond at 8" Slab
89	229°-32'	14'-10"	None	14½, 31		Yes	No	No Bond at 8" Slab
90	245°-00'	11'- 6"	None	15½, 33		Yes	No	Good Bond at 3" Slab
91	257°-00'	22'-0"	None	7, 30		Yes	No	
92	249°-55'	25'-0"	None	6, 14½		Yes	No	Hit Sheath
92A	251°-20'	26'-0"	None	4½, 31		Yes	No	
93	289°-47'	9' -5"	None	7, 19		Yes	No	Hit Sheath
94	288°-33'	15'-7"	None	4, 31		Yes	No	Good Bond at 8" Slab

* These holes were cored after concrete removal. Top and bottom of hole are relative to the original concrete surface.

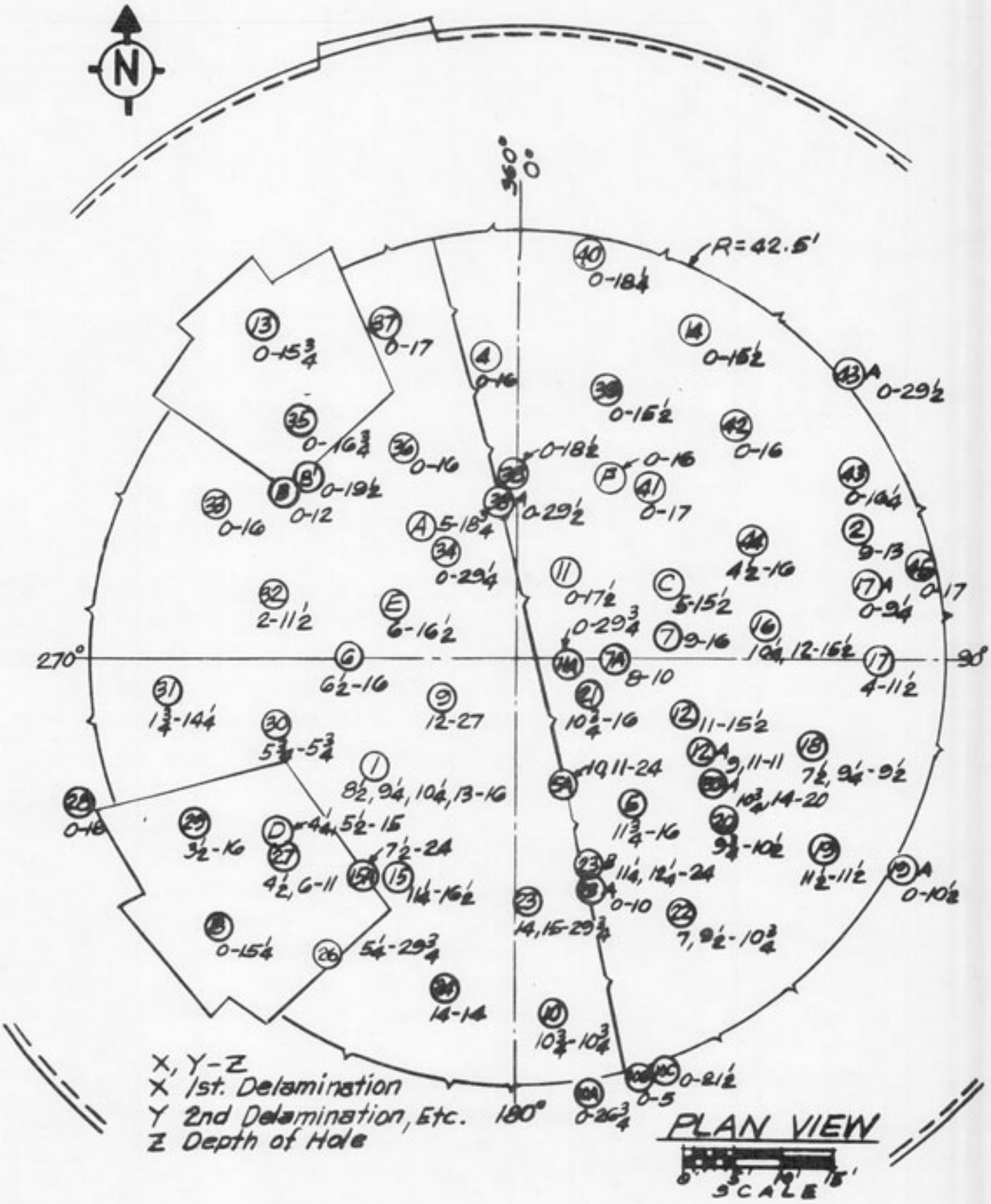

DOME CORING RESULTS

FIG. 3-1

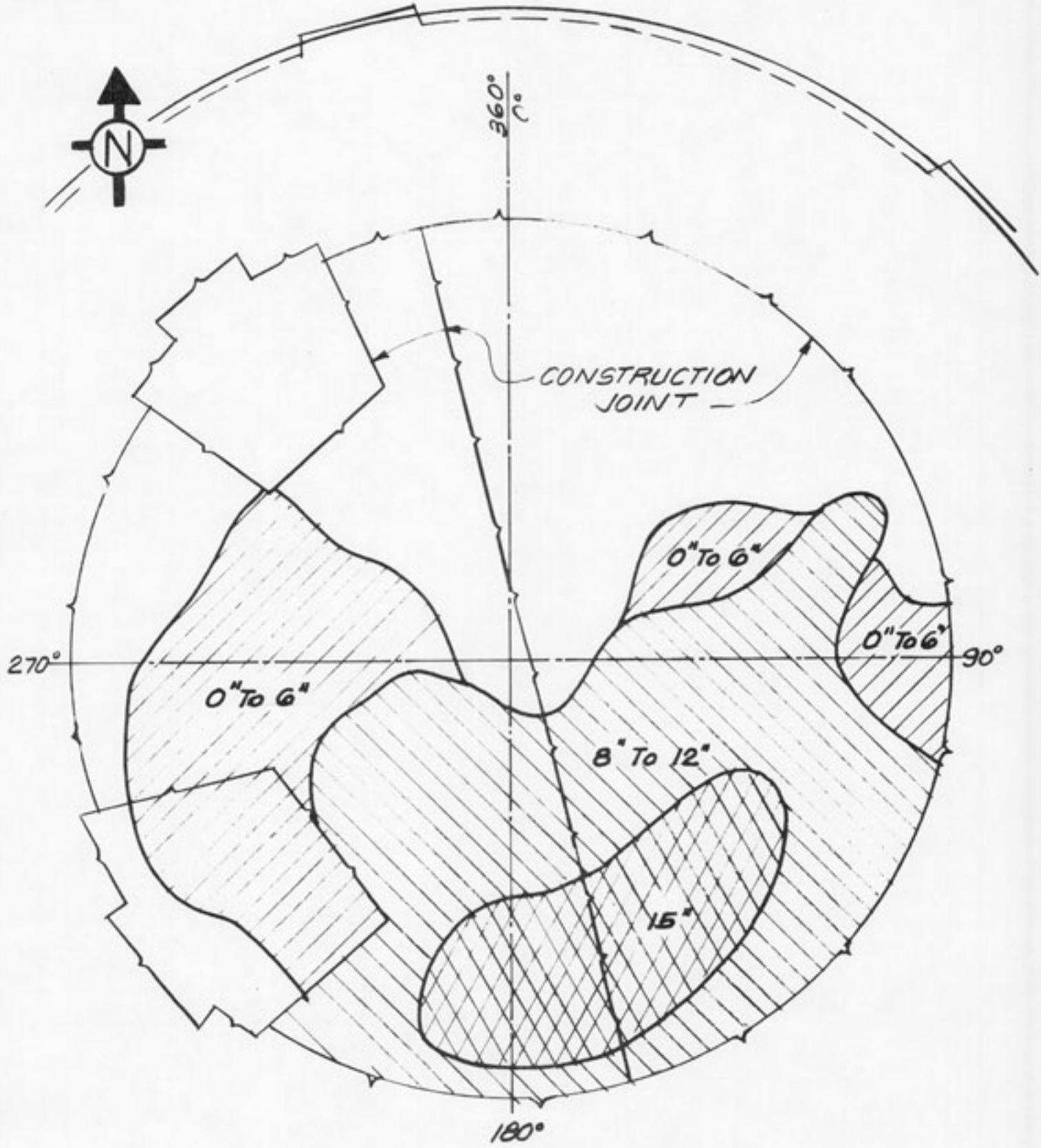

PLAN VIEW

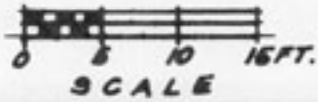

CONTOURS OF DEEPEST DELAMINATIONS

FIG. 3-2

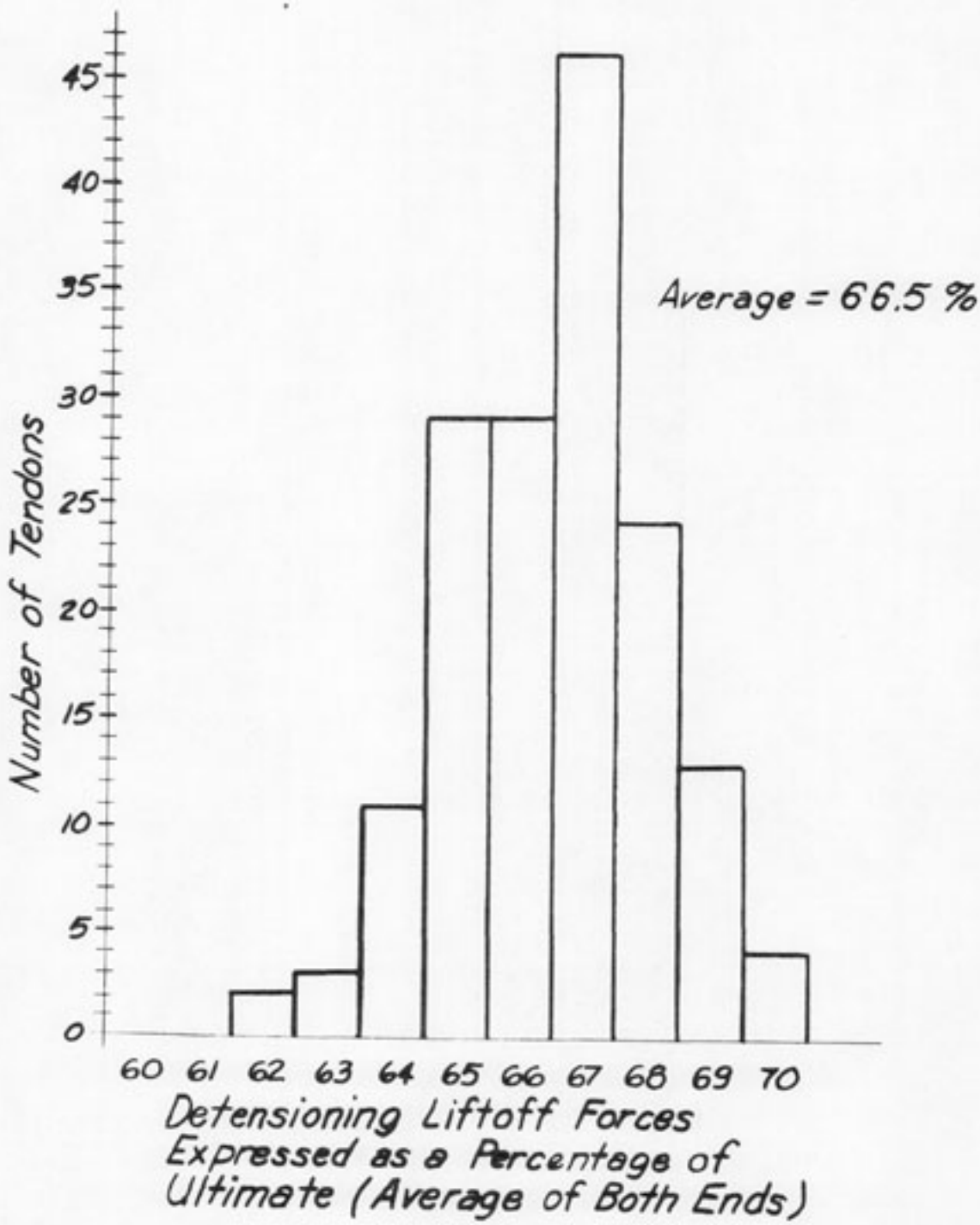

TENDON LIFTOFF VALUES

FIG. 3-3

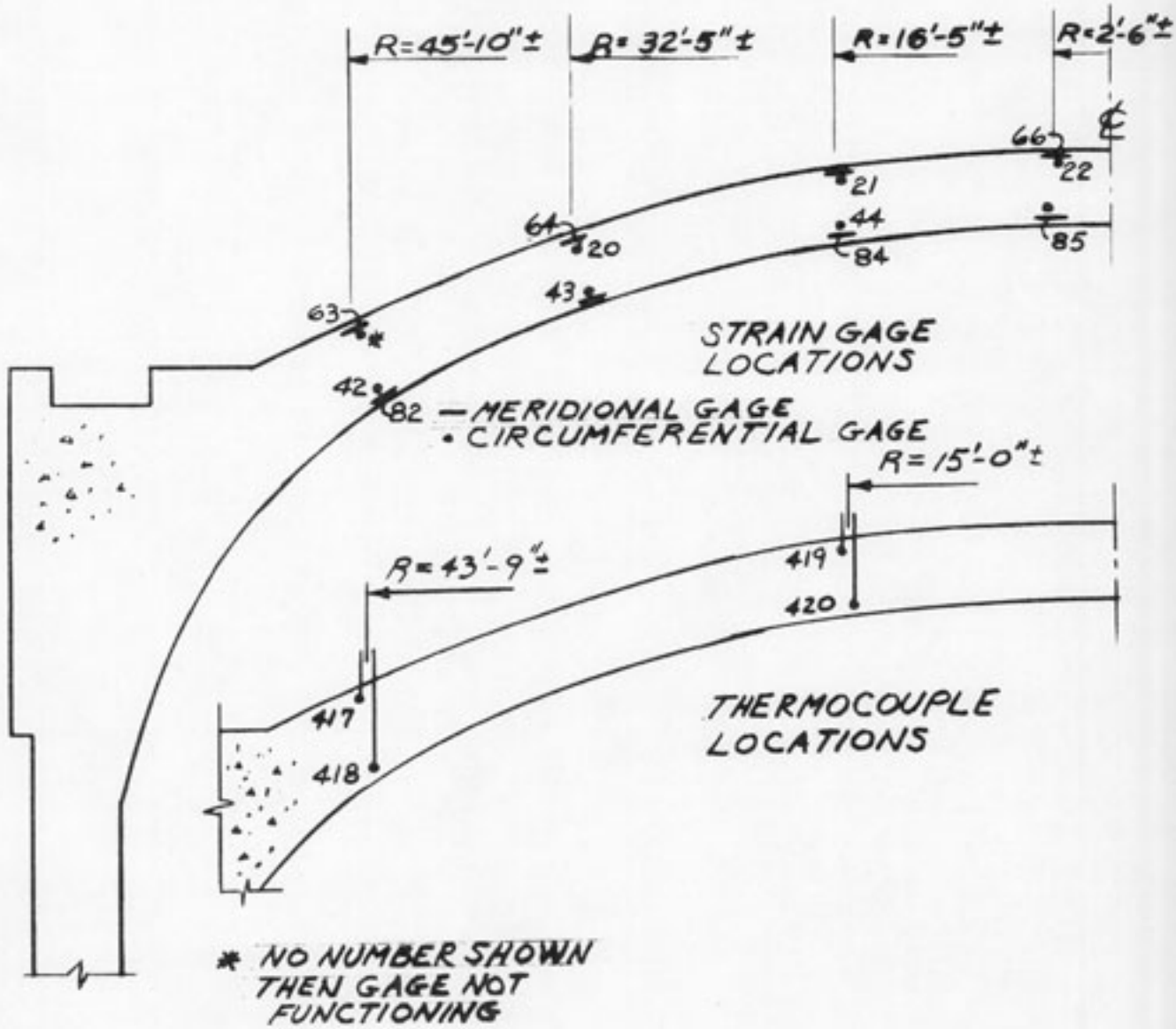

SECTION AT 256°

FIGURE 3-4

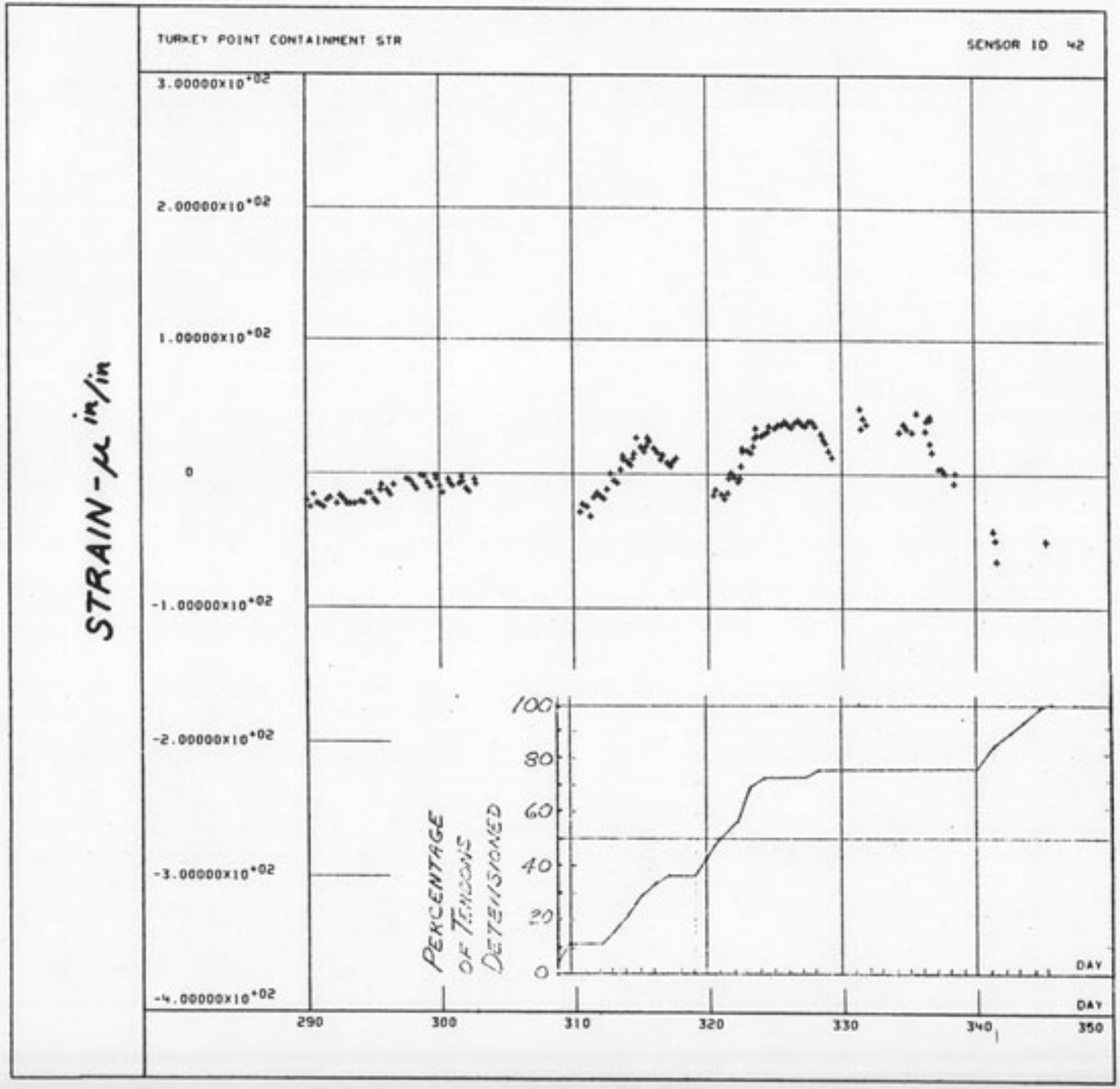
TURKEY POINT CONTAINMENT STR
SENSOR ID 42
STRAIN - μ in/in
3.00000x10+02
2.00000x10+02
1.00000x10+02
0
-1.00000x10+02
-2.00000x10+02
-3.00000x10+02
-4.00000x10+02
290
300
310
320
330
340
350
DAY
PERCENTAGE OF TENDONS DETENSIONED
100
80
60
40
20
0
DAY

FIGURE 3-5

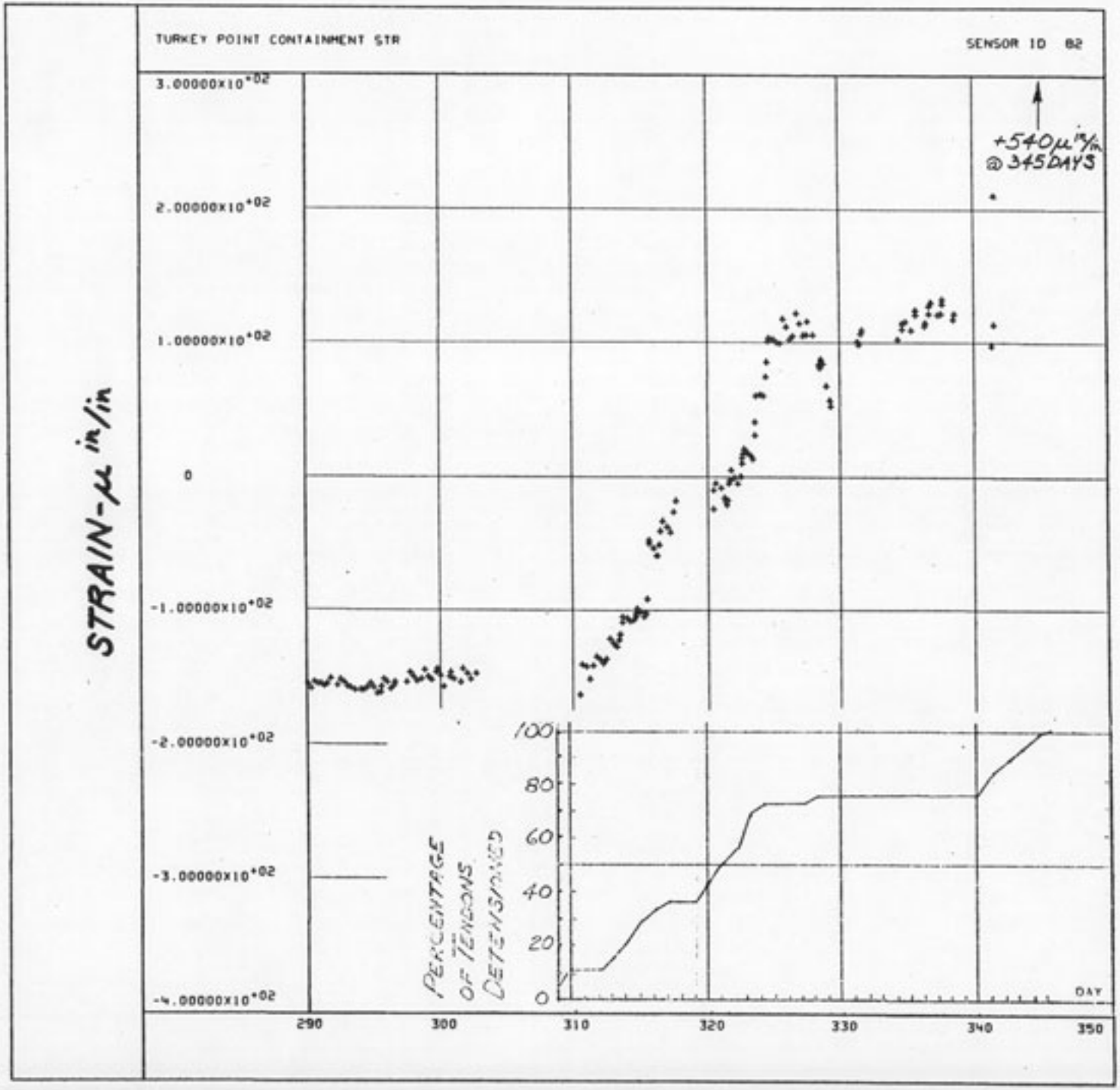
TURKEY POINT CONTAINMENT STR
SENSOR ID 82
STRAIN-μ in/in
3.00000x10+02
2.00000x10+02
1.00000x10+02
0
-1.00000x10+02
-2.00000x10+02
-3.00000x10+02
-4.00000x10+02
+540μ in/in @ 345 DAYS
PERCENTAGE OF TENDONS DETENSIONED
100
80
60
40
20
0
DAY
290
300
310
320
330
340
350

FIGURE 3-6

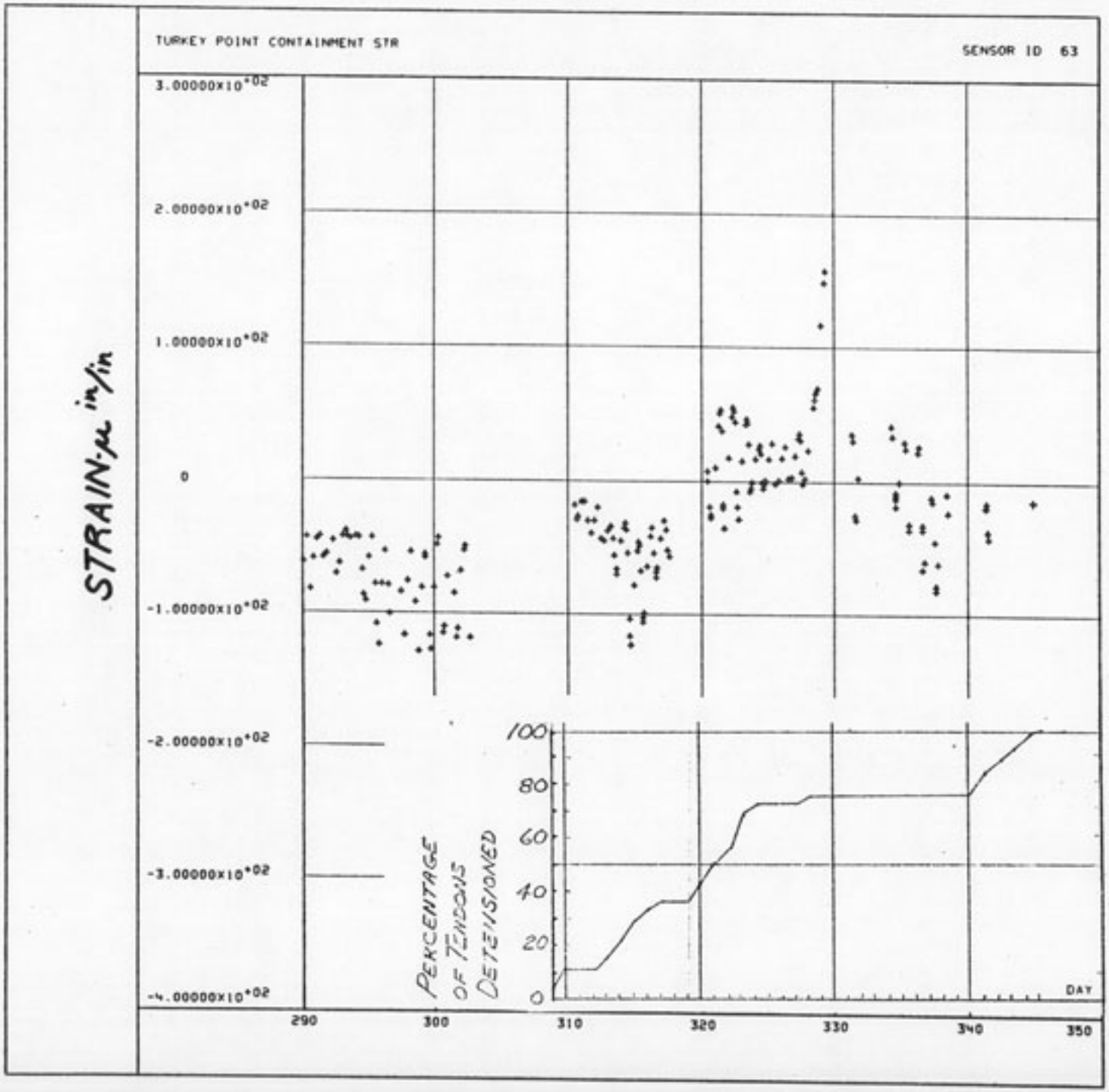
TURKEY POINT CONTAINMENT STR
SENSOR ID 63
STRAIN-μ in/in
3.00000x10+02
2.00000x10+02
1.00000x10+02
0
-1.00000x10+02
-2.00000x10+02
-3.00000x10+02
-4.00000x10+02
290
300
310
320
330
340
350
PERCENTAGE OF TENDONS DETENSIONED
100
80
60
40
20
0
DAY

FIGURE 3-7

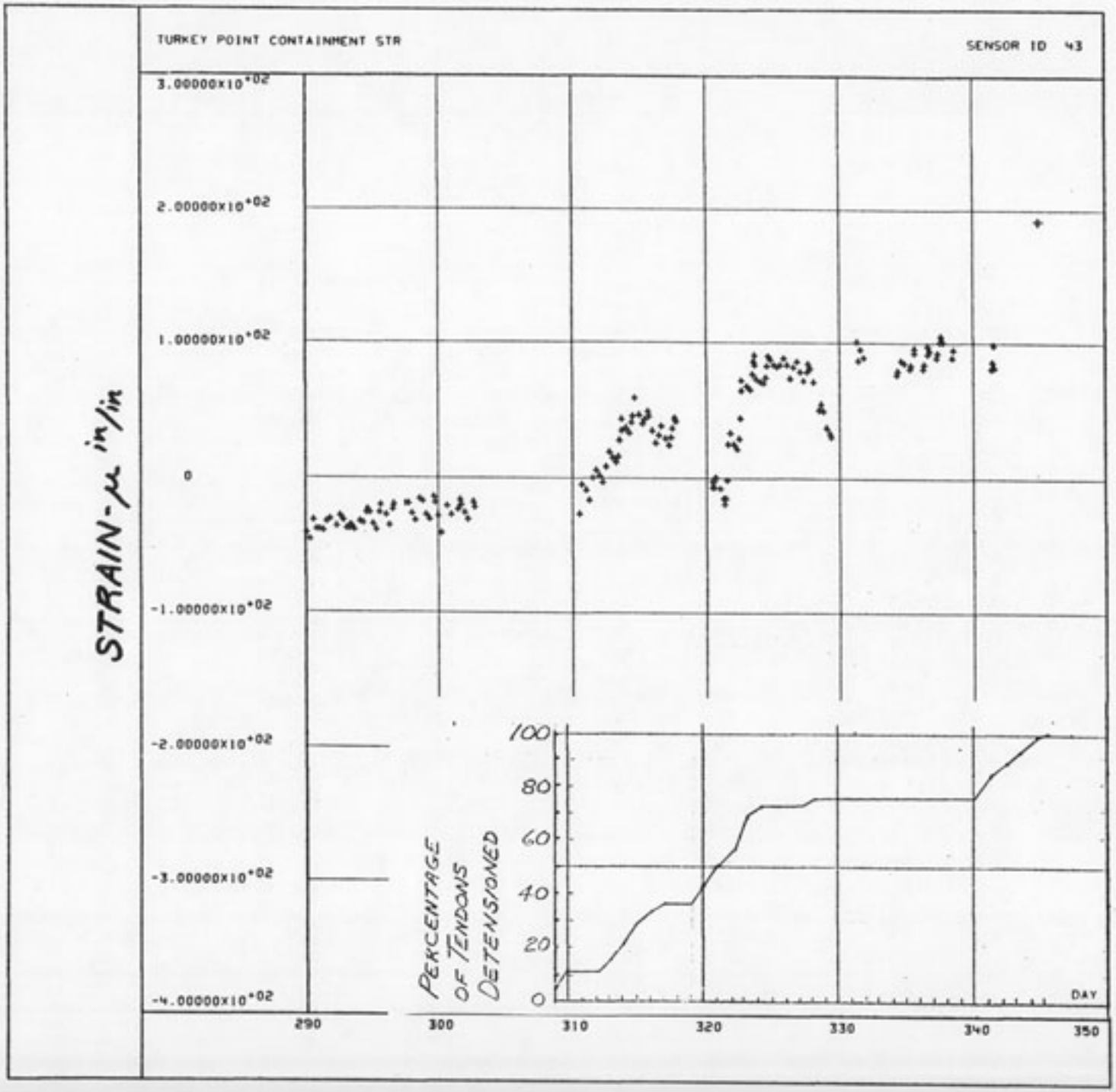
TURKEY POINT CONTAINMENT STR
SENSOR ID 43
STRAIN-μ in/in
3.00000x10+02
2.00000x10+02
1.00000x10+02
0
-1.00000x10+02
-2.00000x10+02
-3.00000x10+02
-4.00000x10+02
290
300
310
320
330
340
350
PERCENTAGE OF TENDONS DETENSIONED
100
80
60
40
20
0
DAY

FIGURE 3-8

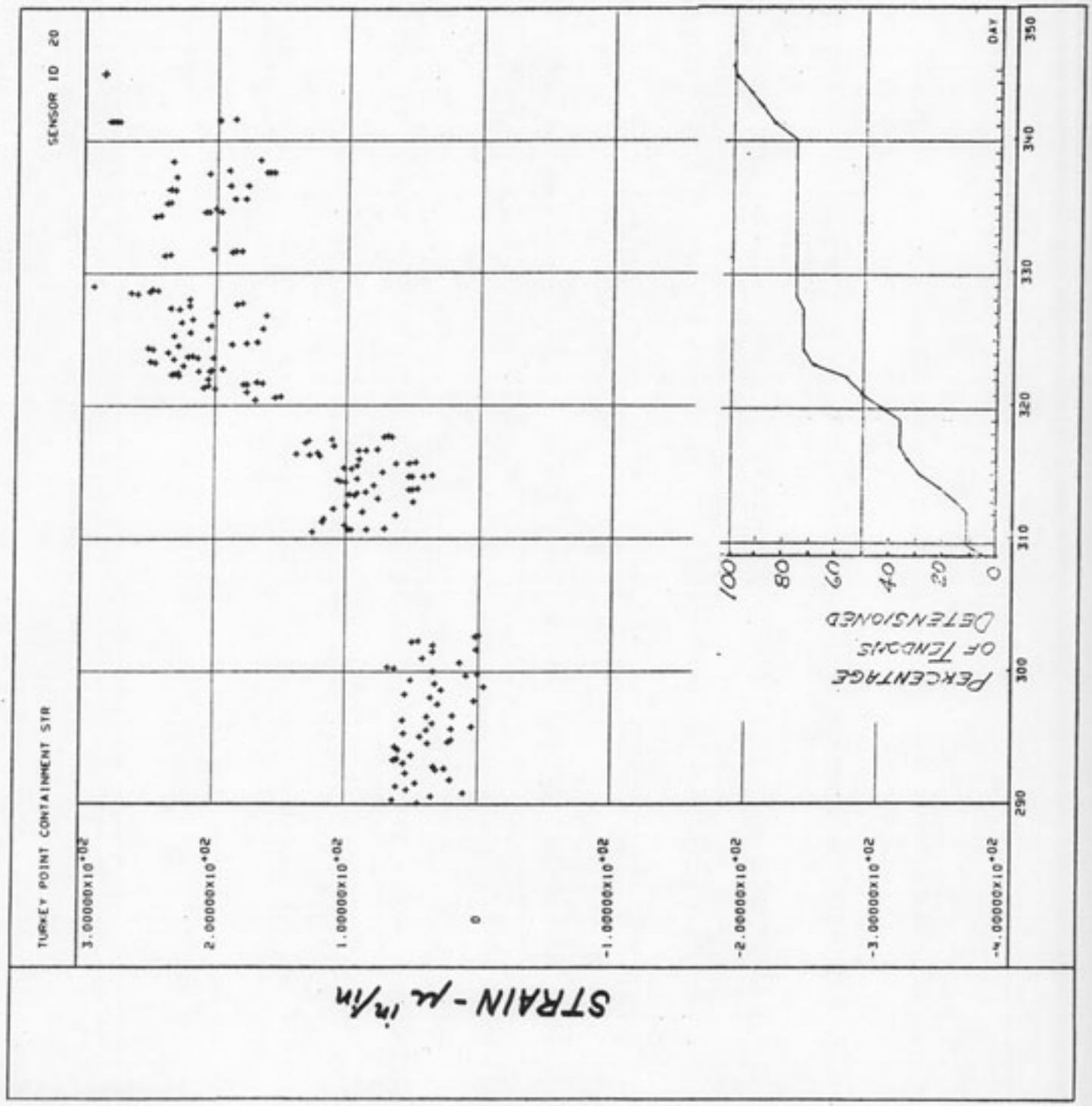
TURKEY POINT CONTAINMENT STR
SENSOR ID 20
3.00000X10+02
2.00000X10+02
1.00000X10+02
0
-1.00000X10+02
-2.00000X10+02
-3.00000X10+02
-4.00000X10+02
290
300
310
320
330
340
350
DAY
100
80
60
40
20
0
PERCENTAGE OF TENDONS DETENSIONED
STRAIN - μ in/in

FIGURE 3-9

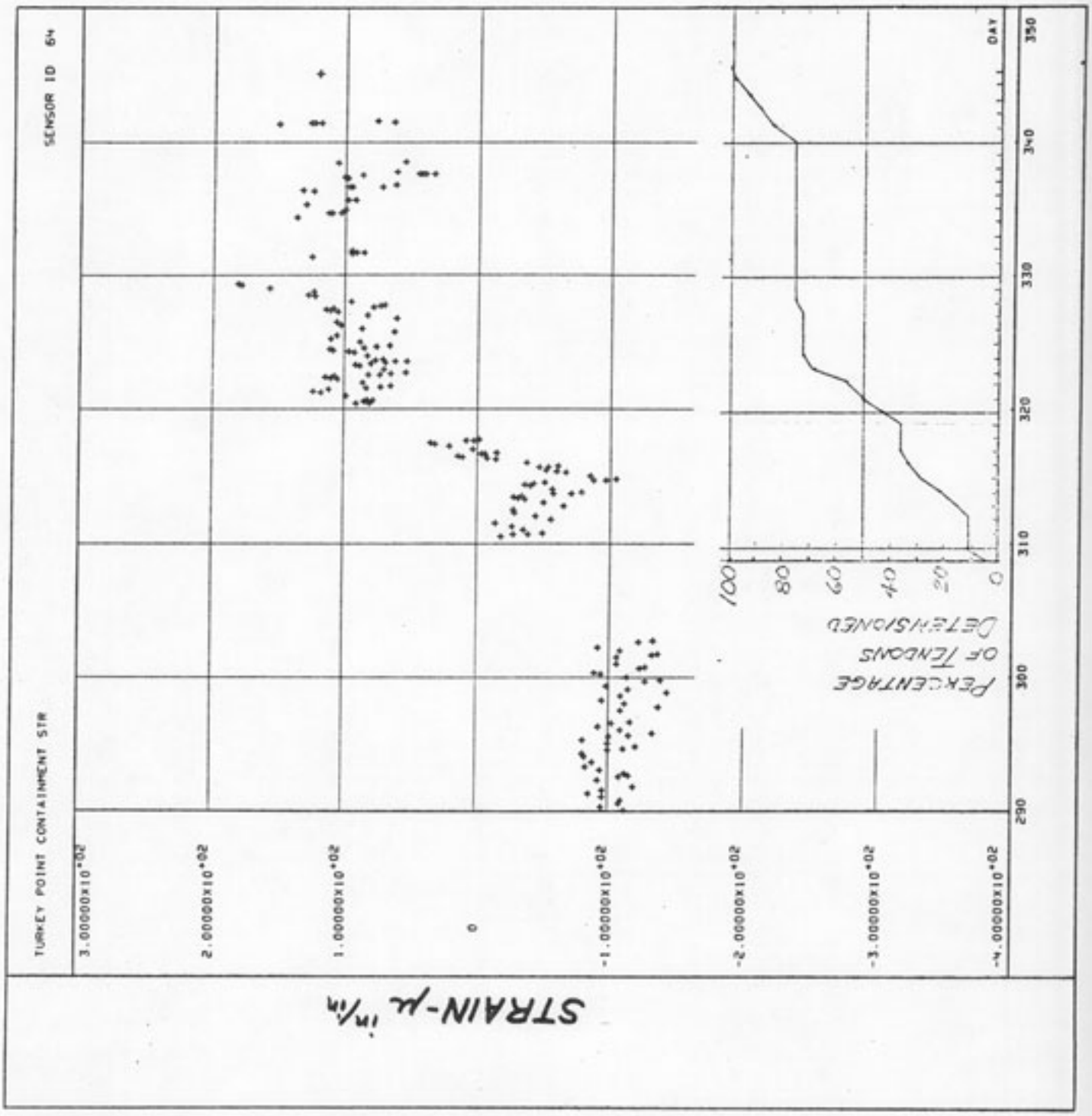
TURKEY POINT CONTAINMENT STR
SENSOR ID 64
STRAIN-μ in/in
3.00000x10+02
2.00000x10+02
1.00000x10+02
0
-1.00000x10+02
-2.00000x10+02
-3.00000x10+02
-4.00000x10+02
290
300
310
320
330
340
350
DAY
PERCENTAGE OF TENDONS DETENSIONED
100
80
60
40
20
0

FIGURE 3-10

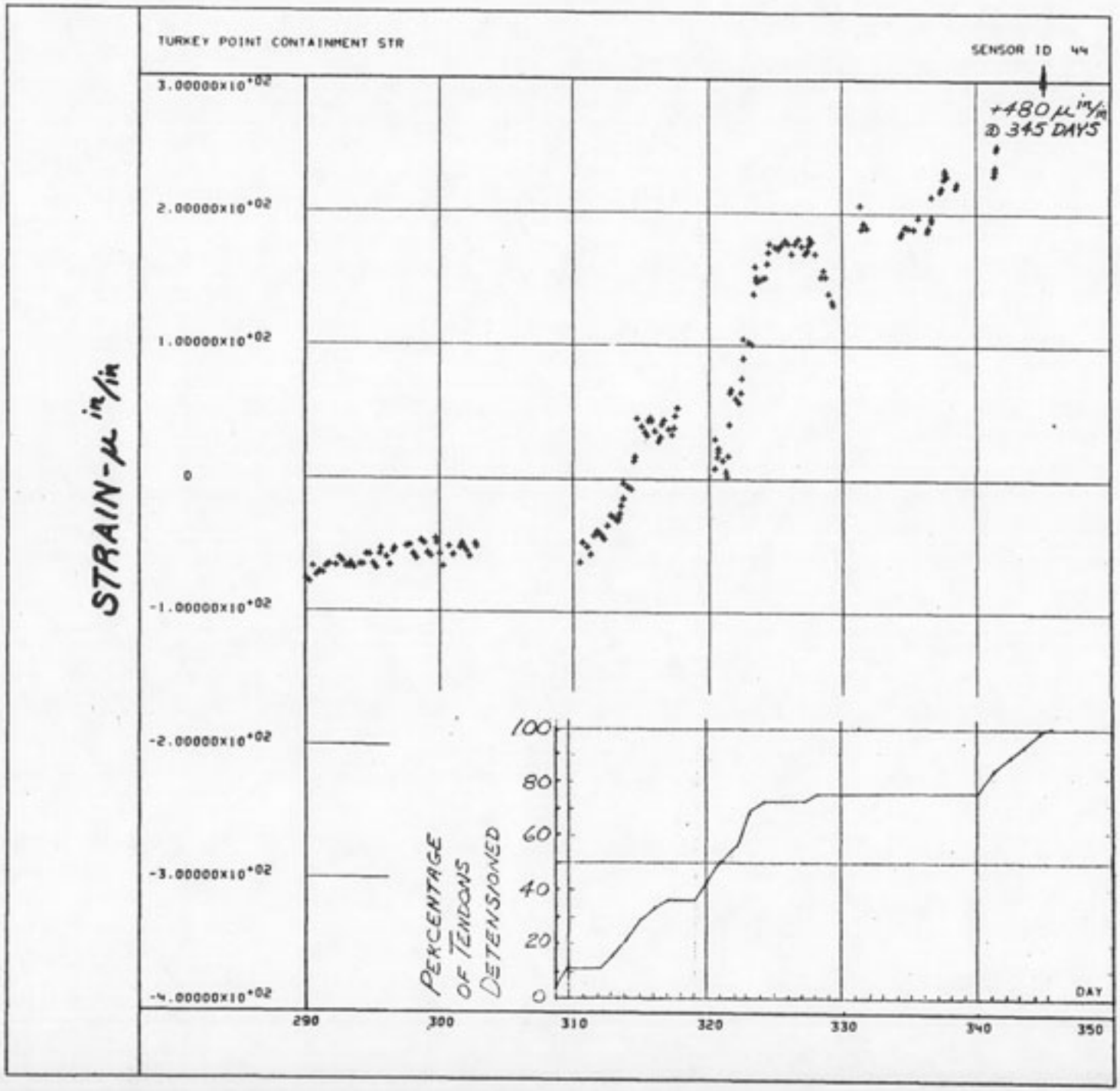
TURKEY POINT CONTAINMENT STR
SENSOR ID 44
+480 μ in/in @ 345 DAYS
STRAIN-μ in/in
3.00000x10+02
2.00000x10+02
1.00000x10+02
0
-1.00000x10+02
-2.00000x10+02
-3.00000x10+02
-4.00000x10+02
290
300
310
320
330
340
350
PERCENTAGE OF TENDONS DETENSIONED
100
80
60
40
20
0
DAY

FIGURE 3-11

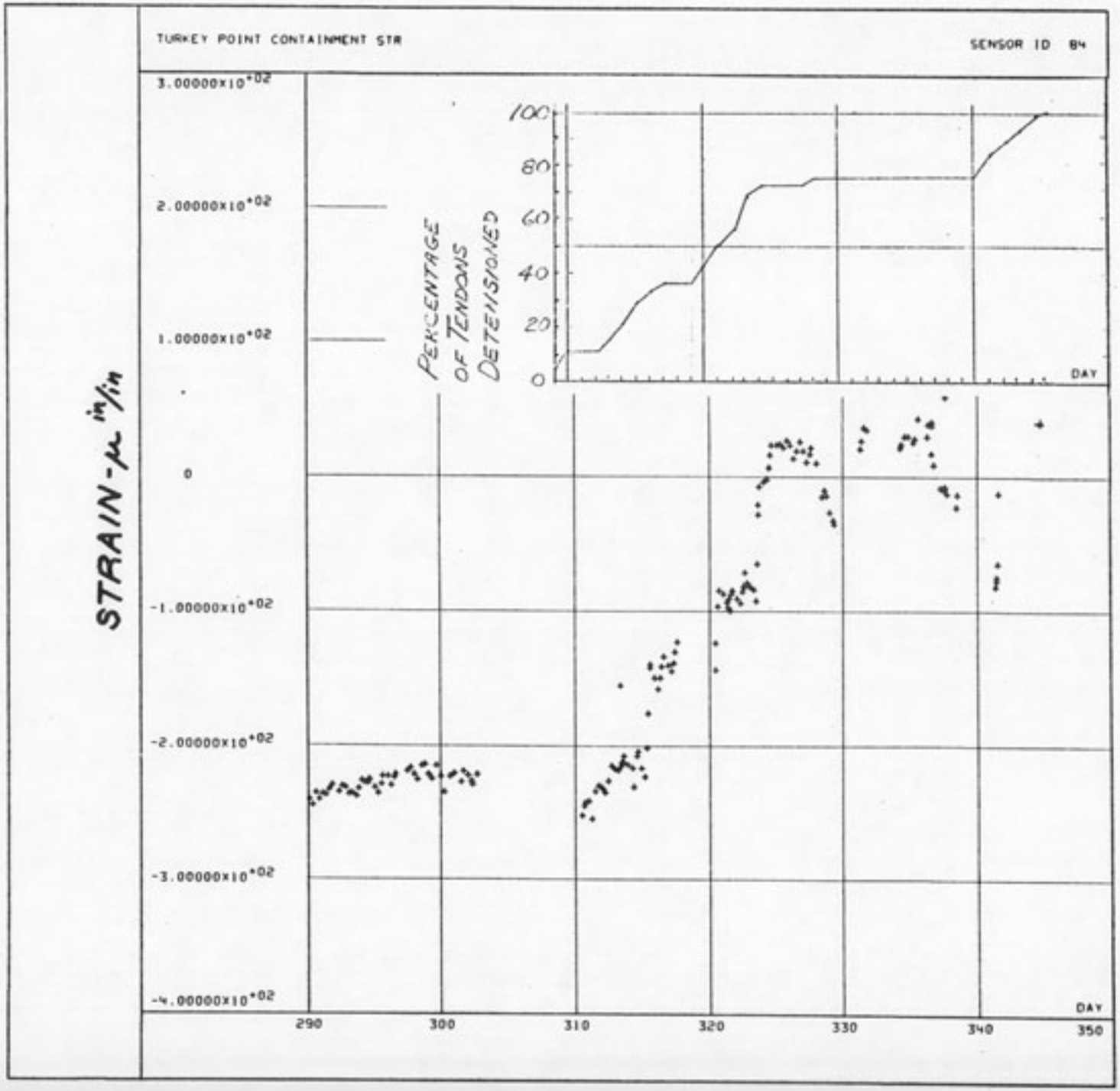
TURKEY POINT CONTAINMENT STR
SENSOR ID 84
STRAIN-μ in/in
3.00000x10+02
2.00000x10+02
1.00000x10+02
0
-1.00000x10+02
-2.00000x10+02
-3.00000x10+02
-4.00000x10+02
PERCENTAGE OF TENDONS DETENSIONED
100
80
60
40
20
0
DAY
290
300
310
320
330
340
350
DAY

FIGURE 3-12

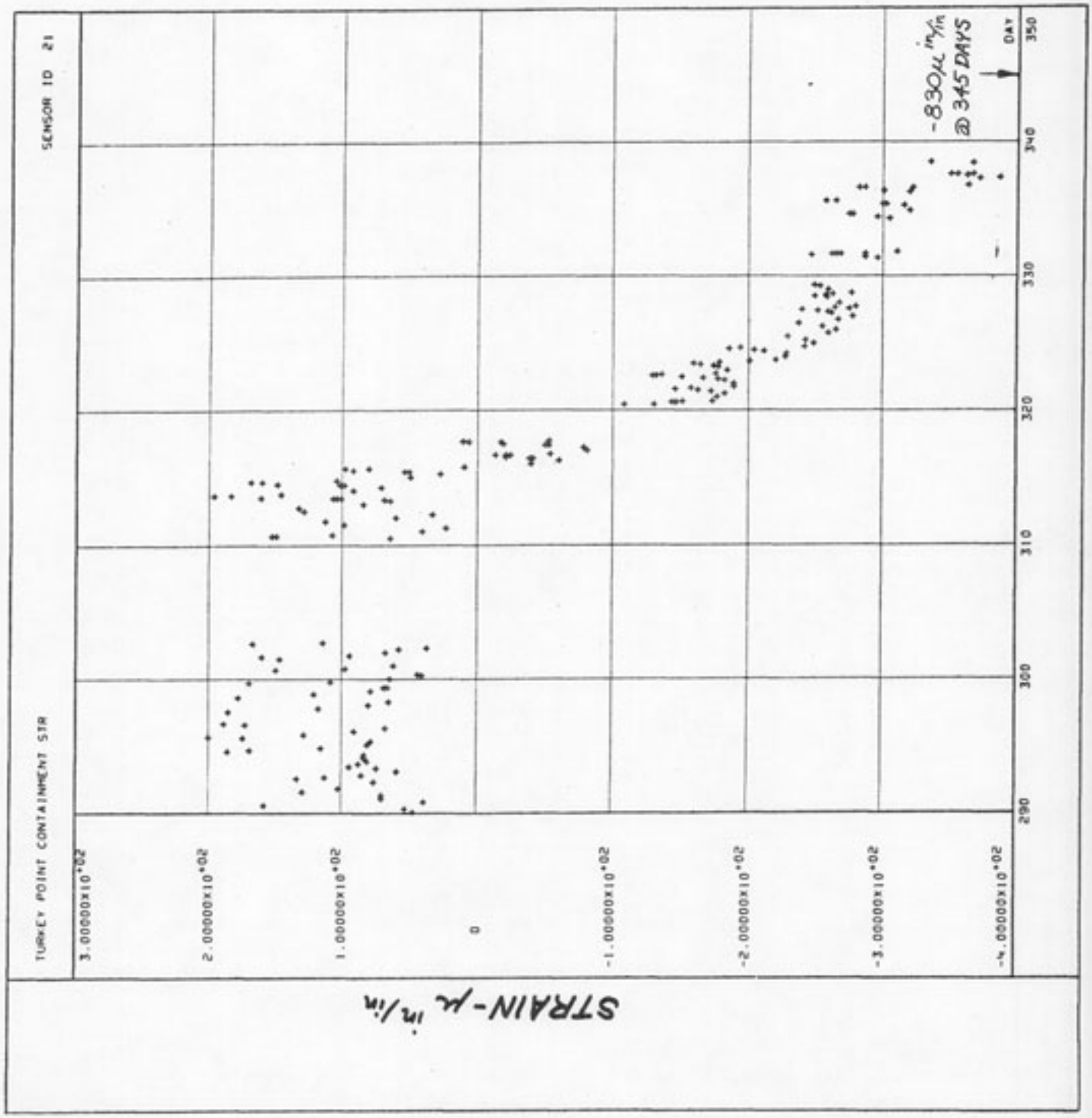
TURKEY POINT CONTAINMENT STR
SENSOR ID 21
3.00000x10+02
2.00000x10+02
1.00000x10+02
0
-1.00000x10+02
-2.00000x10+02
-3.00000x10+02
-4.00000x10+02
290
300
310
320
330
340
350
DAY
-830 μin/in @ 345 DAYS
STRAIN-μ in/in

FIGURE 3-13

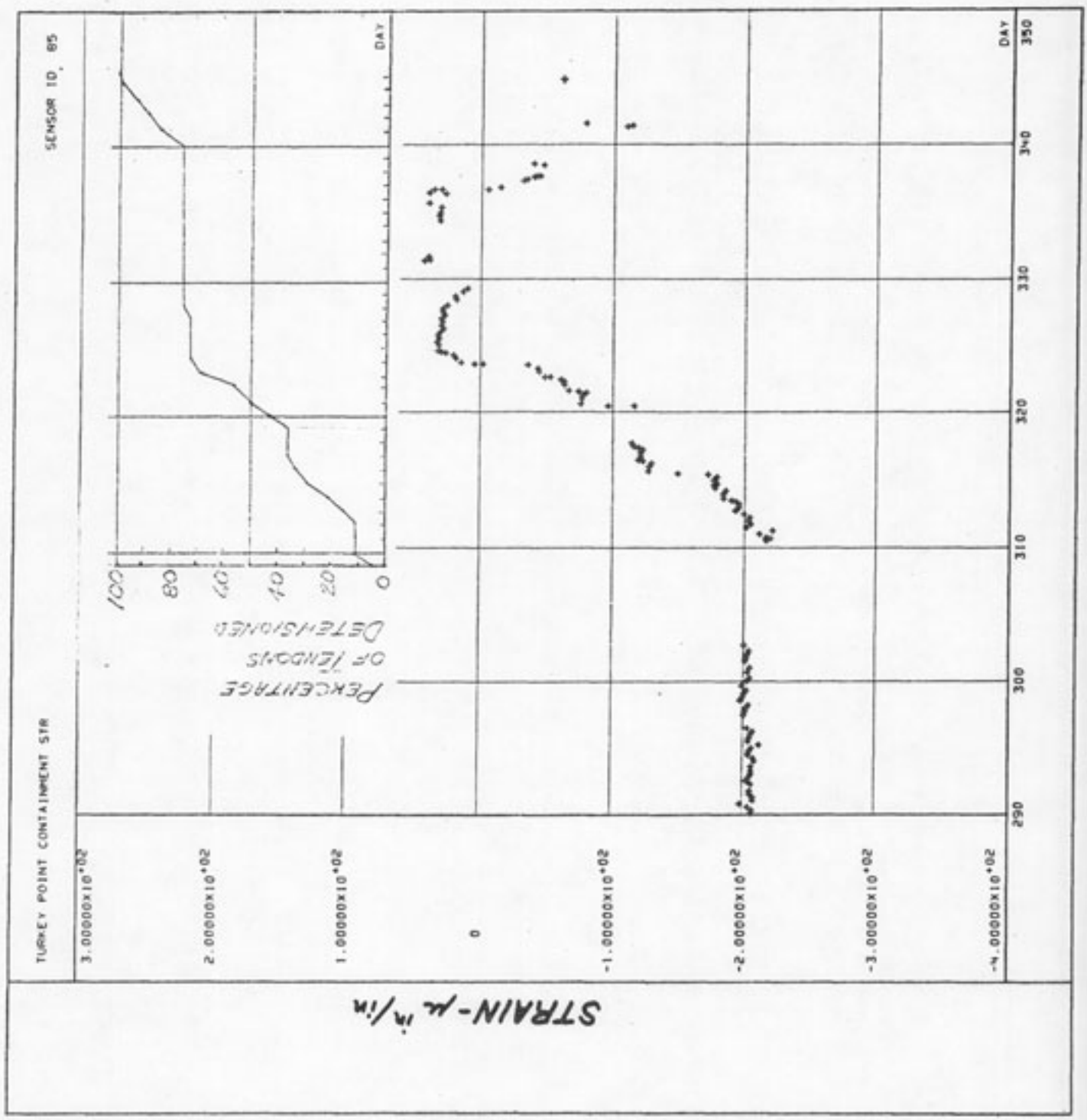
TURKEY POINT CONTAINMENT STR
SENSOR ID. 85
STRAIN-μ in/in
3.00000x10+02
2.00000x10+02
1.00000x10+02
0
-1.00000x10+02
-2.00000x10+02
-3.00000x10+02
-4.00000x10+02
290
300
310
320
330
340
350
DAY
PERCENTAGE OF ICNDCNS DETERMINED
0
20
40
60
80
100
DAY

FIGURE 3-14

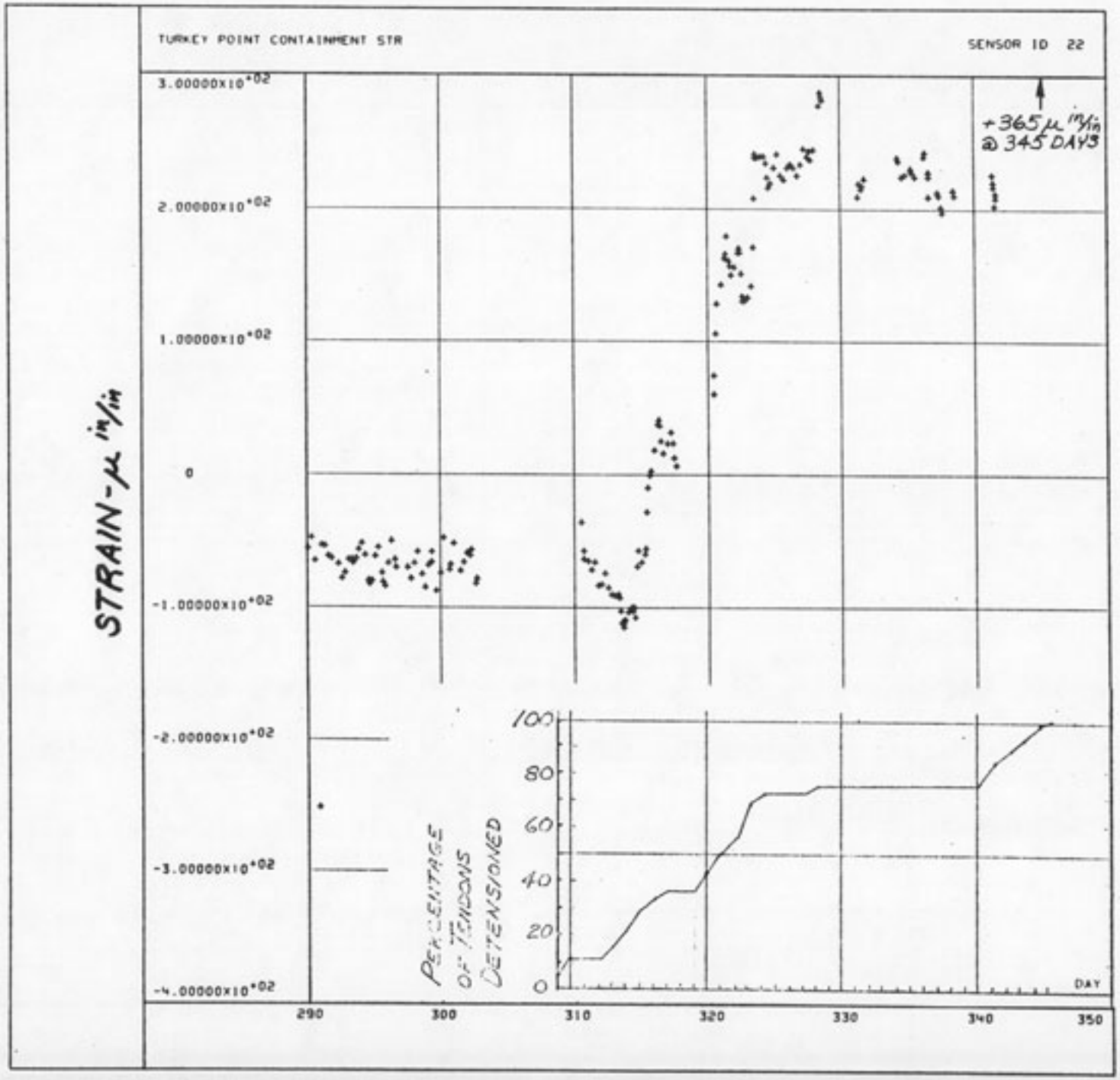
TURKEY POINT CONTAINMENT STR
SENSOR ID 22
STRAIN-μ in/in
3.00000x10+02
2.00000x10+02
1.00000x10+02
0
-1.00000x10+02
-2.00000x10+02
-3.00000x10+02
-4.00000x10+02
+365μ in/in
@ 345 DAYS
PERCENTAGE OF TENDONS DETENSIONED
100
80
60
40
20
0
DAY
290
300
310
320
330
340
350

FIGURE 3-15

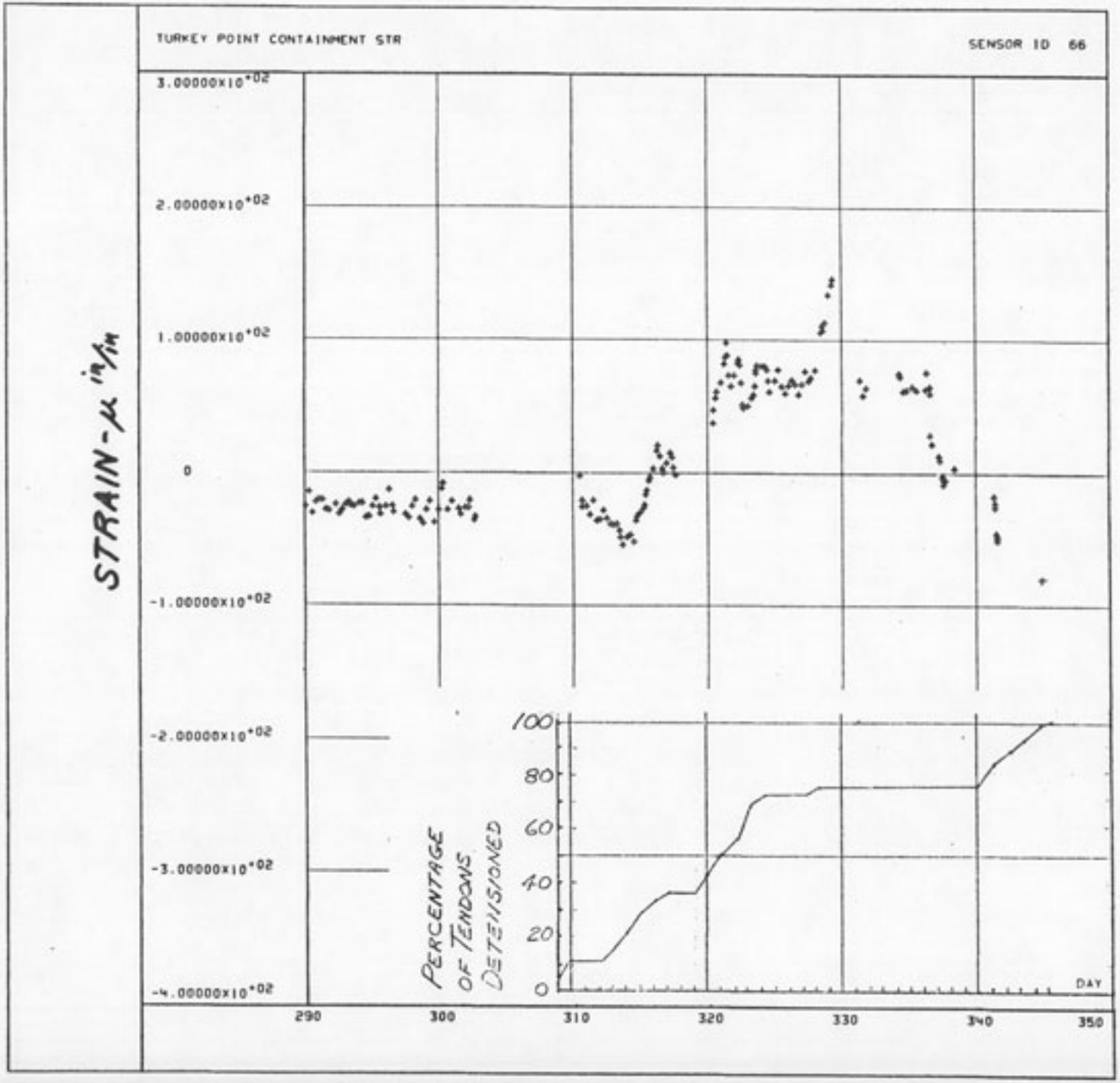
TURKEY POINT CONTAINMENT STR
SENSOR ID 66
STRAIN-μ in/in
3.00000x10+02
2.00000x10+02
1.00000x10+02
0
-1.00000x10+02
-2.00000x10+02
-3.00000x10+02
-4.00000x10+02
290
300
310
320
330
340
350
PERCENTAGE OF TENDONS DETENSIONED
100
80
60
40
20
0
DAY

FIGURE 3-16

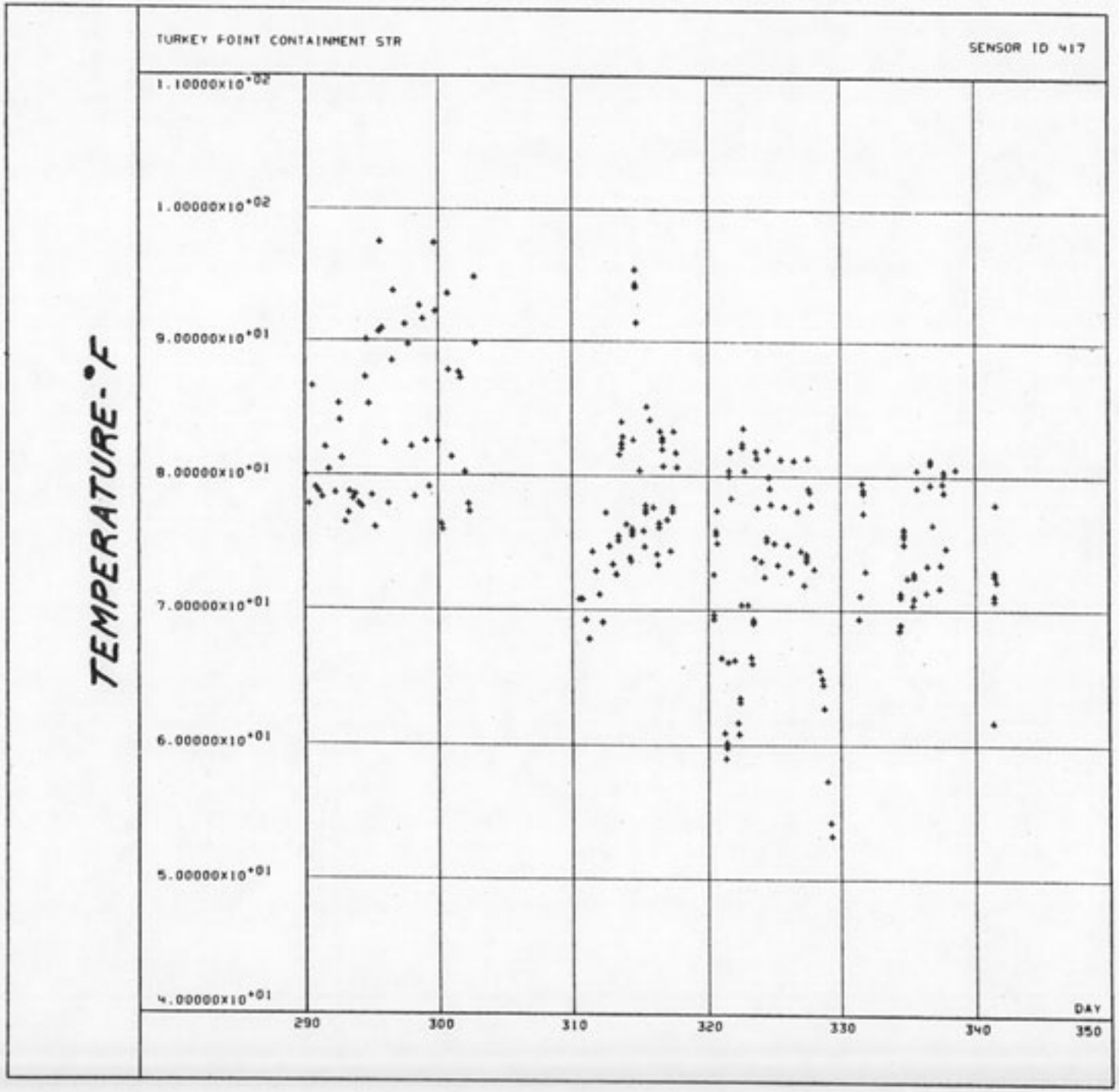
TURKEY POINT CONTAINMENT STR
SENSOR ID 417
TEMPERATURE-°F
1.10000x10+02
1.00000x10+02
9.00000x10+01
8.00000x10+01
7.00000x10+01
6.00000x10+01
5.00000x10+01
4.00000x10+01
290
300
310
320
330
340
350
DAY

FIGURE 3-17

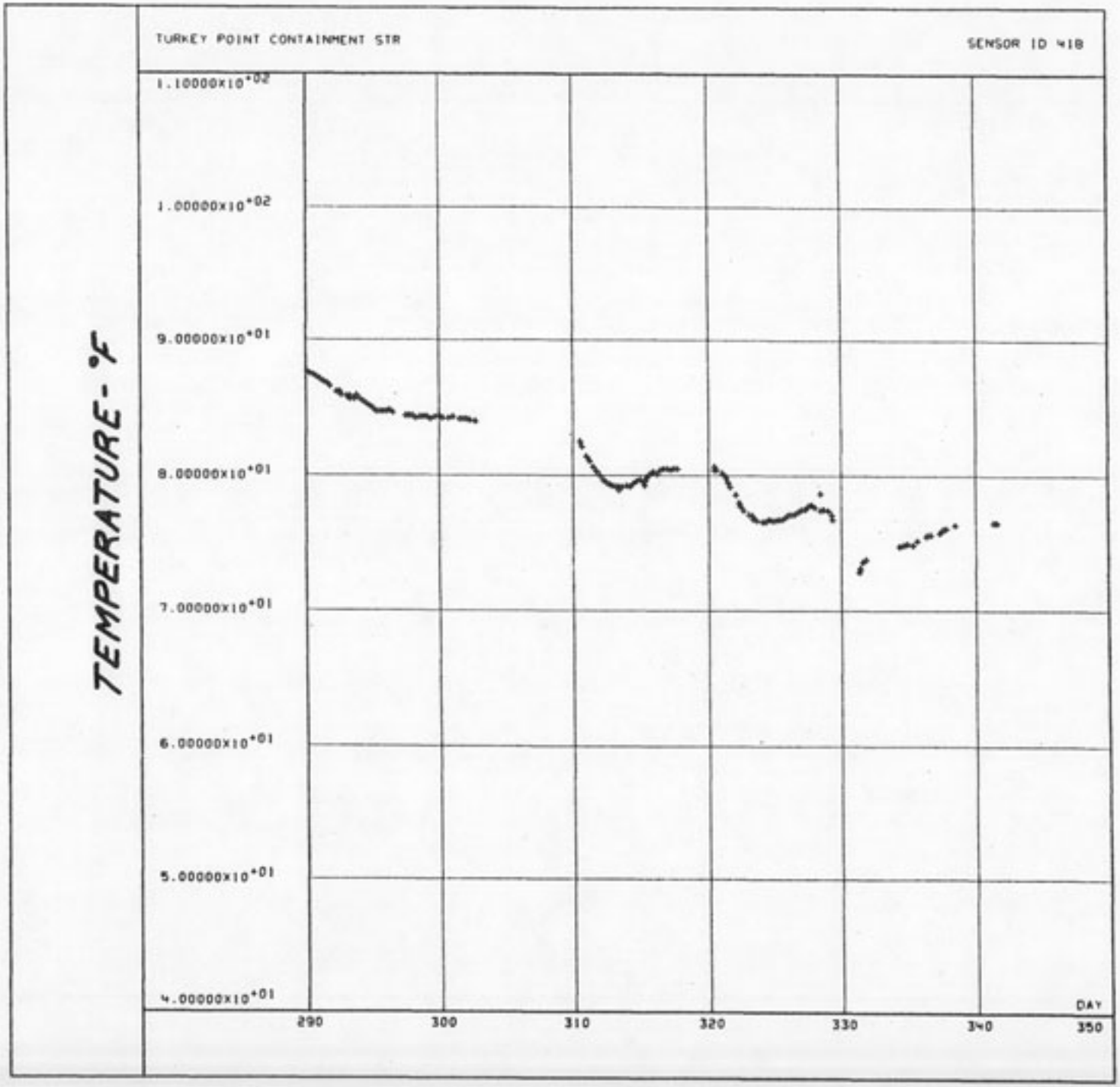
TURKEY POINT CONTAINMENT STR
SENSOR ID 418
TEMPERATURE- °F
1.10000x10+02
1.00000x10+02
9.00000x10+01
8.00000x10+01
7.00000x10+01
6.00000x10+01
5.00000x10+01
4.00000x10+01
290
300
310
320
330
340
350
DAY

FIGURE 3-18

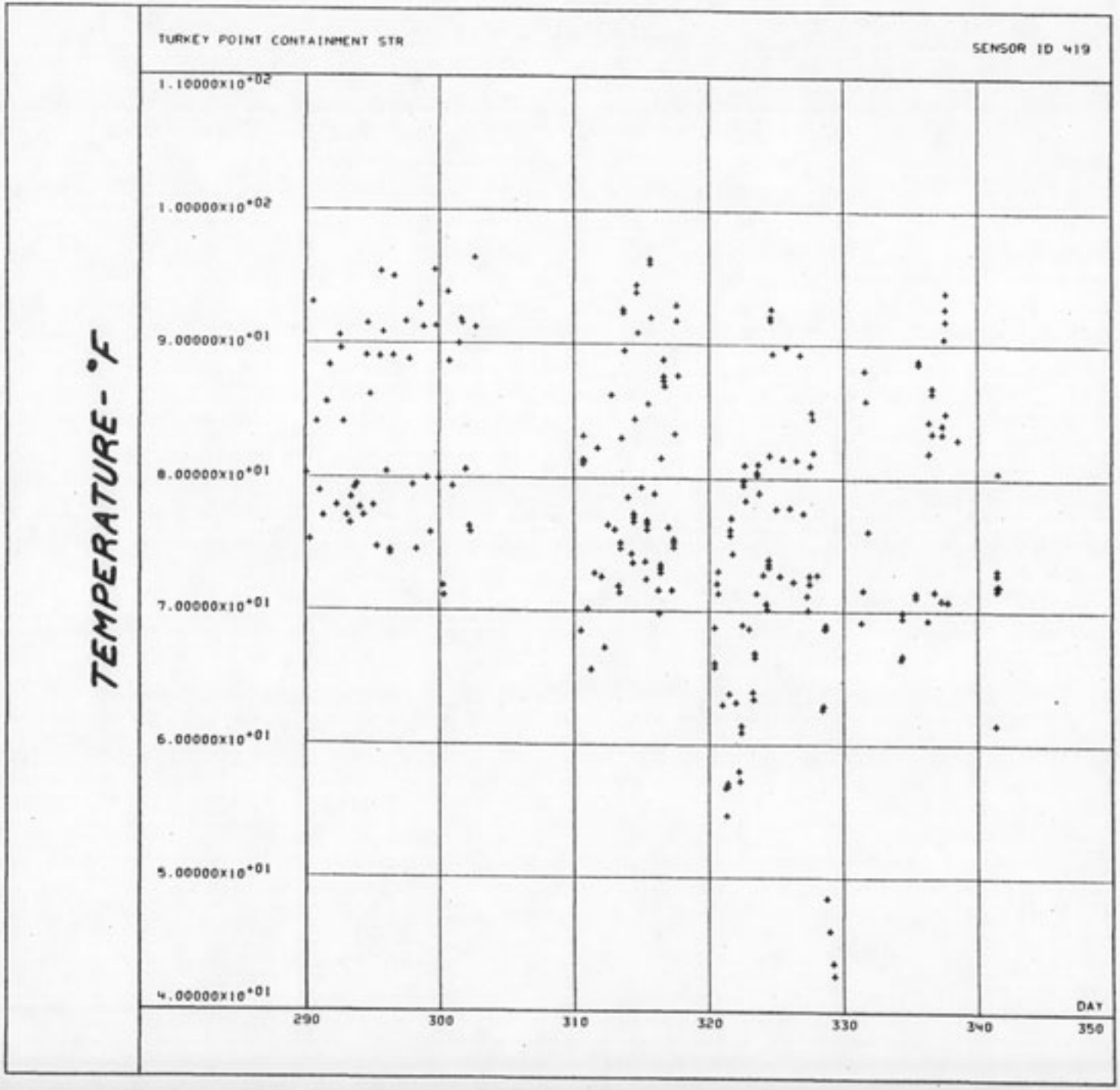
TURKEY POINT CONTAINMENT STR
SENSOR ID 419
TEMPERATURE- °F
1.10000x10+02
1.00000x10+02
9.00000x10+01
8.00000x10+01
7.00000x10+01
6.00000x10+01
5.00000x10+01
4.00000x10+01
290
300
310
320
330
340
350
DAY

FIGURE 3-19

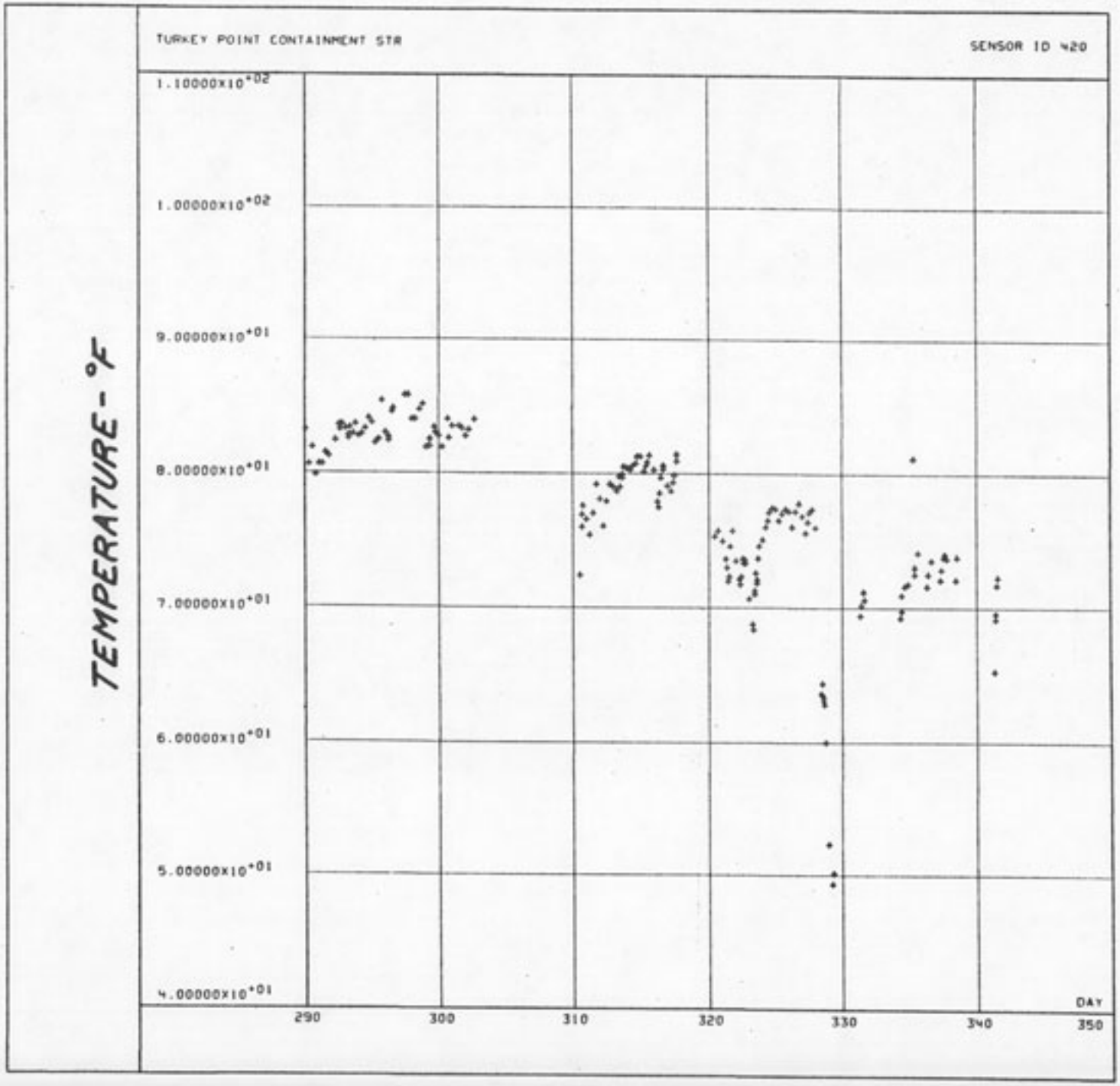
TURKEY POINT CONTAINMENT STR
SENSOR ID 420
TEMPERATURE - °F
1.10000x10+02
1.00000x10+02
9.00000x10+01
8.00000x10+01
7.00000x10+01
6.00000x10+01
5.00000x10+01
4.00000x10+01
290
300
310
320
330
340
350
DAY

FIGURE 3-20

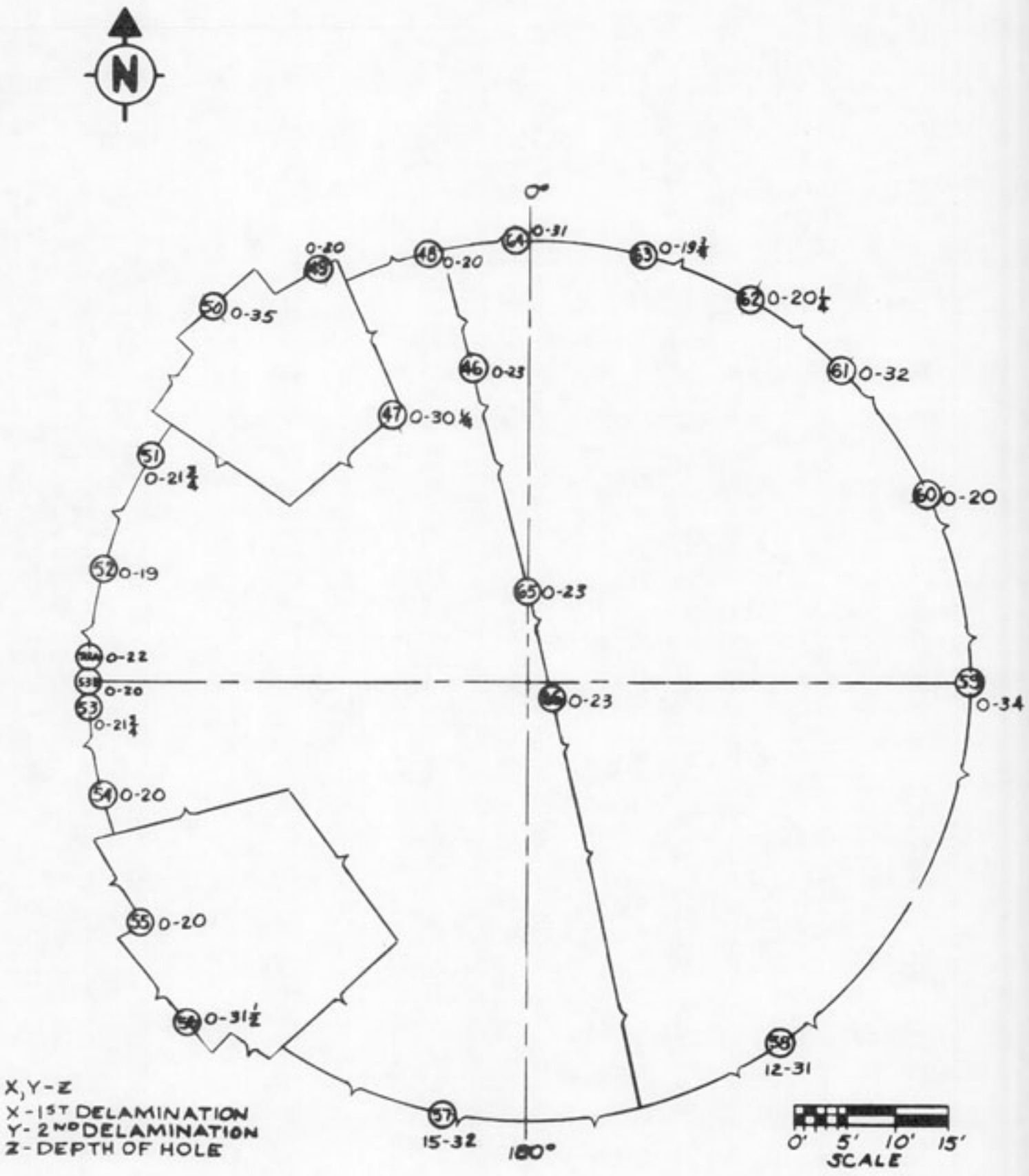

CORING ON CONSTRUCTION JOINT

FIGURE 3-21

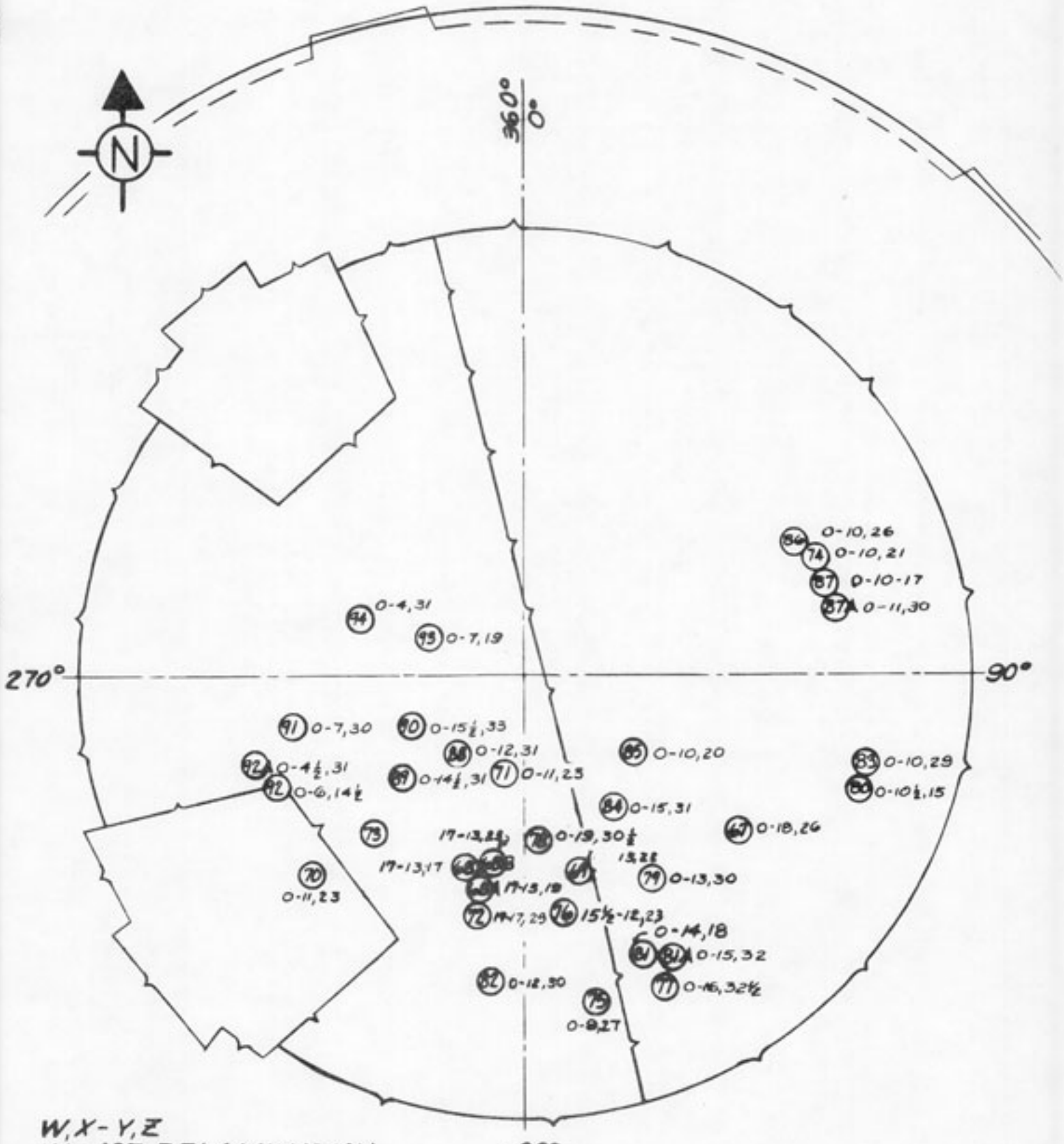

W, X - Y, Z
W - 1ST DELAMINATION
X - 2ND DELAMINATION
Y - STARTING HOLE DEPTH
Z - STARTING HOLE DEPTH

PLAN VIEW

0 5 10 15FT.
SCALE

CORING AFTER CONCRETE REMOVAL

FIGURE 3-22

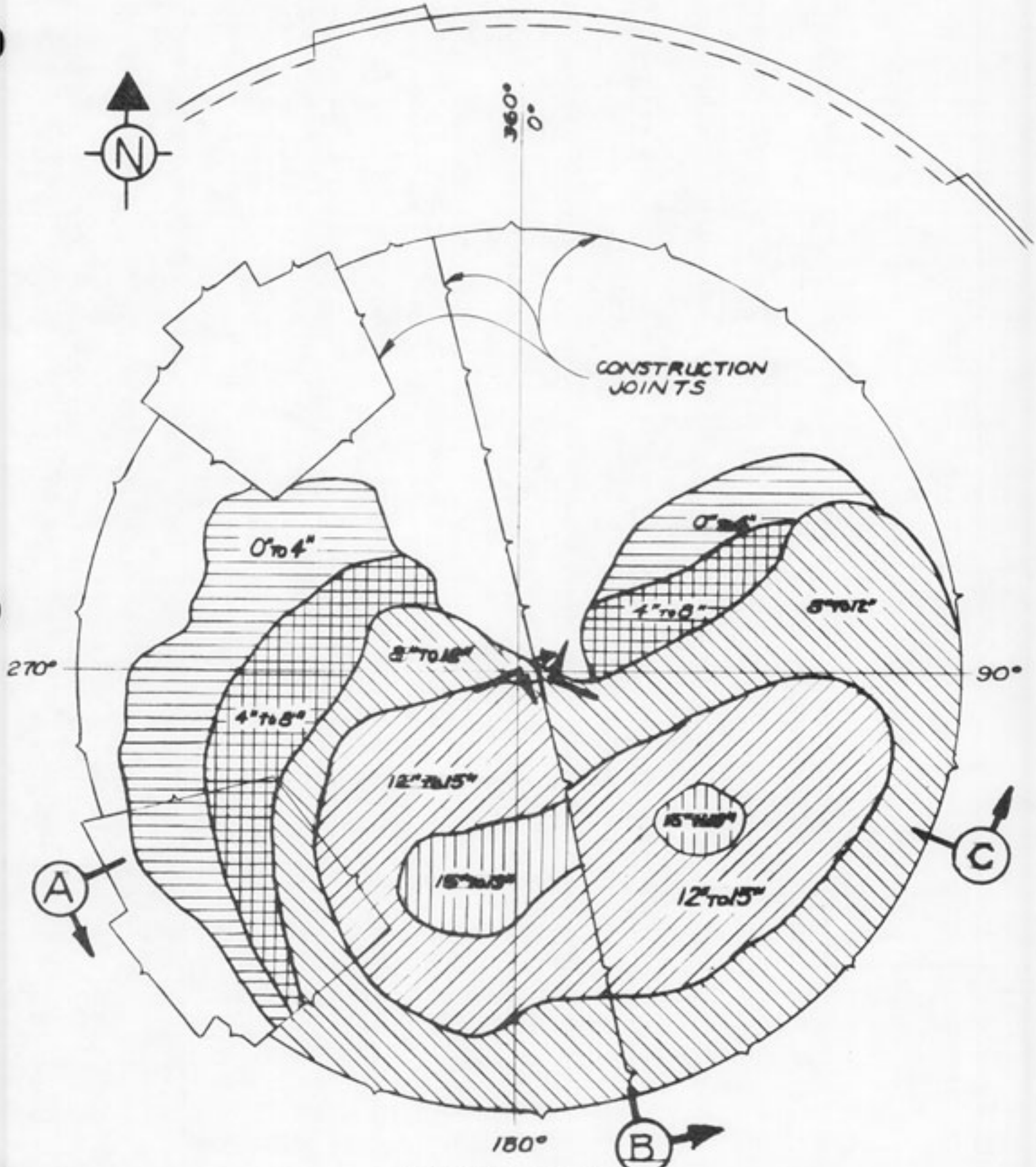

CONTOURS OF DEEPEST DELAMINATIONS VERIFIED BY CONCRETE REMOVAL AND CORING

FIGURE 3-23

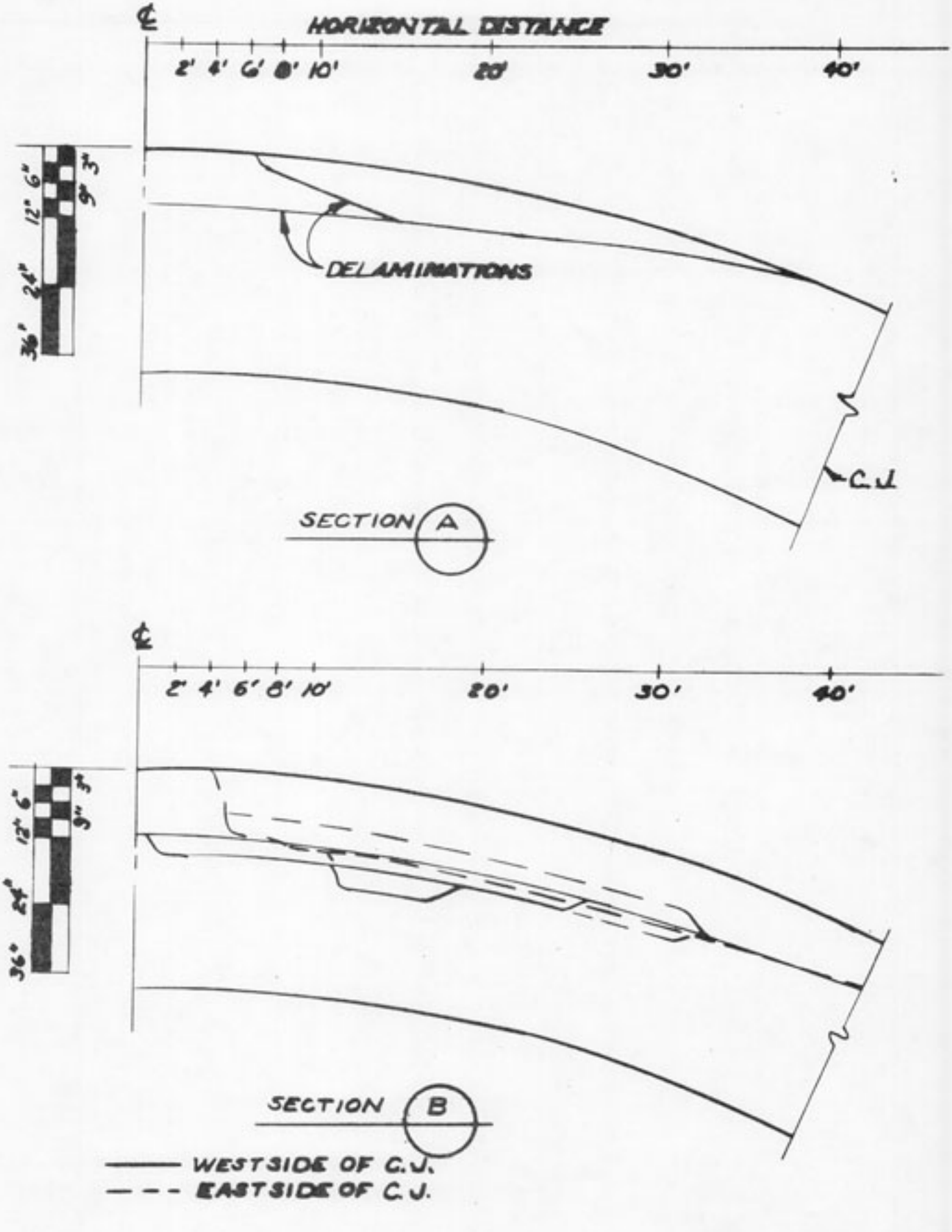

SECTION SHOWING
DELAMINATIONS

FIGURE 3-24

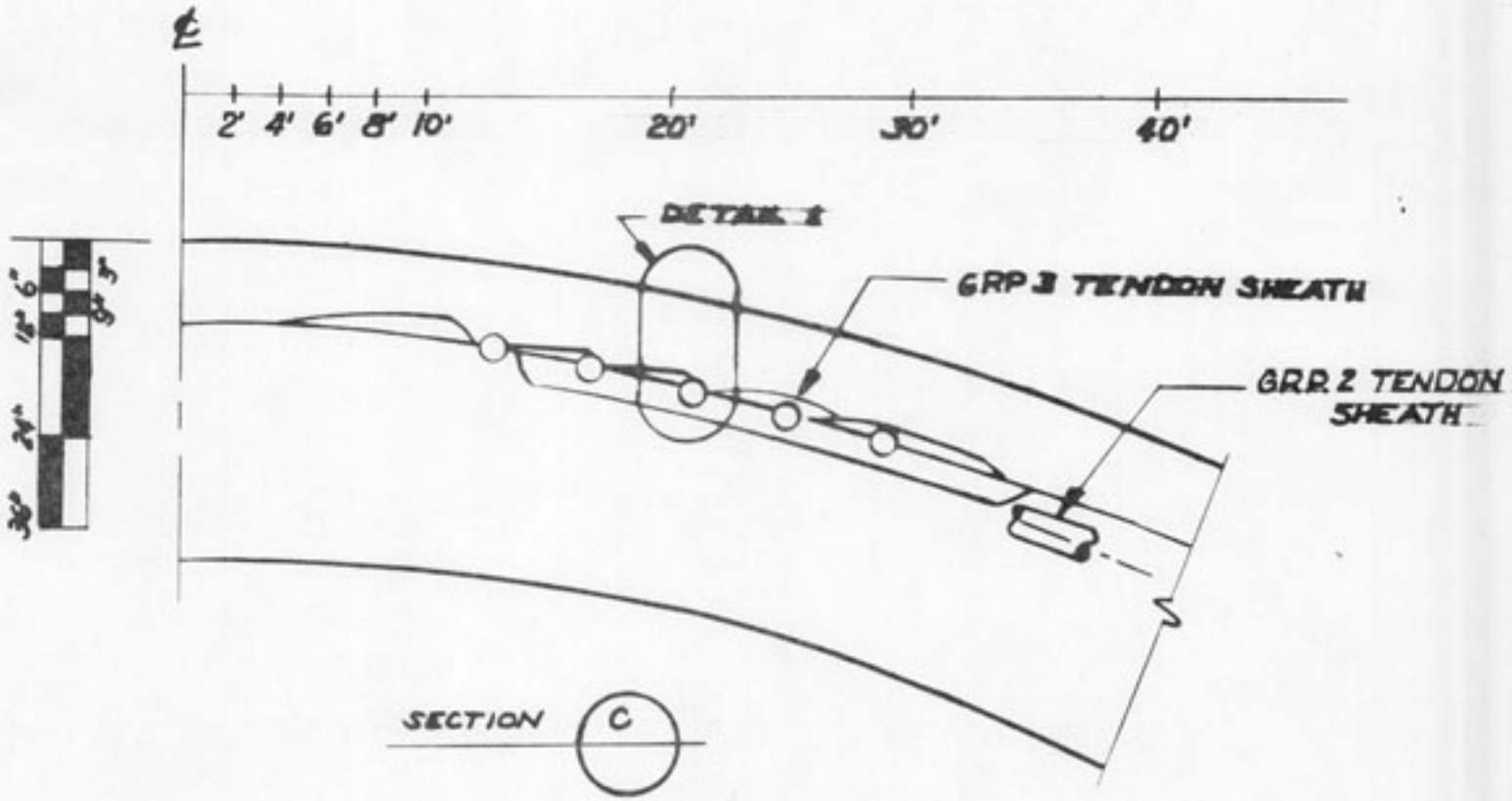

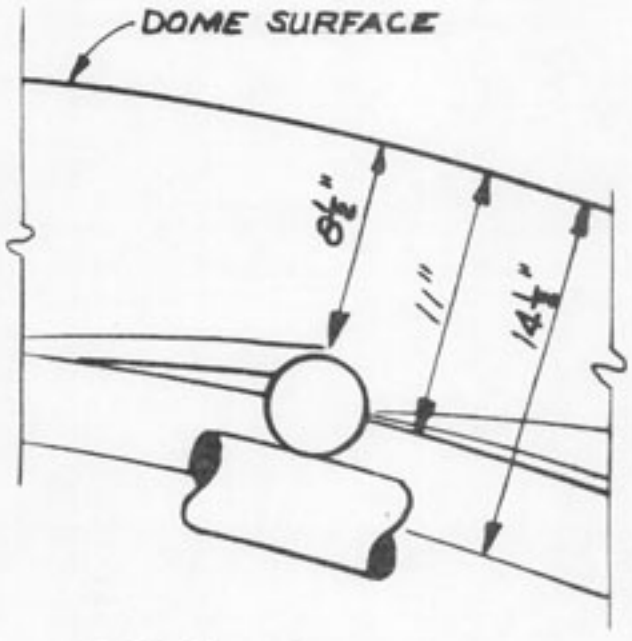

DETAIL 1

SECTION SHOWING
DELAMINATIONS

FIGURE 3-25

EAST SIDE OF DOME
DURING CONCRETE REMOVAL

FIGURE 3-26

WEST SIDE OF DOME
DURING CONCRETE REMOVAL

FIGURE 3-27

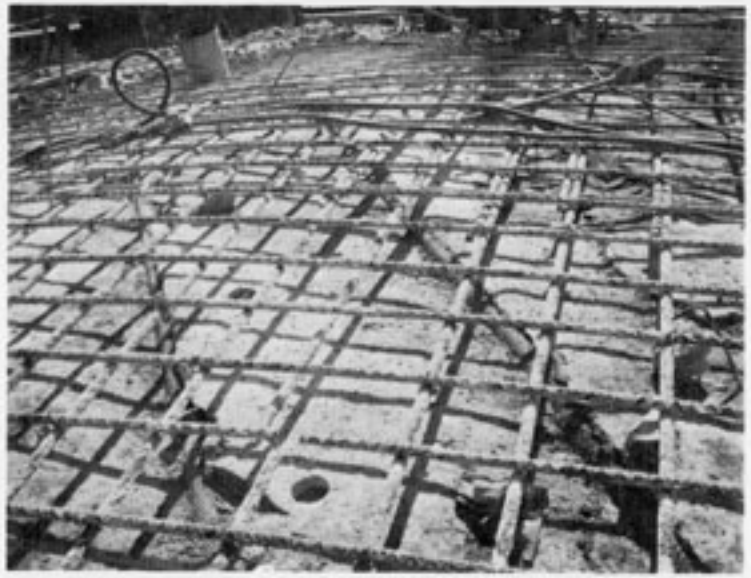

Looking south along West side. Note step effect of first delamination in region of top group 3 tendons.

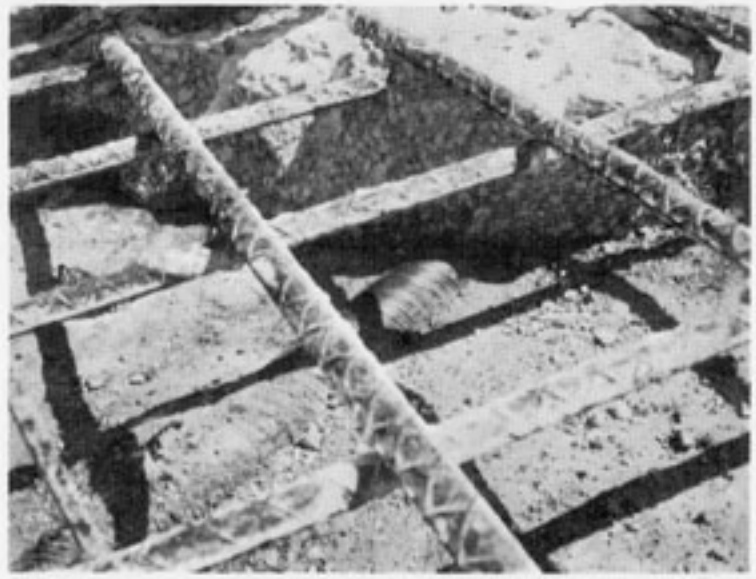

Looking S.E. along delamination through top group 3 tendon on east side. Note same depth on both sides of tendon.

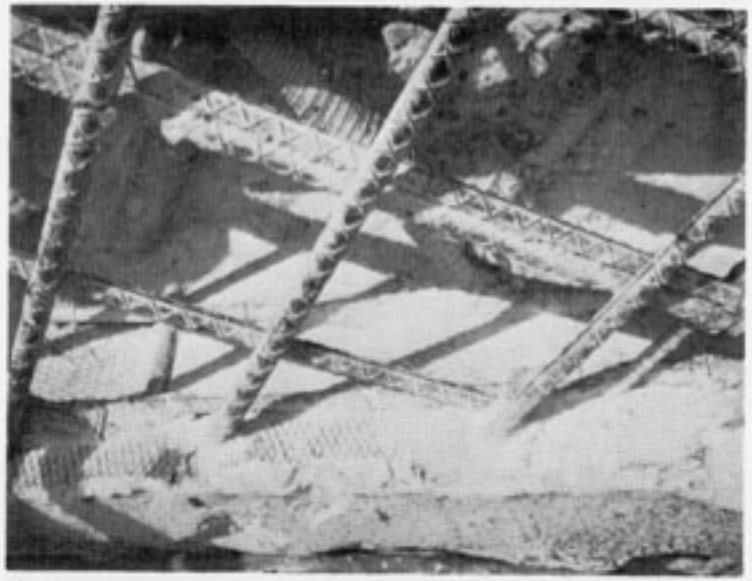

Meridional construction joint 10'-15' south of apex to a depth of 18".

Meridional construction joint 15'-20' south of apex to a depth of 18".

FIGURE 3-28

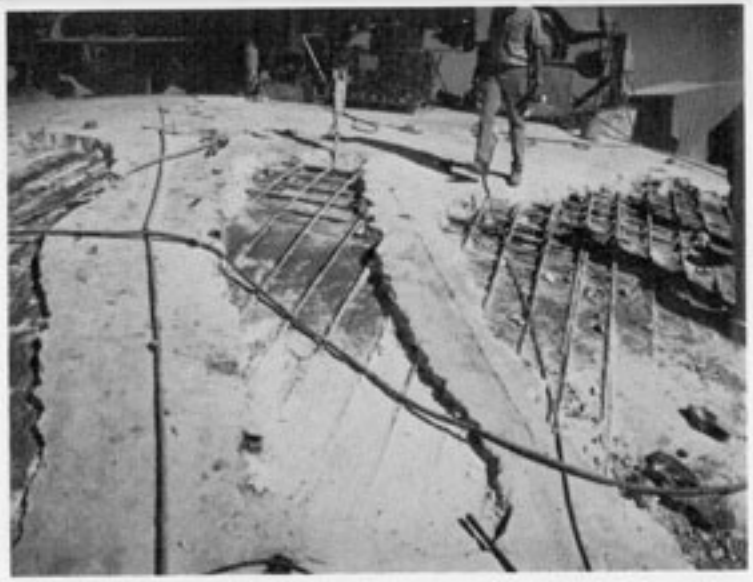

West side of dome in region of azimuth 256°. Note grease stain on delamination and outcropping.

Multiple delaminations at aximuth 316° and radius 8'.

Northeastern corner of the S.W. blockout. Note void at corner and lack of bond along sides.

Looking southeast at radial construction joint of the N.W. blockout. Note poor consolidation and separation from expanded metal.

FIGURE 3-29

4.0 MATERIALS INVESTIGATION

An extensive study was made to recheck the adequacy of the Turkey Point concrete to perform its intended function. The study involved documenting the physical and chemical properties of constituent materials, together with standard testing of specimens prepared with the concrete design mixes and tests not normally required. To establish a comparative basis, information on other concretes within Bechtel's experience are also included.

Table 4-1 shows the concrete design mixes for Turkey Point and other structures. The 2P5 mix is applicable for concrete placed before October 21, 1969. The delaminated dome concrete was formulated to the 2P6 design mix.

Table 4-2 shows the chemical and physical tests for the cements. The Turkey Point Cement conforms to the requirements of Type II cement. Low heat of hydration cement (combined limit of 58% on tri-calcium silicate and tri-calcium aluminate) was not specified for Turkey Point. (The ASTM limit of 58% is optional and applies only when specifically requested by the user). However, control of the concrete placement temperature at 70 F was specified and "Retardwell" was used to slow down the rate of hydration of the cement.

Table 4-3 shows the properties of the fine and coarse aggregate for Turkey Point. The coarse aggregate was specified as 1" minus since larger sizes were considered too absorbtive.

Tables 4-4 and 4-5 show the chemical analyses for both the water and ice used in the mixing of the concretes. In all cases the water and ice are suitable for their intended purpose.

Table 4-6 lists the air entraining agents used in the various concretes and Table 4-7 lists the water reducing agents. All are within specification requirements.

Table 4-8 shows the physical concrete properties based on initial testing which was performed to verify the adequacy of the design mixes for their

intended use and to obtain design data for creep, shrinkage, etc. With the exception of the lower splitting tensile strength on Turkey Point all other properties are comparable. However all calculated tensile stresses are considerably lower than the values given in Table 4-8.

Table 4-9 shows the comparison of uniaxial compression strength for concrete cylinders cast during dome concrete placement and also for concrete taken from the delaminated area of the Turkey Point Dome. All cylinders sampled from concrete when cast show strengths exceeding 5000 psi.

Table 4-10 shows additional splitting tensile strength results for the various concretes. Comments are the same as for Table 4-8.

Table 4-11 shows the results of direct tensile tests on concrete taken from the dome. The average of 8 tests was 352 psi. As is common, the direct tensile strengths are less than those calculated from the results of the cylinder splitting tests.

Another series of tests were performed to determine the stress and strain values for uniaxial tension and compression given in Table 4-12 and 4-13. To provide evidence that a state of biaxial compressive strain would not lead to a condition more critical than that indicated by uniaxial compression tests, a series of tests were performed. The tests were made by placing a concrete cylinder with a membrane around it in a pressure chamber. The chamber could apply an essentially frictionless pressure load to the cylindrical surface while the ends remained free of load. There was a test technique problem in preventing oil from causing a premature failure due to penetration of the membrane or collapsing of subsurface voids and creating a longitudinal tension force. As shown in Table 4-14, it was difficult to cause a failure, resulting from radial pressure alone, however the results do show that the biaxial capability of the concrete strength is equal or greater than the uniaxial capability.

In both biaxial and uniaxial compression the failure mechanism was by formation of crack planes parallel to the applied loading direction for

the Turkey Point and other concretes. When loading a cylinder in uniaxial compression, first cracking would occur in the longitudinal direction. Individual columns would then form and eventually fail in shear on inclined planes with resulting multiple failure surfaces. The texture of the compression failure surfaces were much closer to that of the dome delamination surface than were those resulting from uniaxial tension. Figure 4-1 shows a delaminated surface of a core together with both a tension and compression failure specimen. This fact, together with the knowledge that multiple delaminations existed in the dome, confirms the conclusion that the dome delamination resulted from large compression forces essentially parallel to the surface. These large forces resulted in a concrete strain failure on surfaces parallel to the dome. The testing was for short duration loads, and strengths for long term loads are typically lower. Therefore, it is reasonable to assume that the delaminations occurred because of long term loads that caused relatively widespread compressive stresses of approximately .75 to .85 f'_c parallel to the surface. (For the Turkey Point concrete .75 f'_c is typically equal to 4500 psi).

Petrographic analyses of concrete have been performed by 2 independent laboratories, namely: Erlin Associates of Northbrook, Illinois through Pittsburgh Testing Laboratory and by Dr. Richard C. Mielenz, Vice President of Research and Development, Master Builders Company of Cleveland, Ohio.

The result of their examinations shows the concrete to be a competent material with:

(1) A low water-cement ratio.
(2) A good air void system.
(3) No sign of alkali-carbonate reaction.
(4) A good distribution of sound coarse aggregate.
(5) No sign of metallic aluminum or hydrogen gas formation due to pumping through aluminum pipe.

TABLE 4-1

TABULATION OF DESIGN MIX QUANTITIES
(For 1 Cubic Yard)

	JOB & JOB NUMBER					
	TURKEY POINT 5610	TURKEY POINT 5610	CONTAINMENT A	CONTAINMENT B	CONTAINMENT C	CONTAINMENT D
Mix Number (28 Day Strength)	2P5* (5000 PSI)	2P6* (5000 PSI)	(5000 PSI)	(5000 PSI)	(5000 PSI)	(5000 PSI)
Cement	588#	635#	526#	479#	580#	611#
Fly Ash	-	-	93#	85#	-	-
Sand	1290#	1254#	1210#	1227#	1080#	1131#
3/4" Aggregate	1660#	1638#	937#	996#	1100#	893#
1½" Aggregate	-	-	1033#	1095#	1100#	954#
Water (W/C Ratio)	279# (0.47)	260# (0.40)	246# (0.48)	229# (0.48)	265# (0.46)	225# (0.37)
Water Reducing Agent	12.65 OZ.	13.5 OZ.	11 OZ.	24 OZ.	12 OZ.	13 OZ.
Air Entraining Agent	1.5 OZ.	1.6 OZ.	10.5 OZ.	4 OZ.	10 OZ.	4.6 OZ.

* Mix 2P5 lost approximately 1500 PSI strength when the pump was used. Adopted new mix 2P6 with an extra ½ sack of cement to offset this loss.

TABLE 4-2

CHEMICAL & PHYSICAL TESTS OF CEMENT IN ACCORDANCE WITH ASTM C-150

AVERAGE OF USER TESTS RUN ON THE SITE DURING THE APPROX. PERIOD OF TIME THE DOME WAS POURED (EXCEPT FOR CALVERT CLIFFS). ALL USER TESTS RUN BY INDEPENDENT TESTING LABORATORIES.

ASTM TYPE I' REQUIREMENTS LISTED IN PARENTHESIS

	Chemical Properties									Physical Properties													
	SiO_2 (21%) (Min)	Al_2O_3 (6%) (Max)	Fe_2O_3 (6%) (Max)	MgO (5%) (Max)	SO_3 (2.5%) (Max)	Loss on Ign. (3%) (Max)	Insol. Res. (.75%) (Max)	C_3A (8%) (Max)	C_3A &C_3S (58%) (Max)	Specific Wagner (1600 CM^2/G) (Min)	Surface Blaine (2800 CM^2/G) (Min)	Soundness -Autoclave Expansion- (0.80%) (Max)	Time of Gillmore Initial (60 Min) (Min)	Time of Gillmore Final (10 Hr) (Max)	Setting Vicat (45 Min) (Min)	Air Content % by Vol. (12% Max.)	Comp. Strength 3d (1000 PSI) (Min	Comp. Strength 7d (1800 PSI) (Min	Comp. Strength 28d (3500 PSI) (Min)	Tensile Strength 3d (125) (PSI) (Min)	Tensile Strength 7d (250) (PSI) (Min)
TURKEY PT. #5610 TYPE II CEMENT	21.7	4.13	3.16	1.04	2.12	1.16	.22	5.57	*70.9	2070	3862	0.007%	2 Hr.	5 Hr. 13 Min.	1 Hr. 26 Min.	7.5%	3322	4456	6300	337 Result of 2 tests. This data not requested.	413		
CONTAINMENT A TYPE II CEMENT	22.9	4.24	4.05	2.29	1.95	1.02	.25	4.39	47.0	--	3500	.03%			2 Hr. 40 Min.	8.0%	1517	2257	4291				
CONTAINMENT B TYPE II CEMENT	21.8	4.98	4.41	2.00	2.22	1.15	.10	5.74	54.3	--	3367	.02%	3 Hr. 55 Min.	5 Hr. 56 Min.		8.05%	2383	3375					
CONTAINMENT C TYPE II CEMENT	22.2	4.3	3.6	2.46	2.27	1.23	.13	5.3	58.7	--	3398	.08%			2 Hr. 33 Min.	7.3%	2253	3380	5493				
CONTAINMENT D TYPE II CEMENT	21.75	4.3	4.25	3.05	2.3	0.8	0.25	4.2	52	-	3655	0.06%	-	-	2 Hr. 32 Min.	7.1%	1715	2923	4224	308	384		

* Each User Test Value & Avg. of all Tests exceed maximum. Since moderate heat of Hydration Cement was not requested and the thermal co-efficient of expansion is low in comparison to other mixes, this is an acceptable value.

TABLE 4-3 (SHEET 1)

FINE & COARSE AGGREGATES TESTED IN ACCORDANCE WITH ASTM C-33

Read Table Down For Each Job (ASTM Req't at Right)		AVERAGE OF USER TESTS SUBMITTED BY EACH JOB FROM TESTS RUN ON THE SITE BY AN INDEPENDENT TESTING LAB WITH THE EXCEPTION OF THE PETROGRAPHIC TESTS. PETROGRAPHIC TESTS RUN BY BECHTEL CORPORATION'S GEOLOGY DEPARTMENT.					
TEST	ASTM TEST DESIGNATION	TURKEY PT. #5610	CONTAINMENT A	CONTAINMENT B	CONTAINMENT C	CONTAINMENT D	REQ'T. BY ASTM C-33
Los Angeles Abrasion	C-131	36.8%	42.8%	34.8%	32.8%	36.0%	Max. Loss = 50%
Clay Lumps Natural Aggregate	C-142	Fine Agg. - None Coarse Agg. "	Fine Agg. - None Coarse Agg. "	Fine Agg. - None Coarse Agg. "	Fine Agg. - None Coarse Agg. "	Fine Agg. - None Coarse Agg. "	Max. Friable Particles Fine Agg: 1% by WT. Coarse Agg: .25% by WT.
Material Finer than #200 Sieve	C-117	Fine Agg. 2.5% 3/4" Coarse Agg. 1.5%	Fine Agg. 2% 3/4" Coarse Agg. 1.1% 1½" " " 1.0%	Fine Agg. 5.9% 3/4" Coarse Agg. 0.6% 1½" " " 0.1%	Fine Agg. No Data 3/4" Coarse Agg. No Data 1½" Coarse Agg. No Data	Fine Agg. 0.4% 3/4" Coarse Agg. 0.5% 1½" " " 0.6%	Fine Agg: 3-5% Max. MFG Fine Agg: 5-7% Max. Coarse Agg: 1% Max. Crushed Coarse Agg: 1.5% Max.
Mortar Making Properties	C-87	Satisfactory	Satisfactory	Satisfactory	Satisfactory	Satisfactory	Not less than 95%
Organic Impurities	C-40	Lighter than STD.	Lighter than STD.	Lighter than STD.	Lighter than STD.	Lighter than STD.	Darker than STD.
Potential Reactivity (Chemical)	C-289	F.&C. Agg. - Innocuous	F.&C. Agg. - Innocuous	F.&C. Agg. - Innocuous	F.&C. Agg. - Innocuous	F.&C. Agg. - Innocuous	Reactive when S_c-R_c Plot falls to RT of Curve.
Sieve Analysis	C-136	F.&C. Agg. Sieve Anal - OK Fine Agg. F.M. = 2.51 3/4" Agg. F.M. = 6.8	F.&C. Sieve Anal - OK Fine Agg. F.M. = 2.51 3/4" Agg. F.M. = 7.26 1½" Agg. F.M. = 7.76	F.&C. Sieve Anal - OK Fine Agg. F.M. = 2.69 3/4" Agg. F.M. = 6.95 1½" Agg. F.M. = 7.86	F.&C. Sieve Anal - OK Fine Agg. F.M. = 2.68 3/4" Agg. F.M. = 6.44 1½" Agg. F.M. = 7.93	F.&C. Sieve Anal - OK Fine Agg. F.M. = 2.91 3/4" Agg. F.M. = 6.46 1½" Agg. F.M. = 7.96	As listed in tables for F&C Agg.
Soundness	C-88	F. Agg. 8% C. Agg. 8%	F. Agg. 6.4% C. Agg. 6.4%	F. Agg. 6.7% C. Agg. 6.7%	F. Agg. 3.9% C. Agg. 3.9%	F. Agg. 4.5% C. Agg. 4.5%	F. Agg. - Sodium Sul. - 10% Max. C. " - " " 12% "
Specific Gravity and Absorption for Coarse Aggregate	C-127	3/4" Agg. S.G.=2.44 " " ABS=3.4%	3/4" Agg. S.G.=2.72 " " ABS=1.5% 1½" Agg. S.G.=2.76 " " ABS=0.9%	3/4" Agg. S.G.=2.82 " " ABS=0.33% 1½" Agg. S.G.=2.82 " " ABS=0.31%	3/4" Agg. S.G.=2.88 " " ABS=0.4% 1½" Agg. S.G.=2.88 " " ABS=0.4%	3/4" Agg. S.G.=2.59 " " ABS=1.6% 1½" Agg. S.F.=2.58 " " ABS=1.6%	Spec. Grav - No Limit. Absorption - " "

TABLE 4-3 (SHEET 2)

FINE & COARSE AGGREGATES TESTED IN ACCORDANCE WITH ASTM C-33

Read Table Down For Each Job (ASTM Req't at Right)		AVERAGE OF USER TESTS SUBMITTED BY EACH JOB FROM TESTS RUN ON THE SITE BY AN INDEPENDENT TESTING LAB WITH THE EXCEPTION OF THE PETROGRAPHIC TESTS. PETROGRAPHIC TESTS RUN BY BECHTEL CORPORATION'S GEOLOGY DEPARTMENT.					
TEST	ASTM TEST DESIGNATION	TURKEY PT. #5610	CONTAINMENT A	CONTAINMENT B	CONTAINMENT C	CONTAINMENT D	REQ'T. BY ASTM C-33
Specific Gravity and Absorption for Fine Agg.	C-128	S.G. = 2.52 ABS = 3.8%	S.G. = 2.69 ABS = 1.8%	S.G. = 2.83 ABS = 0.5%	S.G. = 2.63 ABS = 0.5%	S.G. = 2.62 ABS = 0.7%	Spec. Grav - No Limit. Absorption - " "
Petrographic Analysis	C-295	Manufactured Fine Aggregate: Calcite - 80% Quartz - 20% Manufactured Coarse Aggregate: Calcite - 67% Quartz - 30% Chalcadony - 3% & Opal	Alluvial Fine Agg: Alluvial Glacial Limestone-100% Manufactured Coarse Agg: Crushed Quarried Dolomite - 100%	Manufactured Fine Aggregate: Crushed Dolomite-100% Manufactured Coarse Aggregate: - same -	Alluvial Fine Agg: Alluvial River Sand Quartz - 50% Feldspar - 35% Muscovite Magnitite Kyanite, Actinolite, 15% Garnet & Expodite Manufactured Coarse Aggregate: Quarried Dolomite-98% Talc, Quartz Magnitite & Hemotite } 2%	Alluvial Fine Agg: Quartz - 86% Sandstone - 5.5% Siltstone - 3.0% Claystone - 5.5% Claystone comprised of Kaolin & Montmorillonite Expanding Clays Alluvial Coarse Agg: - same -	Method Only

TABLE 4-4

WATER ANALYSIS

	AVERAGE VALUE OF TESTS RUN BY INDEPENDENT TESTING LABORATORIES AND SUBMITTED BY EACH JOBSITE (ALL VALUES ARE EXPRESSED IN PPM EXCEPT pH)																					
	Change in Setting Time Compared to Distilled Water		Reduction in Strength Compared to Distilled Water	Fe	Ca	Mg	Na &K	Hardness As $CaCO_3$	Alkalinity as $CaCO_3$		Total Dissolved Solids	CO_3	HCO_3	SO_4	Cl	OH, As $CaCO_3$	CO_3, As $CaCO_3$	HCO_3 As $CaCO_3$	COLOR	Turbidity	pH	CO_2
	Initial	Final							P.	M.O.												
TURKEY POINT #5610				.365*	95.8	2.4*	285*	242	0	189	258	0*	250*	28*	19	0*	0*	205*	0	3	7.23	29*
CONTAINMENT A	7%*	0%*	4.6%* (7 Days)																			
CONTAINMENT B				.64	61.	16.	2.8	220	0	184	230	0	223	20	16		0	223			7.05	32
CONTAINMENT C								14*		31*	64*				4.5*							
CONTAINMENT D	-	-	5%* (28 Days)								120*									*	7.78*	

* Result of 1 Test

TABLE 4-5

ICE ANALYSIS

	AVERAGE VALUE OF TESTS RUN BY INDEPENDENT TESTING LABORATORIES AND SUBMITTED BY EACH JOBSITE (ALL VALUES ARE EXPRESSED IN PPM EXCEPT pH)																					
	Change in Setting Time Compared to Distilled Water		Reduction in Strength Compared to Distilled Water	Fe	Ca	Mg	Na &K	Hardness As $CaCO_3$	Alkalinity as $CaCO_3$		Total Dissolved Solids	CO_3	HCO_3	SO_4	Cl	OH, As $CaCO_3$	CO_3, As $CaCO_3$	HCO_3 As $CaCO_3$	COLOR	Turbidity	pH	CO_2
	Initial	Final							P.	M.O.												
TURKEY PT. #5610				.01*	7*	0*	4.2*	20*	0	35	83	0*	24*	0*	9	0*	0*	20*	2*	2.3	7.42	4.3*
CONTAINMENT A																						
CONTAINMENT B																						
CONTAINMENT C				0.27*	2.8*	0.8*		5		10.7	30				1.5*						7.4*	
CONTAINMENT D	+8%*	+9%*	4%* (7 Days)								72										7.2	

* Result of 1 Test

TABLE 4-6

AIR ENTRAINING AGENT

JOB	BRAND NAME - SUPPLIER	Supplied in Accordance with ASTM Specification
TURKEY PT. #5610	"AIRECON" - UNION CARBIDE	C-260
Containment A	"SIKA AIR" - SIKA CHEMICAL CO.	C-260
Containment B	"M.B.V.R." - MASTER BUILDERS	C-260
Containment C	"SIKA AIR" - SIKA CHEMICAL CO.	C-260
Containment D	"AIRECON" - UNION CARBIDE	C-260

TABLE 4-7

WATER REDUCING AGENT

JOB	BRAND NAME - SUPPLIER	Supplied in Accordance with ASTM Specification
TURKEY PT. #5610	"RETARDWELL" - UNION CARBIDE	C-494 TYPE D
Containment A	"PLASTIMENT" - SIKA CHEMICAL CO.	C-494 TYPE D
Containment B	"POZZOLITH 8" IMPROVED - MASTER BUILDERS	C-494 TYPE D
Containment C	"PLASTIMENT" - SIKA CHEMICAL CO.	C-494 TYPE D
Containment D	"RETARDWELL" - UNION CARBIDE	C-494 TYPE D

TABLE 4-8
CONCRETE PHYSICAL CHARACTERISTICS

	Turkey Point*	Containment A	Containment B	Containment C	Containment D	Remarks
Comp. Strength psi	*Mix 2P5					
28D	7780	5900	7240	5617	6420	
180D	7760	8000	8620	7925		70°
365D	6790	-	8720	7810		
†Splitting Tensile & Comp. psi	Comp. Tensile	Comp. Tensile	Comp. Tensile	Comp. Tensile	Comp. Tensile	†28 day test in accordance with ASTM 39 & 496
	6340 473	7040 585	5980 555	6100 580	5670 560	
	6050 390	6370 560	6140 525	5980 563	5450 560	
	5980 359	6170 515	5910 520	6150 -	- 485	
Elastic & Creep Strain x 10^{+6} in/in						
1D	272	277	175	245	336	
180D	388	372	224	332	(Load applied	
14600D	543	387	280	405	at 28 days)	Reference to application of load at 180 days, 70° except as noted
Poisson Ratio	0.24	0.25	0.26	0.27	0.18 (28 days)	
"E" x 10^{-6} psi						
Inst. 1D	6.2	6.4	8.9	7.32		
Sust. 180D	3.9	4.1	6.7	4.52		
Sust. 14600D	2.8	3.2	5.4	3.70		
Auto. Vol. x10^{+6}						
180D	-2	-15	-17	-120	-2	@70°F
365D	-4	-23	-32	-145	-	
Therm. Exp.x10^{+6} in/in per °F	5.1	6.3	6.9	6.8	7.4	------
Spec. Heat BTU/"°F	0.268	No Data	0.257	No Data		------
Diff. Ft. ^{2}/hr	0.0340	0.048	0.0513	0.0395	.067	
"E" x 10^{-6} Static psi						Reference to application of load at 180 days, 70° except as noted
1D		4.2	7.3	5.5	4.9	
180D	4.6	6.6	8.3	5.8	(Load applied	
14600D			8.8	6.5	at 28 days)	

TABLE 4-9

COMPRESSIVE STRENGTH (UNIAXIAL COMPRESSION)

	Avg. 28 Day Comp. Strength For Test Cylinders From Dome Concrete (psi)	Comp. Strength For Cylinders Cored From Dome Concrete-40 hr. Water Cure Prior To Testing (psi)	Comp. Strength For Cylinders Cored From Dome Concrete-Tested In A Dry State (psi)
	ASTM C-39	ASTM C-42	-
Turkey Point (Unit 3)	6724 (24 Tests)	6020 6270 } Ave. 9 Mos. old 4910 5570 5280 5840 AVG. = 5648	6810 } Ave. 9 Mos. old 6710 AVG.=6760
Containment A	#1 6968 (28 Tests) #2 7137 (32 Tests)		
Containment B	5510 (28 Tests)		
Containment C	#1 5493 (36 Tests)		
Containment D	6155 (7Tests) From wall; dome not poured		

TABLE 4-10

TENSILE STRENGTH (SPLIT CYLINDER TEST)

	Tensile Strength Of Cylinders Cored From Dome Concrete (psi)	Tensile Strength Of Test Cylinders Made From Same Mix As Dome Concrete (psi)
	ASTM C-496	ASTM C-496
Turkey Point (Unit 3)	743-W (7 mo.old) 740-W (10 mo. old) 753-W (12 mo. old) 652-D (9 mos. old) 719-D (9 mos. old) 562-D (9 mos. old) Avg. = 745 - W Avg. = 644 - D	390-W (20 days old) 360-W (20 days old) 746-W (28 days old) 473-W (73 days old) 785-D (28 days old) Avg. = 492 - W Avg. = 785 - D
Containment A		585-W, 615-W) 560-W, 620-W) 515-W, 595-W) Avg. = 580 - W all 28 days old
Containment B		575-W) 590-W) all 28 610-W) days old 590-W) Avg. = 590 - W
Containment C		580-W) 563-W) all 28 347-W) days old 345-W) Avg. = 459 - W
Containment D		560) 560) all 28 days 485) old Avg. = 535 - W

W = Tested Wet
D = Tested Dry

TABLE 4-11

TENSILE STRENGTH (UNIAXIAL TENSION TEST)

Job	Source	Cylinder Number	Tensile Strength (psi)	Maximum Tensile Strain ($x10^{-6}$ in/in	Age	Remarks
Turkey Point	Test made on 2"x6" cylinders cored from 6x12 std. test cylinders made on jobsite with same design mix as in dome.	1185-2	329		31 Days	About 80% of aggregate broke through; 20% pulled off
		1185-1	347		31	About 50% of aggregate broke through; 50% pulled off
		1177-2	241		38	About 75% of aggregate broke through; 25% pulled off
		1177-1	394		38	About 100% of aggregate broke through
		1183-2	341		33	About 90-95% of aggregate broke through; 5-10% pulled off
		1183-1	392	112.5@ 371psi	33	About 90-95% of aggregate broke through; 5-10% pulled off
		1186-2	368	102.5@ 340psi	31	About 90-95% of aggregate broke through; 5-10% pulled off
		1186-1	405	112.5@ 402psi	31	About 90-95% of aggregate broke through; 5-10% pulled off
			AVG.=352			

TABLE 4-12

UNIAXIAL TENSION TESTS

Project	Age days	σ_z - Stress psi		ε_z - Strain μ in/in*		ε_ϕ - Strain μ in/in*	
Turkey Point 6" x 12" Cyl.	28	+405)		+105)		-20)	
	28	+370)	+392+	+110)	+108	-20)	-22
	28	+400)		+110)		-25)	
Turkey Point NX core-From Dome Concrete	11 mo	+330)		+80)		-22)	
	11 mo	+365)	+347	+105)	+93	-25)	-24
Containment A 6" x 12"	42	+490)		+90)		-20)	
	21	+420)	+455	+125)	+ 108	-16)	-18
Containment B							
Containment C 6" x 12"	80	+404)		+70)		-15)	
	75	+410)	+408	+75)	+72	-16)	-16
	73	+415)		+72)		-16)	
Containment D 6" x 12"	28	+340)		+76)		-08)	
	28	+300)	+321	+64)	+69	-08)	-9
	28	+324)		+66)		-12)	

* Smallest strain at ultimate load. Some specimens continued to strain while maximum load was held.

\+ Average

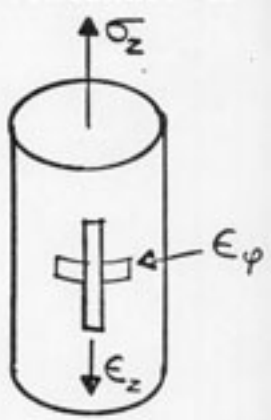

TABLE 4-13

UNIAXIAL COMPRESSION TESTS

Project	Age days	σ_z-Stress psi	ε_z-Strain μ in/in	ε_ϕ-Strain μ in/in
Turkey Point 6" x 12" cyl.	28 28	-5500 -6030	-2700 -2650	+450 @ 5000 psi +400 @ 5000 psi
Containment A 6" x 12"	21 21	-6700 -7000	-2000 -2000	+350 @ 6000 psi +475 @ 6000 psi
Containment B 6" x 12"				
Containment C 6" x 12"	61 56	-7050 -6600	-1850 -1850	+550 @ 6000 psi +400 @ 6000 psi
Containment D 6" x 12"	48 48	-6550 -6800	-1850 -1750	+550 @ 6000 psi +400 @ 6000 psi

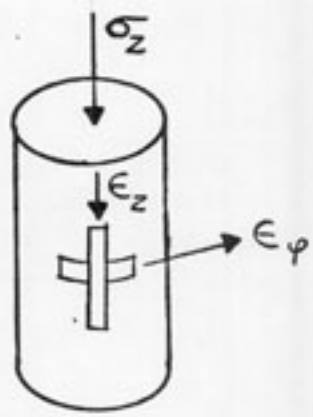

TABLE 4-14

BIAXIAL COMPRESSION TESTS

Project	Age days	σ_r-Stress psi	ε_z-Strain μ in/in	ε_ϕ-Strain μ in/in	Remarks
Turkey Point 6" x 12" cyl.	26	-6000	+545	-	Indicative of ultimate biaxial concrete stress
	25	-5300	+300	-	Possible failure due to hydraulic fluid in void
	25	-4700	-	-	Cracked near end due to failure of membrane
Turkey Point NX core From Dome Concrete	11 mo	-4700	-	-	Tensile break, possible fluid penetration
	11 mo	-6000	+1200	-	Good failure of concrete
Containment A 6" x 12"	45	-4600	+700	-	No failure No cracks
	28	-7500	+1200	-	No failure No cracks
Containment D 6" x 12"	40	-5550	+530	-1030	Membrane failure caused crack in concrete

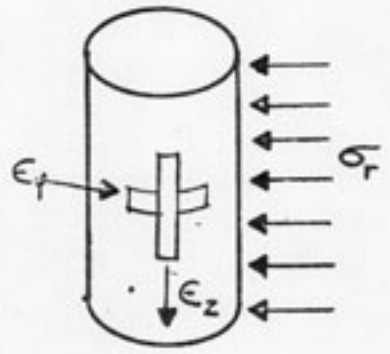

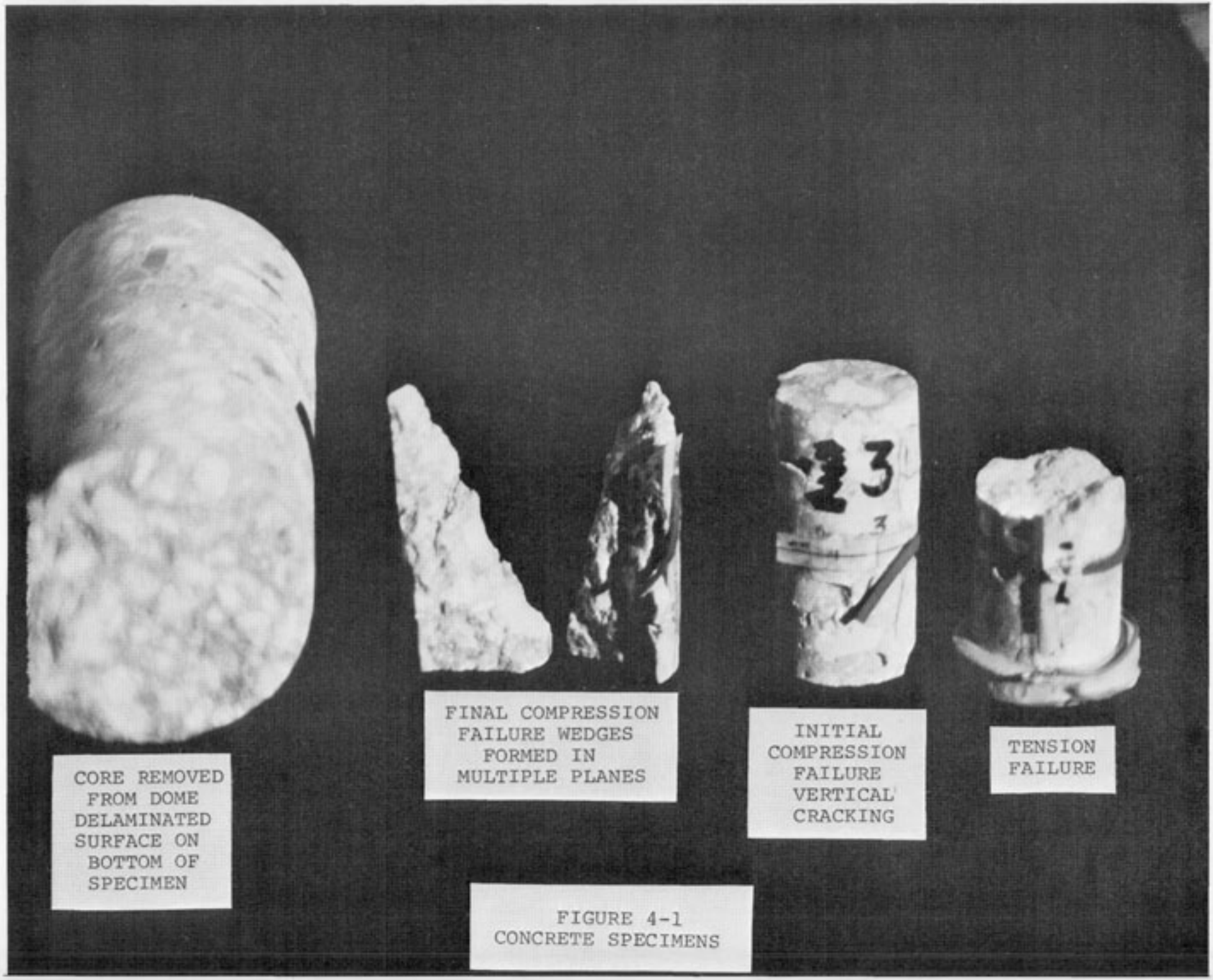

FIGURE 4-1
CONCRETE SPECIMENS

5.0 ANALYTICAL INVESTIGATION

In order to determine why the containment structure dome delaminated various analyses were performed. These analyses covered all the known items which could have caused the delaminations or been a contributing factor.

5.1 CRANE LOADING

A 50 ton Bay City truck crane was set up at the apex of the dome 1 month after completion of concrete placement and 4 months before the start of post-tensioning, for handling tendons and tendon installation equipment. The crane location is shown in Figure 5-1.

The crane loads were resisted by the outriggers. The dead load for a single outrigger is 13K. Considering the rated 5.5K lifted load at a radius of 70 ft. an outrigger downward load of 17.5K results. The dead load, together with a 50% impact factor on the lifted load, yields a maximum downward load of 39K. "Local Stresses In Spherical Shells From Radial Or Moment Loadings" by Bijlaard, Welding Research Council Bulletin No. 34 was used to estimate the stresses from the 39K concentrated load. In the analysis the shell was assumed to be 31" thick with the initial 8" pour neglected. A dome radius of 89' and a 2' diameter loading area was also assumed.

The predicted stresses are as follows:

Maximum Meridional Flexure:	± 86 psi
Maximum Hoop Flexure:	± 26 psi
Maximum Meridional Membrane:	- 11 psi

Due to the low magnitude of the calculated stresses the crane is not considered a significant contributor to delamination causes.

5.2 TEMPERATURE AND MOISTURE

An assumed worst temperature gradient (for compression on the outer surface) is shown in Figure 5-2.

Using the following formula the peak compressive stress on the outside face is predicted to be:

$$\sigma = \frac{\Delta T \sigma E}{1-\nu} = \frac{36(5.\times10^{-6})\ (4.5\times10^{+6})}{(1-.25)} = -1080 \text{ psi}$$

The stress distribution will be similar to the temperature gradient plot with a tendency to reduce to very small values within 4" from the surface.

To simulate a condition of wetting for a prolonged period of time, the following tests were performed. Four concrete specimens, approximately 10" x 10" x 4", removed from the dome were soaked in water. Using a Whittemore strain gage, 3 of the specimens were found to expand to a strain of 167 μ in/in after 14 hours of soaking. After 40 hours of soaking the specimens remained constant with an accumulated strain of 233 μ in/in. One of the 4 specimens had very little change in dimensions. Converting the strain to stress yields

$$\sigma = \frac{\varepsilon E}{(1-\nu)} = \frac{(233\times10^{-6})\ (4.5\times10^{6})}{.75} = -1400 \text{ psi}$$

if the specimen would have been fully restrained.

The stresses from temperature and moisture do not peak simultaneously since one tends to reduce the other. Both are primarily surface effects and they would not cause delaminations 15" in depth. However there is a possibility that these two items could have been a contributor in causing shallow delaminations.

5.3 SHEATHING FILLER PRESSURE

One of two pumps used for sheathing filling had a stall pressure of 250 psi with the other lower. With all vent valves closed the pressure in

the sheaths would not have exceeded 150 psi due to head losses. In a few isolated cases the vent valves were closed, however with only a few tendons affected, this is not of concern. Since the lowest known temperature of the filler during pumping was 90 F, it was assumed that the filler had zero pressure at 85 F. Thermocouple measurements have indicated a temperature of 97 F at an 11" depth when interpolating between the inside and outside readings. Through past testing the filler pressure has been found to rise 8 psi for each 1 F change. Therefore it is possible that a 96 psi pressure could have existed in the sheathing. A finite element analysis was performed subjecting a portion of concrete with a 4" diameter hole 11" deep to a pressure of 100 psi. The analysis indicated that the peak radial stress would be 80 psi at the edge of the hole with the stress rapidly decreasing away from the hole. The radial tension is not high enough to case delaminations and a direct tension load of this kind would not have caused the multiple and shallow delaminations actually found above the sheaths.

5.4 RADIAL TENSION CAUSED BY PRESTRESSING

Since the tendons are not located on the outside surface, radial tension will exist near the outside face of the concrete. To estimate the magnitude of radial tension the analytical calculations were done in two parts and superimposed. The maximum radial tension should exist near the upper layer of tendons, which are 11" from the outer surface, because this is the maximum thickness of concrete without direct radial compression from the tendons.

The first part of the solution considered the effects of all tendons other than the first layer. Since the prestressing essentially loads the shell with a pressure of 100 psi then the pressure from all tendons other than the first layer will be 5/6 (100) = 83.3 psi. Due to displacement compatibility the following relationship must exist

$$\delta = C \frac{P_1 R^2}{E t_1} = C \frac{P_2 R^2}{E t_2} \quad \text{or} \quad P_1 = \frac{t_1}{t_2} P_2$$

Where P_1 is the tension in the top 11" of concrete, P_2 is the applied pressure, t_1 is the thickness of the top layer and t_2 is the total thickness. Then the radial tension is $P_1 = \frac{11}{39}$ (83.3) = 23.5 psi. A finite element analysis of a small portion of the dome was made to evaluate the local effects of the top layer of tendons. The analysis indicated that the peak radial tension was +68 psi occurring near the edge of the tendon sheathing void. The radial stress reduced greatly a few inches from the hole. Superimposing the two results lead to the radial tension distribution shown in Figure 5-3.

The analysis indicates that radial tension is not a major concern due to the magnitude and distribution. In addition a failure from radial tension should not lead to multiple delaminations close to the surface as were found in the investigation of the structure.

5.5 UNBALANCED LOADS FROM PRESTRESSING

A study was made to determine the force distribution on the dome due to the reported prestressing sequence. Each tendon group was divided into 2 zones giving a total of 6 zones. At various times, such as when 50% of the total tendons were tensioned, each zone was examined to determine the amount of normal pressure from the tensioned tendons within a particular zone. The normal pressures from each zone were then superimposed. Since the normal pressure from all the tendons being tensioned is approximately 100 psi, then the resulting pressure also indicates the percentage complete for a particular area. Figure 5-4 shows the results for 40, 50 and 60% completion of prestressing. When 50% of the total tendons were tensioned, one area had effectively 73.8% of its total load whereas another area only had 28.4%.

In order to determine the effect of these unbalanced loads an analysis was performed for a homogeneous containment structure dome. The analysis did not include the effects of concrete cracking or construction joints. The dome was analyzed for the most severe case when the prestressing was 50%

complete. The triangular areas shown in Figure 5-4 were further subdivided by using one large and three small circular areas as shown in Figure 5.5.

Solutions were obtained by loading a dome at the apex by loads distributed over the same areas as those shown in Figure 5-5. After obtaining this data a final solution was obtained by superimposing the effects of any loaded circular area which appreciably affected the location under consideration. The following table shows the maximum calculated stresses on the outside surface, together with the results of applying 100% of the prestressing load (100 psi pressure) distributed uniformly over the dome surface.

	Calculated Stresses (psi)	
	Unequal 50% Loading	Uniform 100% Loading
Meridional		
Membrane	- 727	-1389
Bending	- 974	- 300
Combined	-1701	-1689
Circumferential		
Membrane	- 876	-1450
Bending	- 660	- 200
Combined	-1536	-1650

As indicated above the bending stresses are great enough, so that when combined with membrane stresses, the combined stresses at 50% loading are slightly higher than the stresses under full uniform loading. These loads are considered to be a contributor.

5.6 CONSTRUCTION JOINTS

In the analysis of why the delaminations occured the construction joints deserved special attention because of the following:

(1) As shown by the coring results, the delaminations reached a maximum depth adjacent to the meridional construction joint.

(2) The delaminations appear to have some degree of symmetry about the meridional construction joint with a tendency to approach the surface as they progress away from this joint.

(3) Sheathing filler is present in the meridional construction joint indicating that separation existed.

To establish a base case for the dome stress distribution and magnitude, due to dome prestressing, a shell computer program was utilized. The program handles axisymmetric loads and uses a classical solution after the shell has been divided into small cone frustums. The results of this analysis for a homogeneous containment structure are given in Figures 5-6 and 5-7. The maximum combined meridional stress was found to be -1689 psi at the outer surface. And the maximum combined circumferential stress was found to be -1650 psi at the outer surface.

To determine the effects of the circumferential construction joints in conjunction with dome prestressing an analysis was performed using the shell program previously described. The construction joints were simulated by hinges. The line of thrust was through the center of the elements and therefore the results do not consider the effects of an eccentric thrust.

Figures 5-8 and 5-9 show the distribution and magnitude of stress at the outside surface. The analysis indicates that this case is even less severe in the meridional direction, than the base case since the stress at the outside surface of the dome is -1620 psi. Due to the assumed hinges the circumferential stress increased considerably at a radius of 42 feet with a magnitude at the outer surface of -2600 psi. This stress increase could have been a local contributor to the delaminations.

As the field investigation progressed more evidence became available that many areas surrounding the meridional construction joint were not

of the quality necessary to resist the applied loads without considerable redistribution of load. Figure 5-10 shows a condition which could have resulted in the formation of delaminations. Since expanded metal was used as a form for the joint, voids or soft spots could have resulted. As the structure was prestressed high compressive stresses would result at localized areas. As shown in Section 4 a high compressive stress will result in a strain failure in a plane parallel to the load. If the joint area was effectively reduced to 1/3 of the dome thickness then the resulting stress would be 4,500 psi, enough to cause failure. Figure 5-11 shows another case which could result in delaminations. In this case, the joint had poor tensile capability due to the lack of bond. When the prestressing loads occurred the joint would rotate due to the unbalanced loading. This condition would force the structure to carry high loads near the upper surface. Again high stresses would result and the strain failure would occur. Eventually equilibrium would be obtained.

Two plexiglass domes were obtained to help visualize the phenomenon of the joint rotation. One of the domes was a hemisphere and the other was a hemisphere cut in half and then taped together so that only shear could be transmitted through the joint. Figures 5-12 and 5-13 show the split plexiglass dome before and after applying a load across the joint. Two plexiglass tabs were mounted normal to the surface, pointing inward, on each side of the simulated joint. The photographs indicate that as the load is applied the joint rotates, opening at the bottom.

An analysis was performed (using the shell program previously described) to simulate the effects of having the membrane force distributed over a small area near the surface with resulting eccentricity. In order to simplify the analysis a hemisphere was used with its equator as the construction joint. The geometry of the shell together with its comparison with the real shell geometry are shown on Figure 5-14. The shell was loaded with 100 psi in the area included by the 52° angle. The results which are also given in Figure 5-14 illustrate that both the

reduce joint area and eccentricity of membrane load leads to large calculated stresses. This analysis illustrates how faulty construction joints lead to stresses high enough to be considered one of the main contributors in causing the delaminations.

An analysis was performed which considered both the effects of the unbalanced loads from post-tensioning together with eccentric thrust at the dome construction joints. The analysis was performed by using a finite element program for non-axisymmetrical structures with non-axisymmetrical loads. The analytical model considered the portion of the dome inside the 42.5' radius circumferential construction joint shown in Figure 2-2. The model considered this joint hinged. The meridional construction joint and the construction joints around the ventilation blockouts were also hinged. A radius of 89' and a thickness of 39" were assumed in the analysis.

In the first part of the analysis the structure was loaded with the unbalanced load resulting when post-tensioning was 50% complete as shown in Figure 5-4. Due to the assumed boundary conditions all the forces at the construction joints acted through the center of the section with no eccentricity. The stresses resulting at the outer surface from this loading condition are shown on Figures 5-15 and 5-16 for the meridional and circumferential directions. The peak meridional stress is - 1420 psi (compression) and the peak circumferential stress is - 1220 psi.

In the second part of the analysis the membrane forces were assumed to have a line of thrust at the top of the circumferential and meridional construction joints. The membrane forces at the joints from the first part of the analysis were multiplied by one-half the dome thickness to

generate moments. The moments were then applied together with the post-tensioning loads. The results of this analysis are given in Figures 5-17 and 5-18 for the meridional and circumferential direction. The peak meridional stresses at the outside surface occur at the circumferential joint with the maximum value being - 2900 psi. The peak circumferential stresses at the outside surface occur at the meridional construction joint with the value being - 2880 psi.

This analysis shows that the unbalanced load from post-tensioning together with rotating construction joints (eccentric thrust) would lead to large predicted stresses. These two items acting in conjunction with each other are considered the major cause for the concrete delaminations.

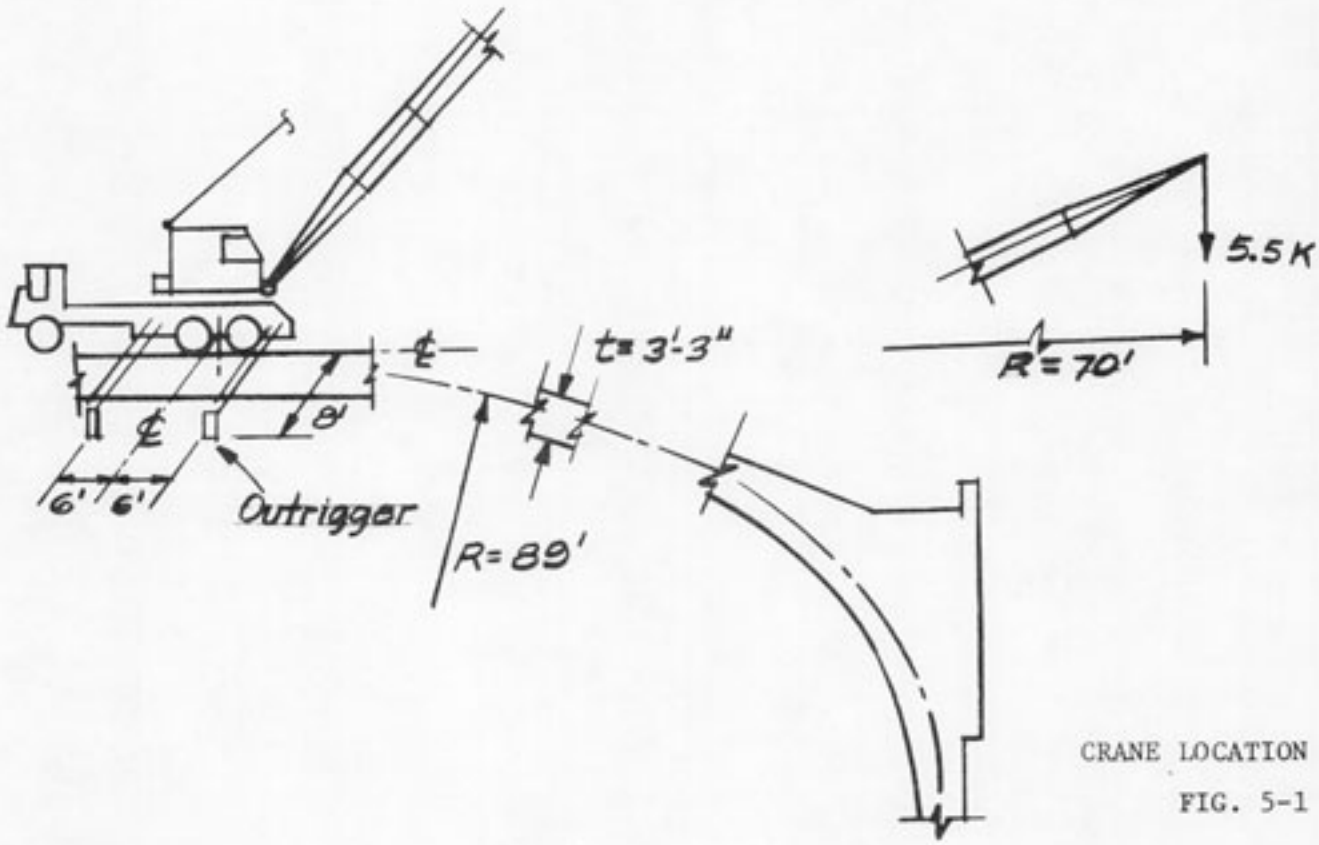

CRANE LOCATION

FIG. 5-1

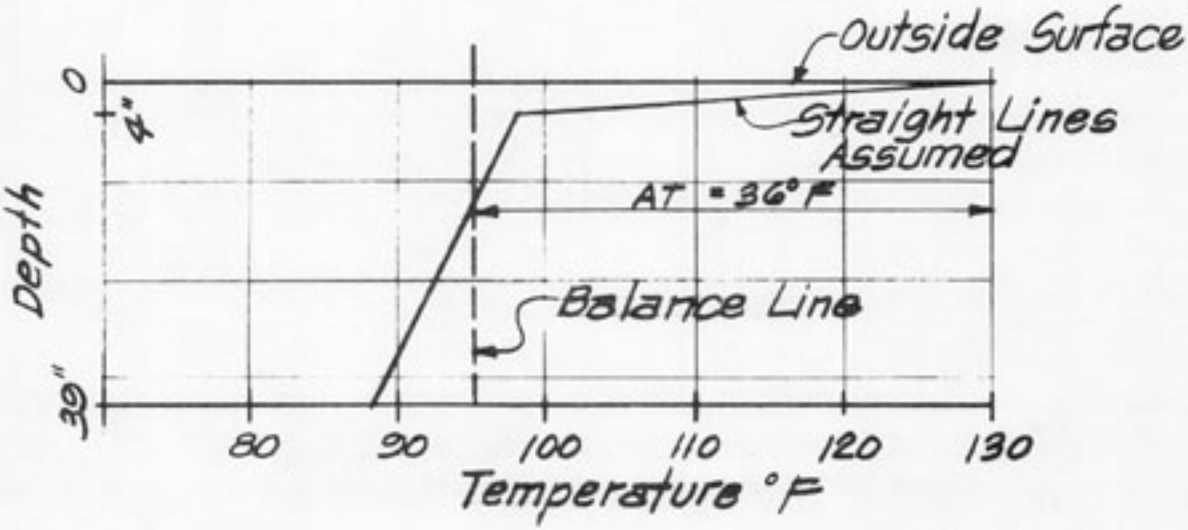

THERMAL GRADIENT

FIG. 5-2

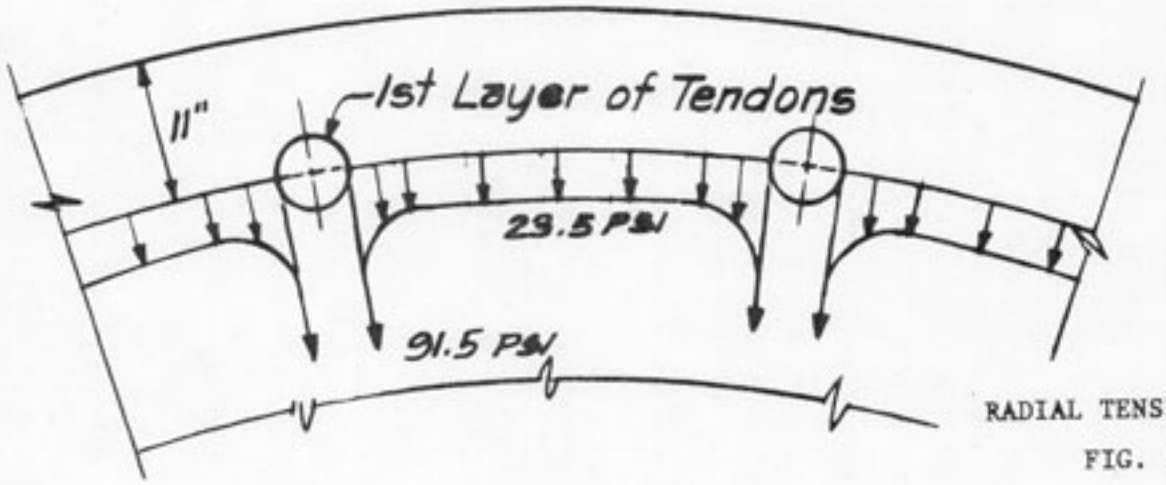

RADIAL TENSION

FIG. 5-3

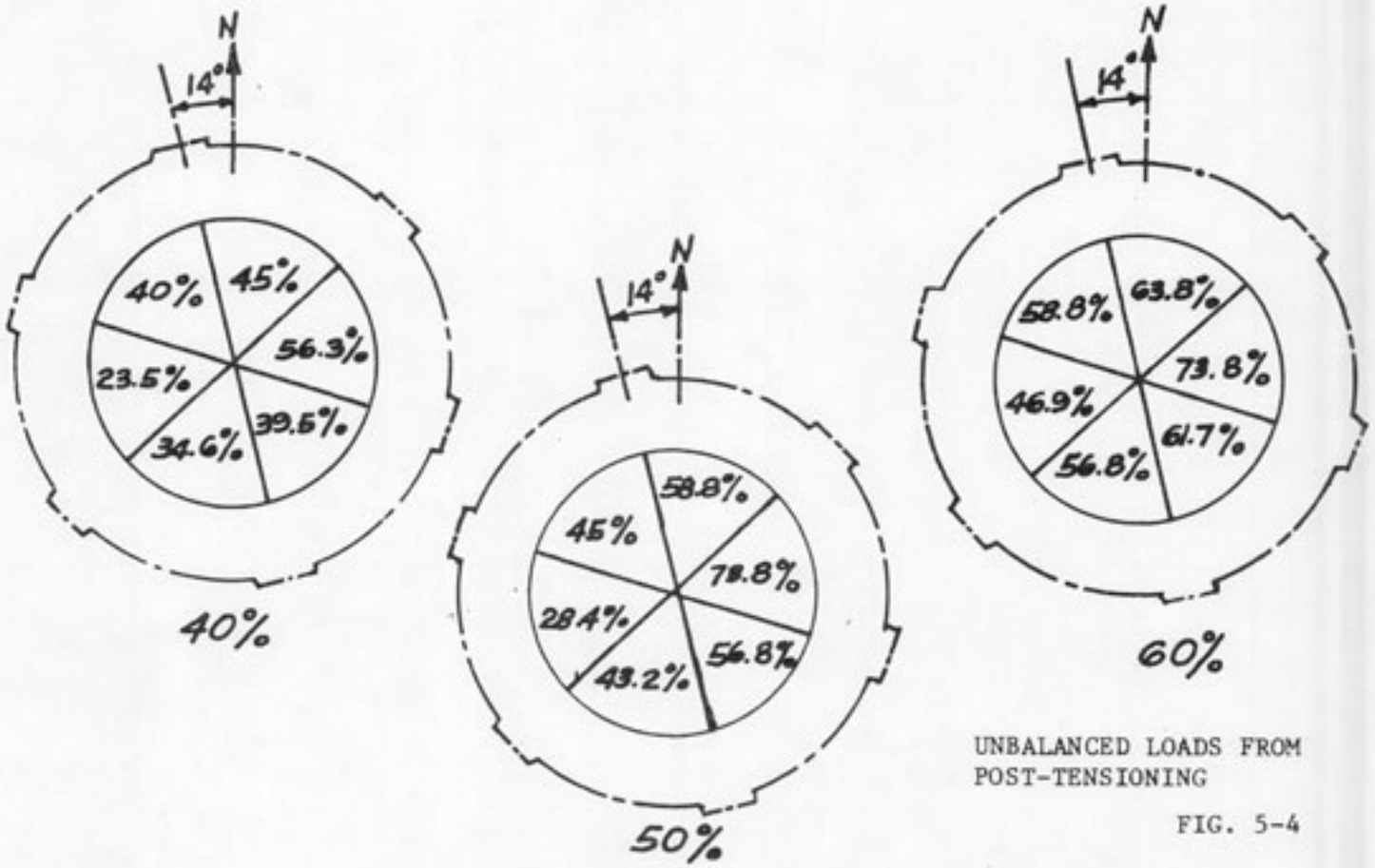

UNBALANCED LOADS FROM POST-TENSIONING

FIG. 5-4

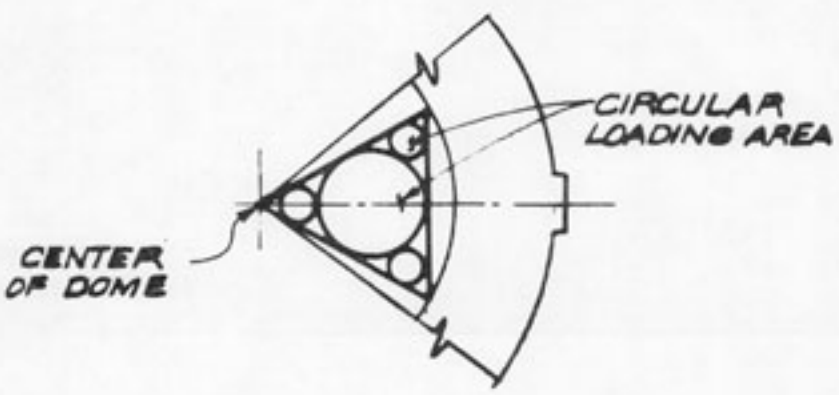

LOADING AREAS

FIG. 5-5

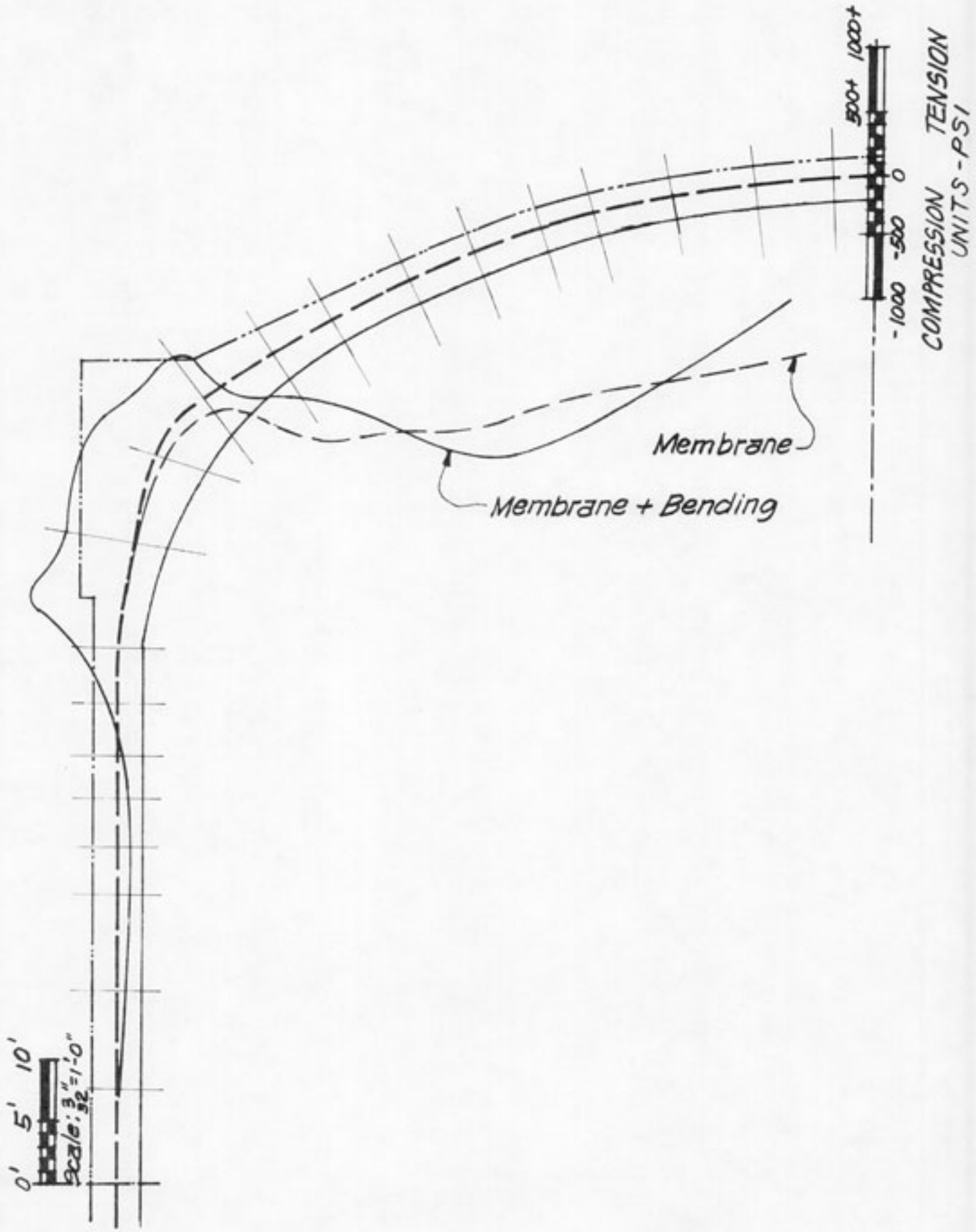

MERIDIONAL STRESS AT THE OUTER
SURFACE FROM DOME POST-TENSIONING

FIG. 5-6

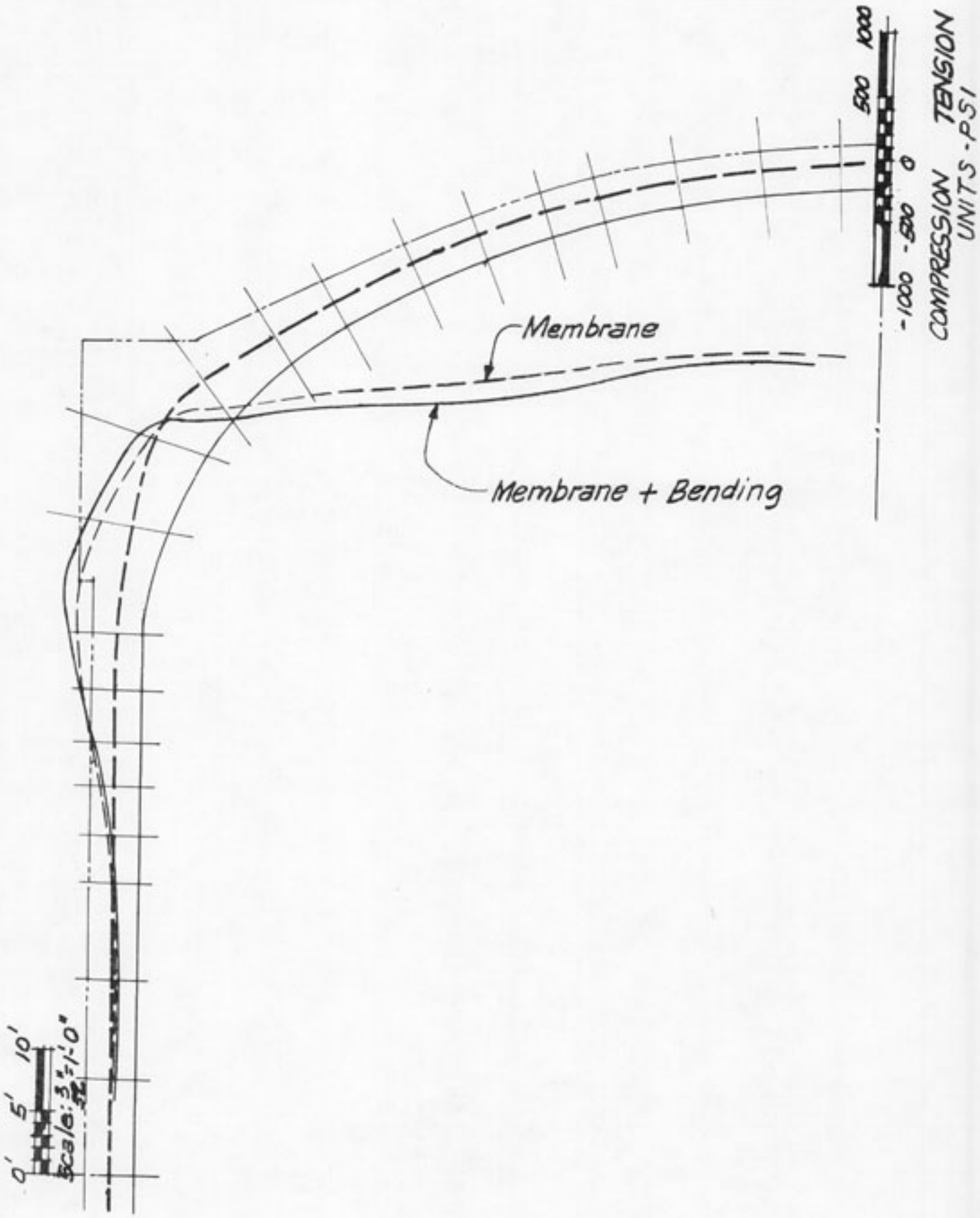

CIRCUMFERENTIAL STRESS AT THE OUTER SURFACE FROM DOME POST-TENSIONING

FIG. 5-7

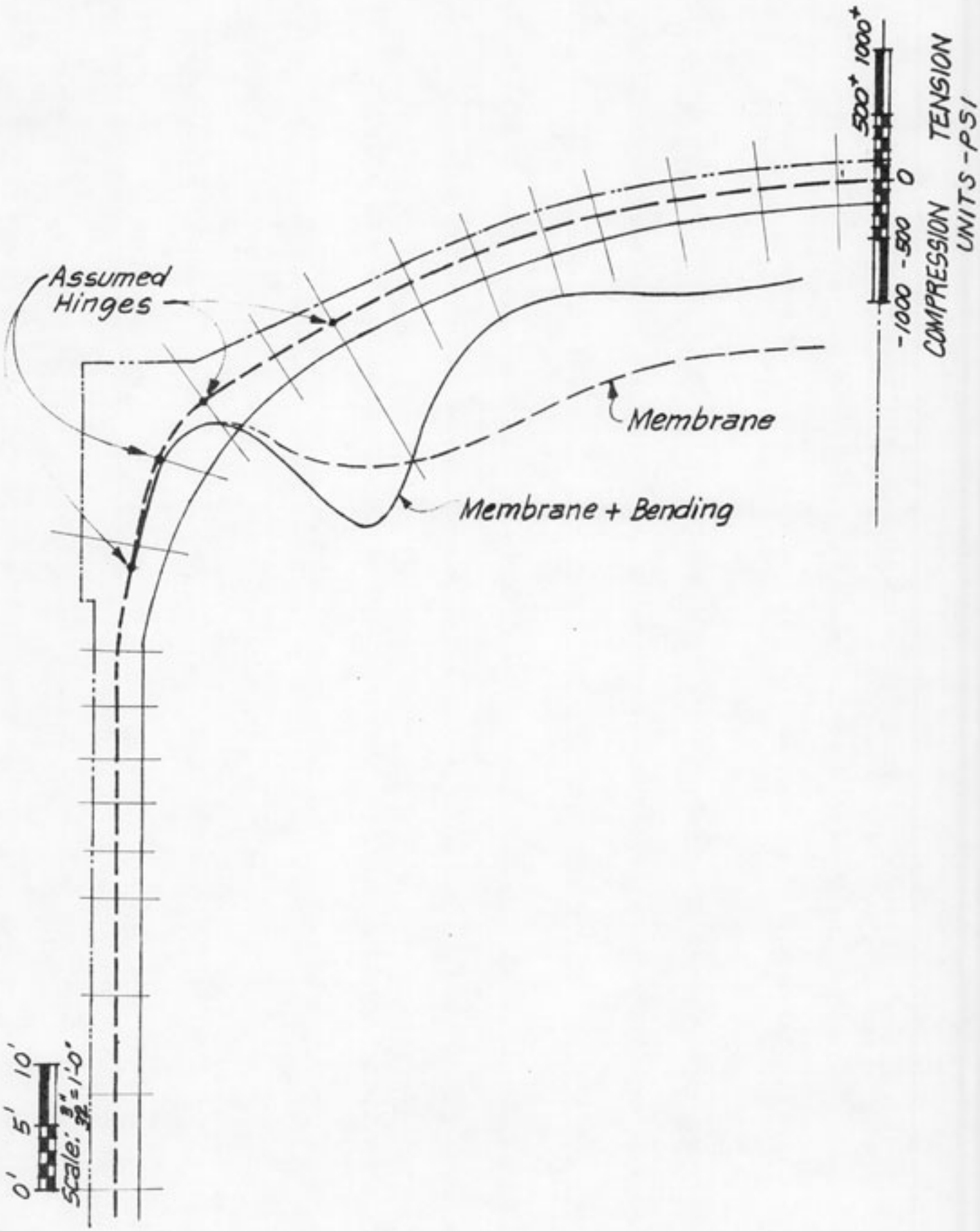

MERIDIONAL STRESS AT THE OUTER SURFACE FROM DOME POST-TENSIONING

FIG. 5-8

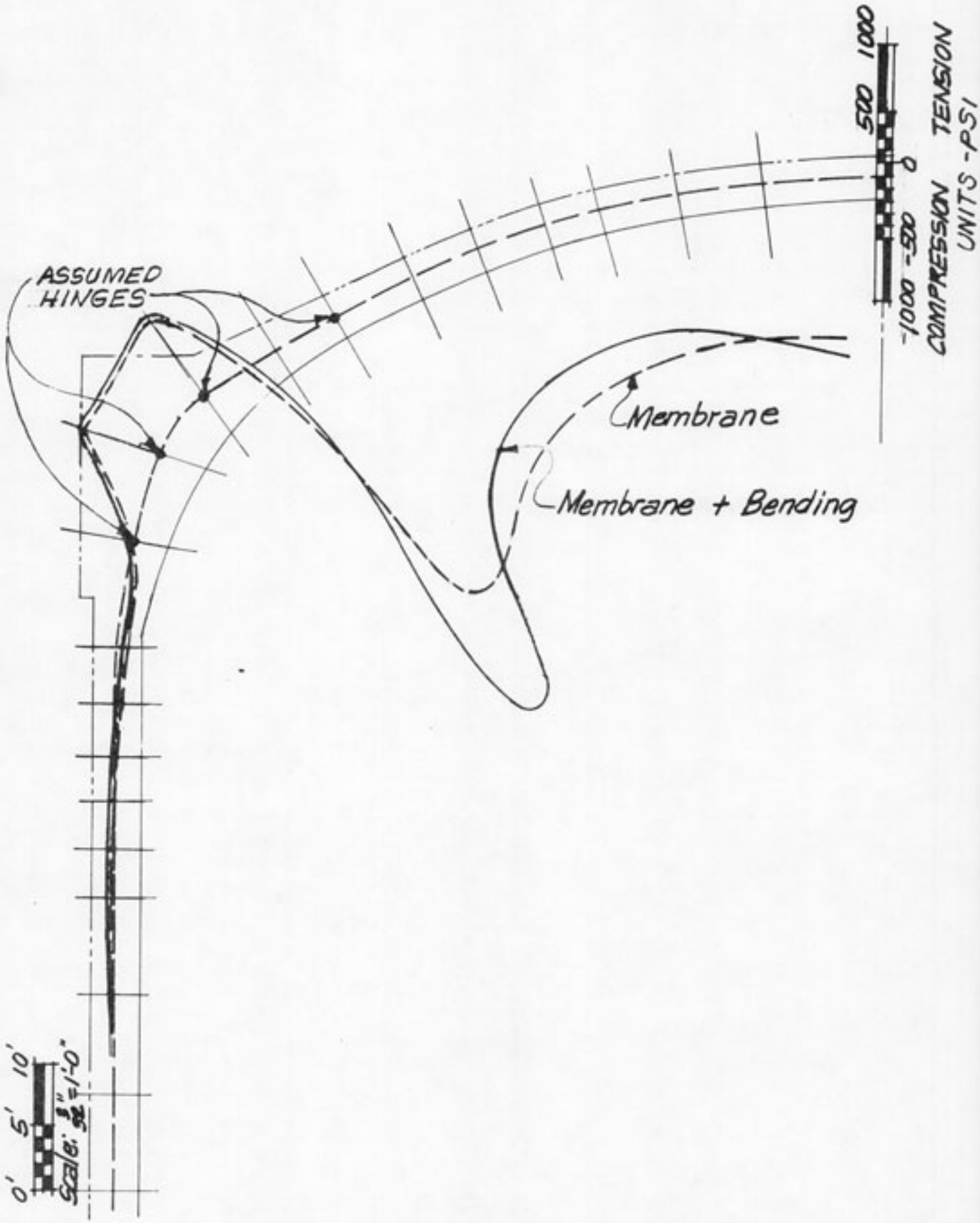

CIRCUMFERENTIAL STRESS AT THE OUTER SURFACE FROM DOME POST-TENSIONING

FIG. 5-9

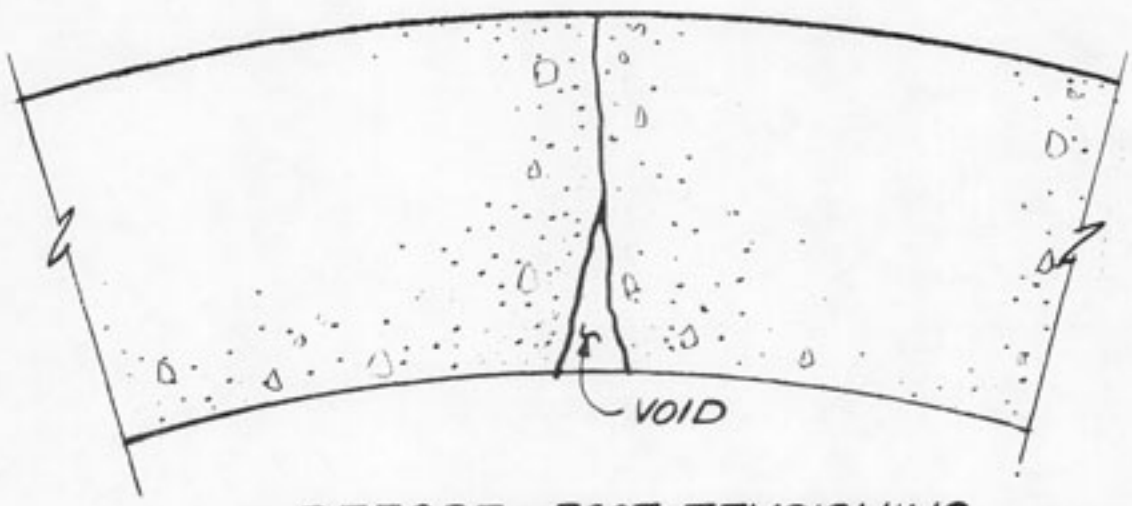

BEFORE POST-TENSIONING

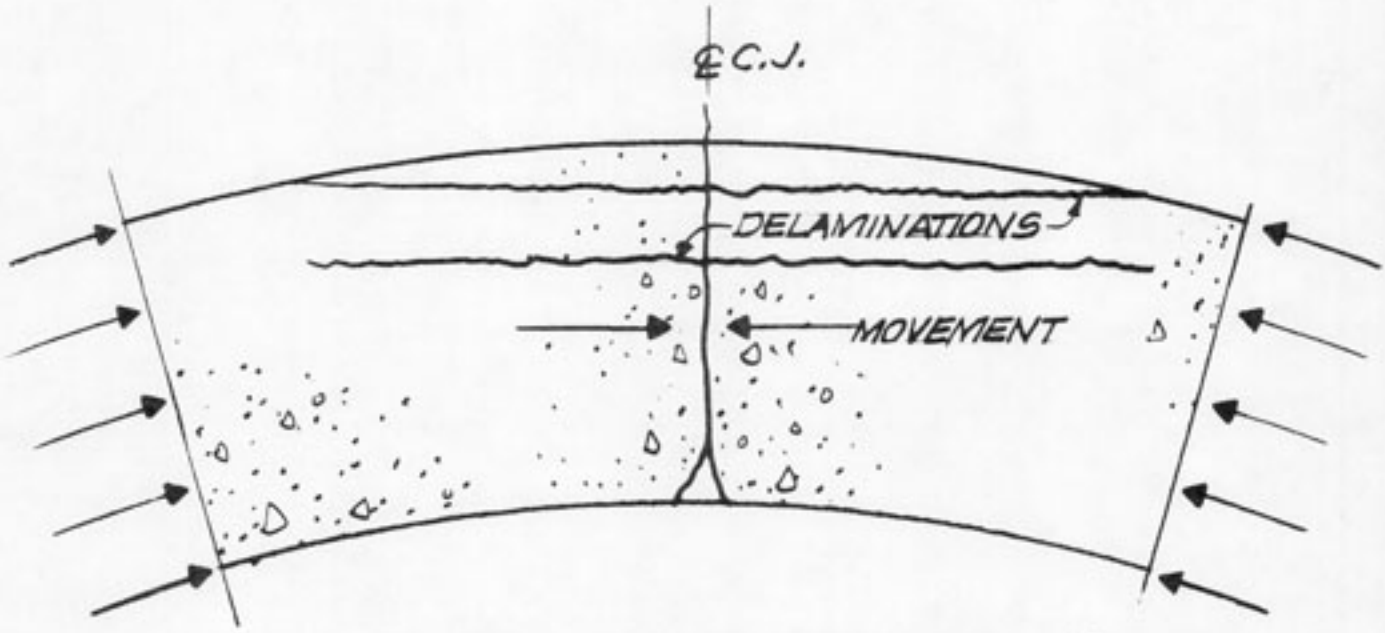

AFTER POST-TENSIONING

NONUNIFORM BEARING CASE 1

FIG. 5-10

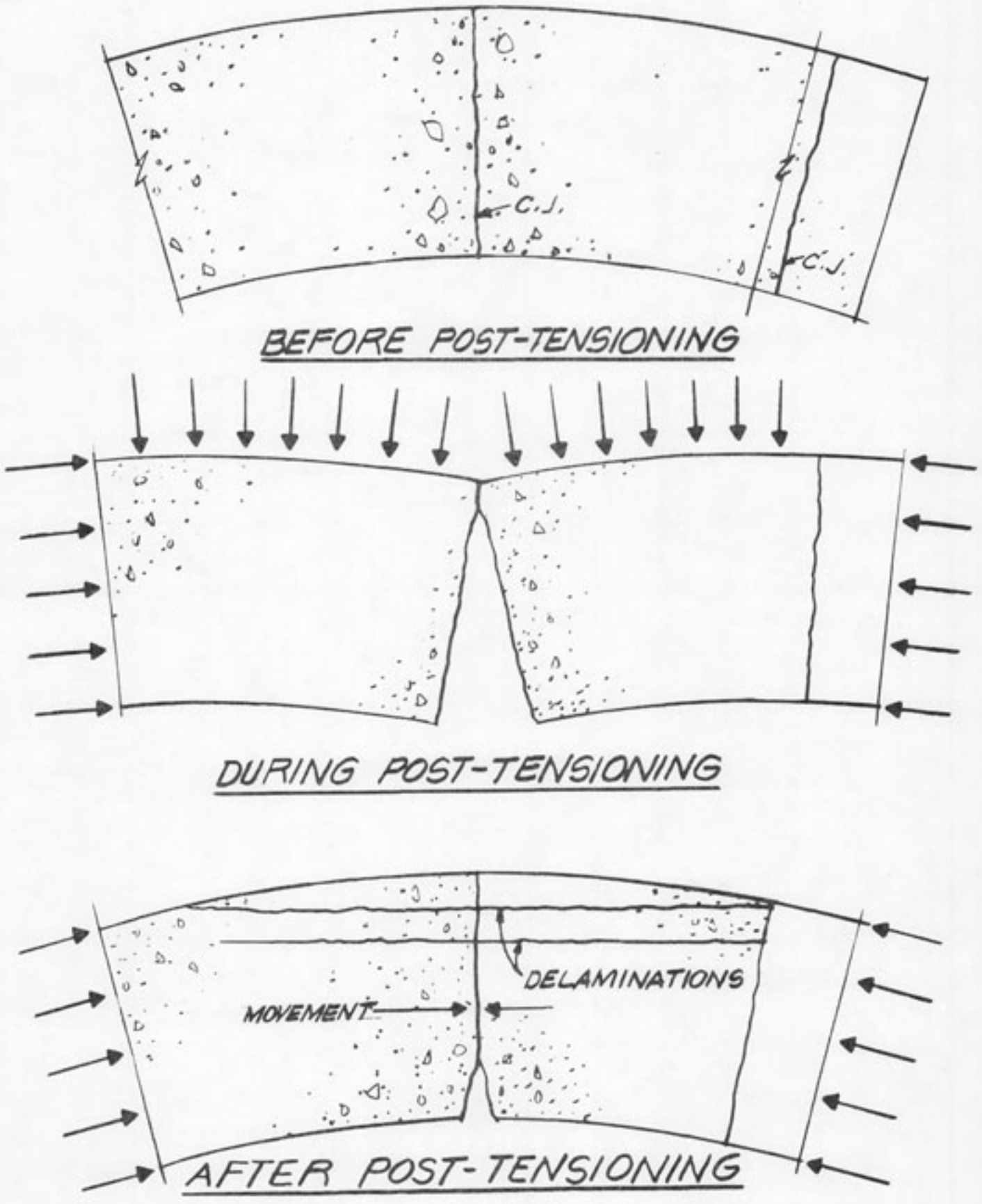

NONUNIFORM BEARING CASE 2

FIG. 5-11

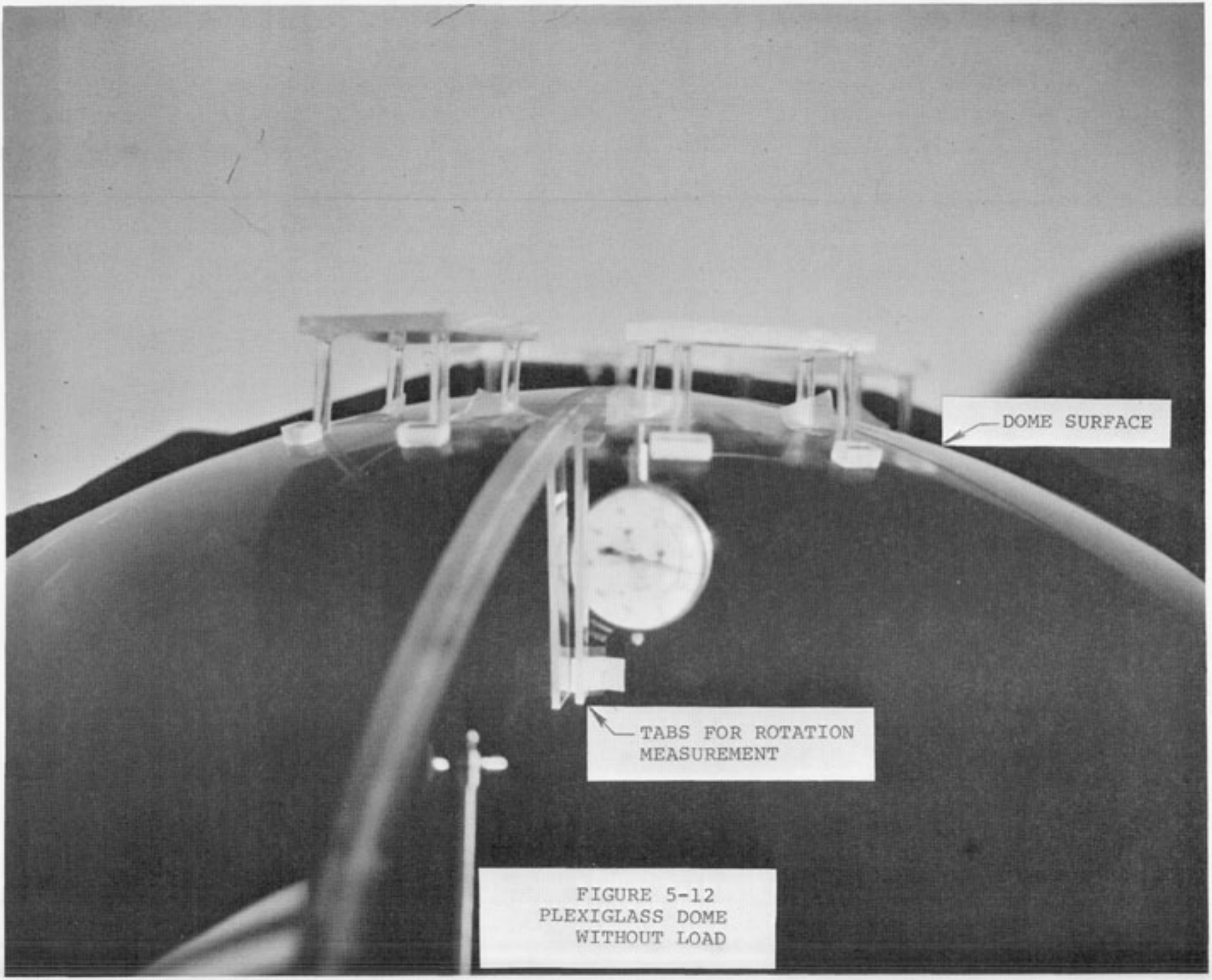

FIGURE 5-12
PLEXIGLASS DOME
WITHOUT LOAD

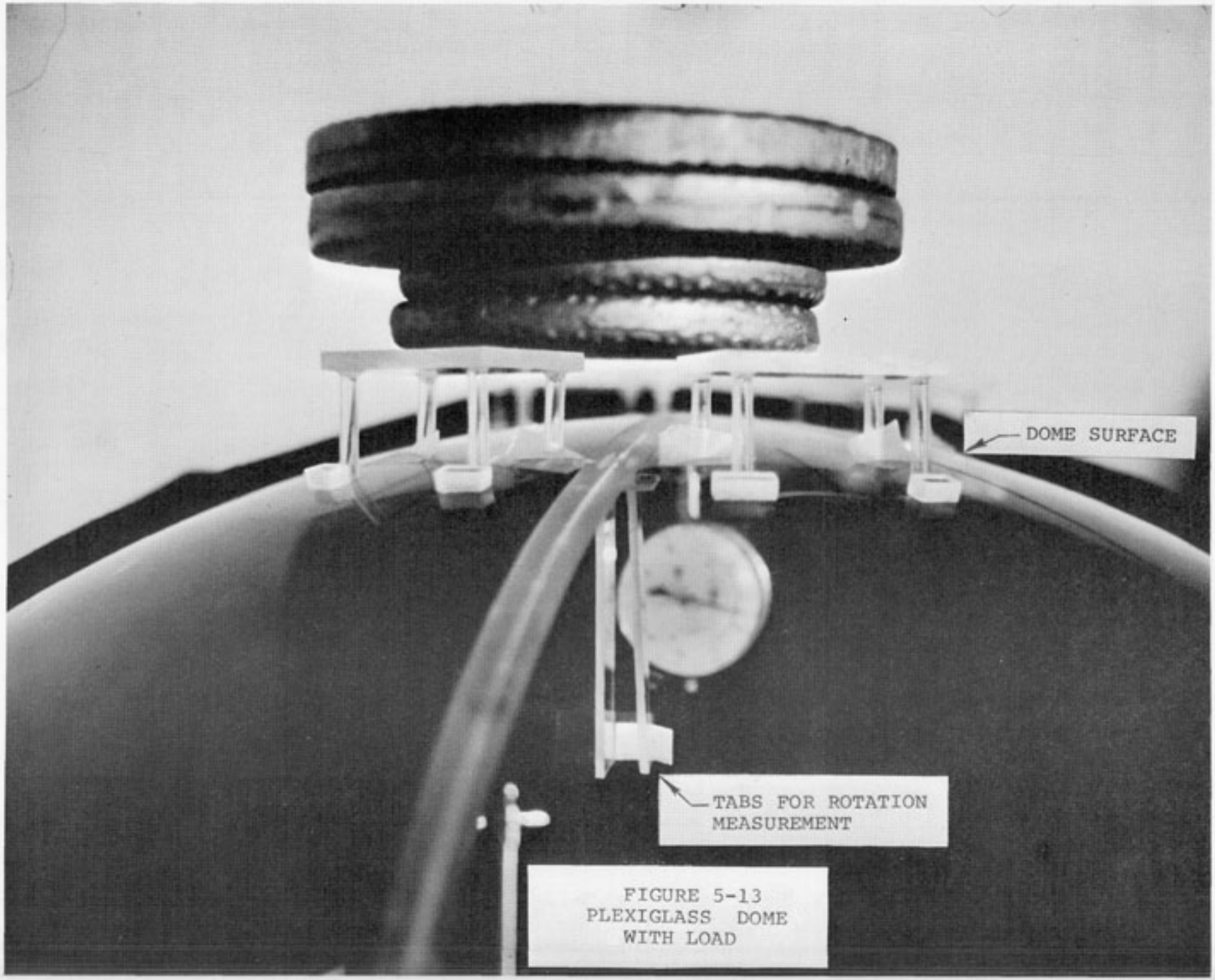

FIGURE 5-13
PLEXIGLASS DOME
WITH LOAD

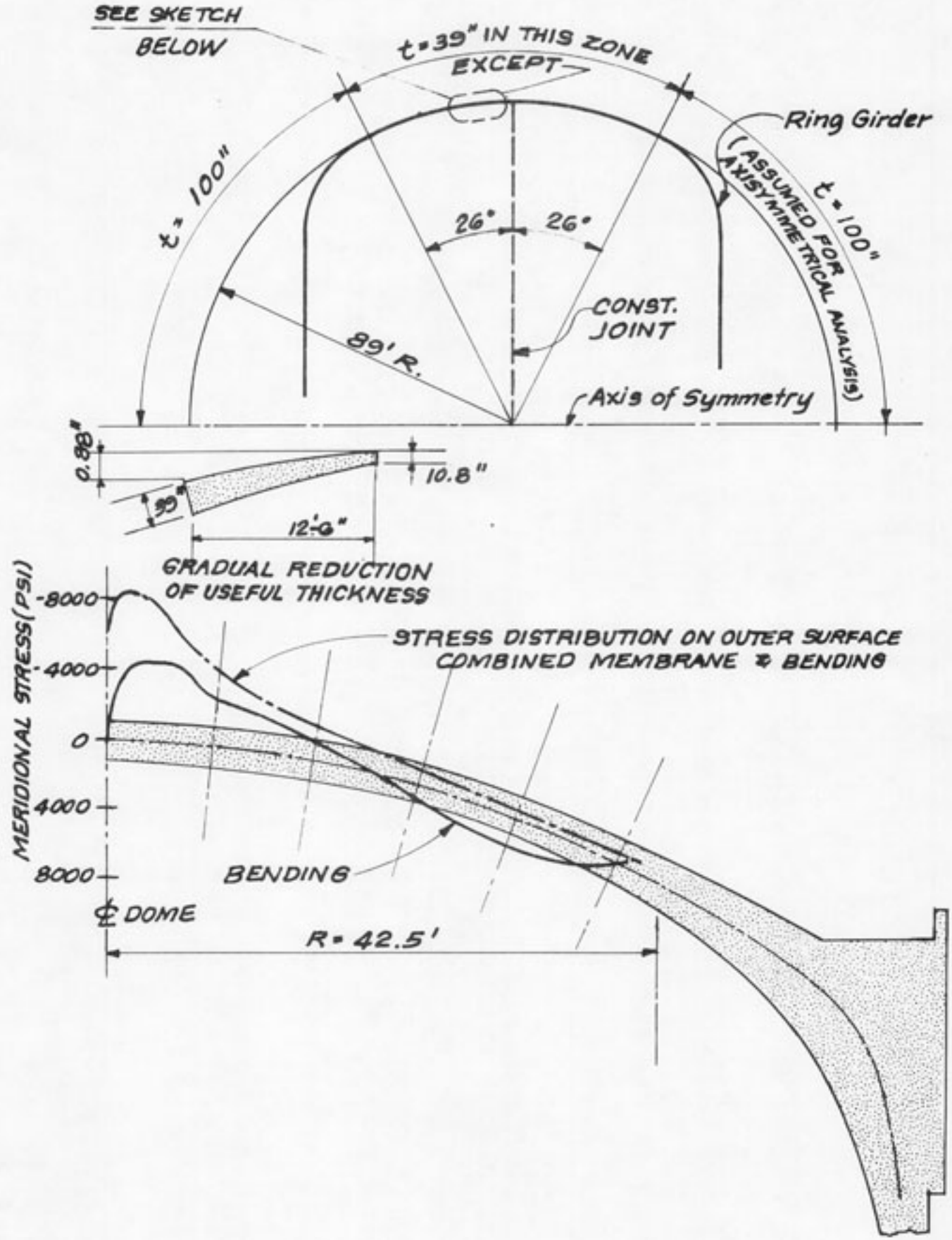

AXISYMMETRICAL SIMULATION OF THE MERIDIONAL CONSTRUCTION JOINT

FIG. 5-14

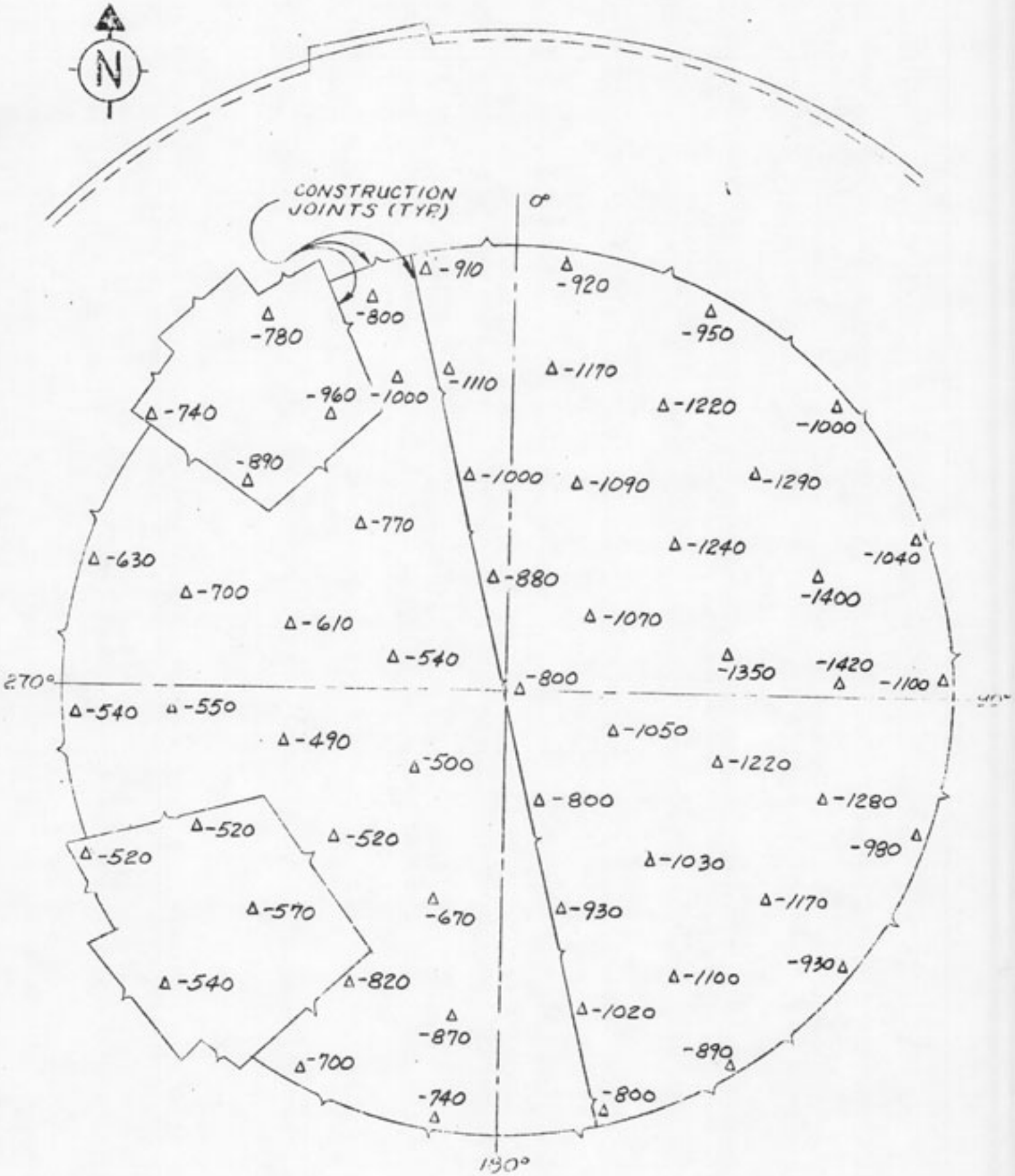

MERIDIONAL STRESSES AT THE OUTSIDE SURFACE FROM THE POST-TENSIONING LOAD AT 50% COMPLETION. ALL JOINTS ASSUMED HINGED WITH MEMBRANE FORCES ACTING AT CENTER OF SECTION.

UNITS-PSI

FIGURE 5-15

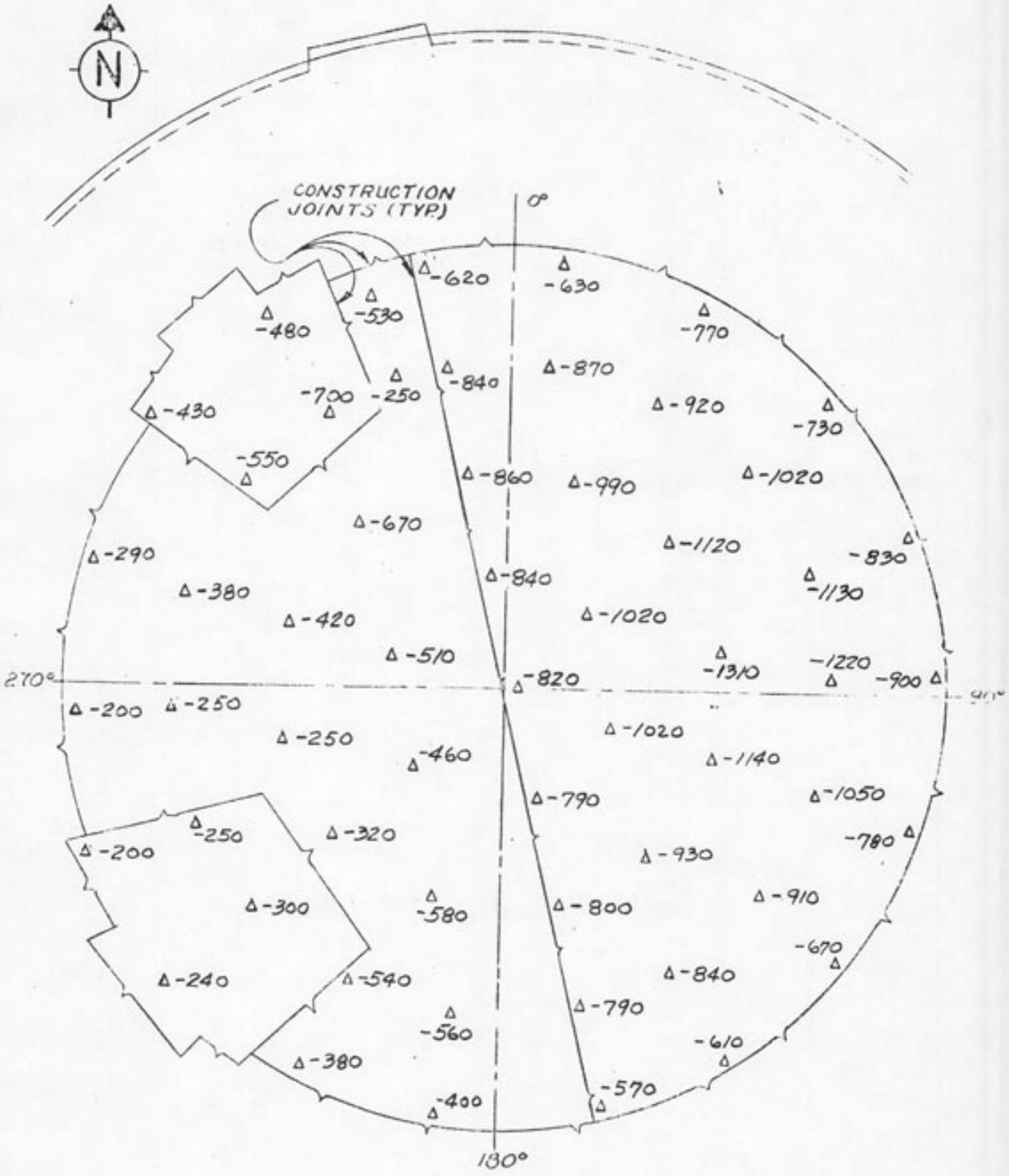

CIRCUMFERENTIAL STRESSES AT THE OUTSIDE SURFACE FROM THE POST-TENSIONING LOAD AT 50% COMPLETION. ALL JOINTS ASSUMED HINGED WITH MEMBRANE FORCES. ACTING AT CENTER OF SECTION.
UNITS-PSI

FIGURE 5-16

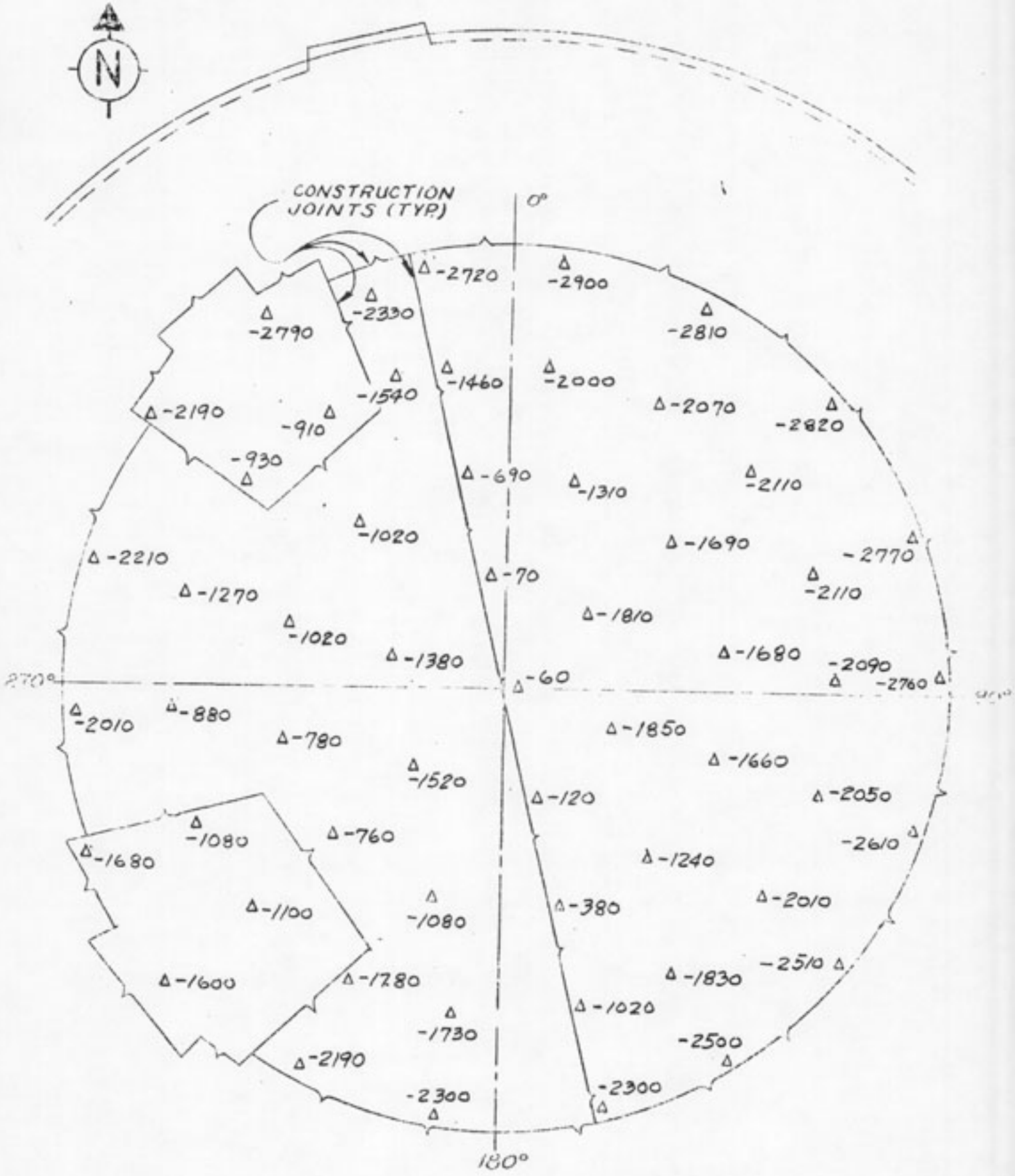

MERIDIONAL STRESSES AT THE OUTSIDE SURFACE FROM THE POST-TENSIONING LOAD AT 50% COMPLETION. ALL JOINTS ASSUMED HINGED WITH THE MEMBRANE FORCES ACTING AT THE TOP OF THE CIRCUMFERENTIAL AND MERIDIONAL JOINTS.

UNITS-PSI

FIGURE 5-17

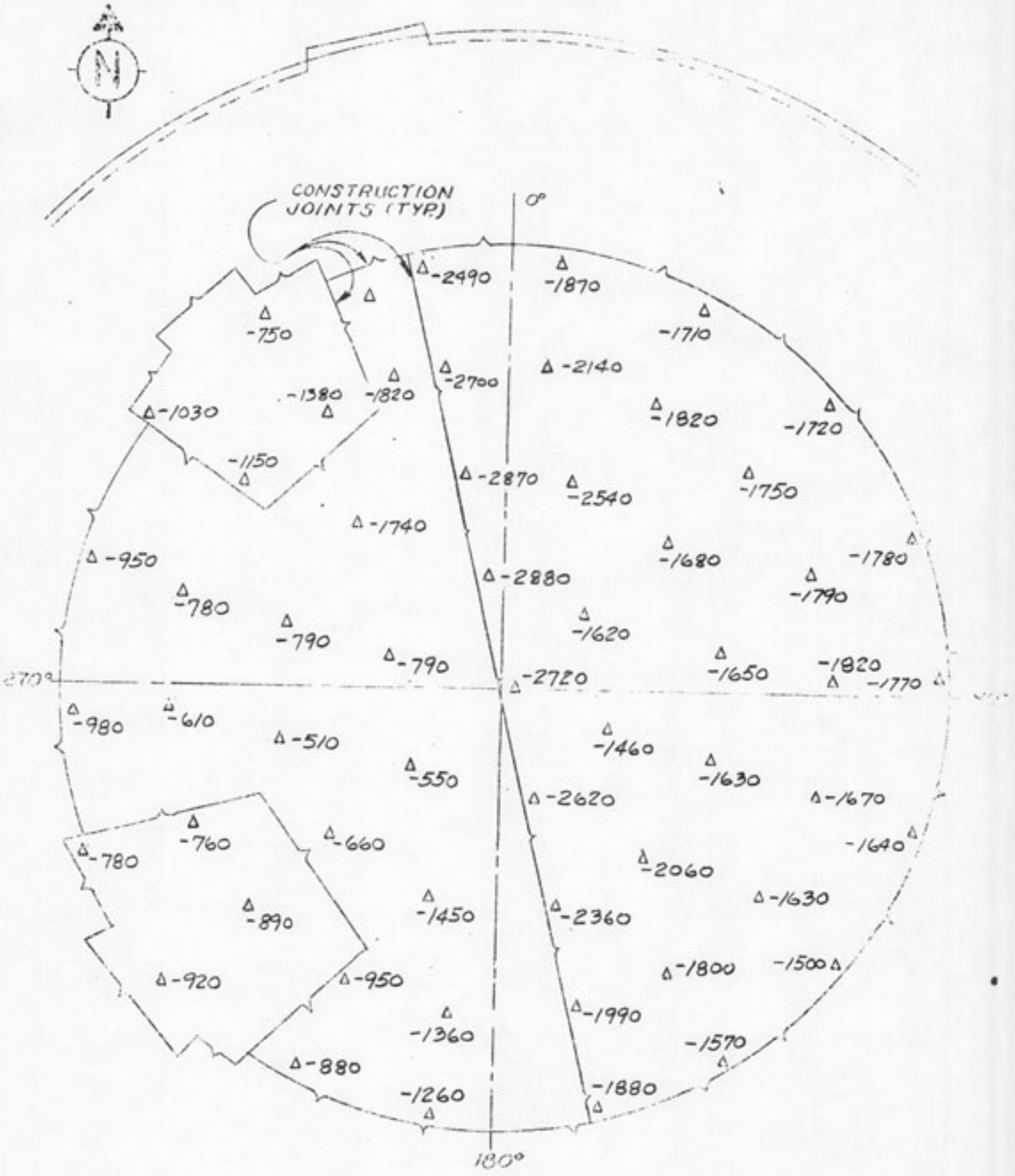

CIRCUMFERENTIAL STRESSES AT THE OUTSIDE SURFACE FROM THE POST-TENSIONING LOAD AT 50% COMPLETION. ALL JOINTS ASSUMED HINGED WITH THE MEMBRANE FORCES ACTING AT THE TOP OF THE CIRCUMFERENTIAL AND MERIDIONAL JOINTS.

UNITS-PSI

FIGURE 5-18

6.0 CONCRETE REPLACEMENT

6.1 COMPATIBILITY OF THE ORIGINAL AND REPLACED CONCRETE

An analysis was performed to determine the compatibility of the replaced and the original concrete. Due to the difference of concrete age when loaded the replaced concrete should creep more than the original concrete. The replaced concrete may be loaded when it is 28 days old, whereas the original concrete will be reloaded when it is over one year old. To simulate this difference in creep the original concrete was assumed to have a modulus of elasticity of 4×10^6 psi and the new concrete was assumed to have a modulus of elasticity of 2×10^6 psi.

The analytical model is shown in Figure 6-1. The amount of replaced concrete was assumed to be a worst case based on the concrete coring information obtained before detensioning. Figures 6-2 to 6-4 show the stress distribution at various section, in the meridional direction. Section B shown in Figure 6-2 will be discussed in detail since it involves the greatest volume of replaced concrete. At this cross section the replaced concrete had a thickness of 15 in. and the original concrete had a thickness of 24 in. in the figure. The dotted line shows the stress distribution for an analysis assuming the same modulus of elasticity throughout the thickness. As shown on Figure 6-2 there is a samll amount of flexure at Section B. The average stress in the top 15" is - 1700 psi and in the bottom is - 1450 psi. The solid line shows the stress distribution with the modulus of elasticity of the top portion as 1/2 of that of the bottom. The average stress in the top 15" is - 1500 psi and the average in the bottom 24" is - 1800 psi. The analysis indicates an increase of - 350 psi in the bottom portion due to the effect of replaced concrete. Since the modulus of elasticity for both the top and bottom portion were based on creep data for a - 1500 psi load, the analysis is yielding conservative results since creep is considered linearly

proportional to applied stress. In reality the bottom portion with the higher stress would creep more than indicated by the analysis and this would increase the stress in the top portion and reduce it in the bottom. With the exception of Section A the increase in stress is quite small in the original concrete. In Section A the stress increase is - 700 psi, however only a small volume of concrete is affected. As shown by the analysis the dome should respond to load essentially the same as it would if the top concrete had not been delaminated and replaced.

The original concrete has been subjected to a larger portion of its originally anticipated creep cycle. The tendons have been subjected to a large portion of the originally anticipated relaxation cycle. The combined magnitude of creep and relaxation to date is illustrated by the tendon and anchor liftoff measurements shown in Figure 3-3. Future tendon relaxation is therefore expected to be somewhat less than the total originally anticipated. Future creep and shrinkage is expected to be about the same or slightly larger than originally anticipated. The effective prestressing forces at end of plant life are expected to be larger than originally anticipated since steel relaxation is the predominant factor in the total long term losses.

The effect of the changes in force resulting from material compatibility do not have a significant effect on the analyses discussed. The prestressing forces assumed are those at completion of restressing and will become smaller. The predicted stress levels will therefore become smaller. Further, the expected change in losses, from those originally anticipated, are small compared to the effective prestress assumed, and almost negligible.

6.2 SURFACE PREPARATION

After the completion of the removal of loose delaminated concrete, the removal depth will be increased so that the minimum depth of concrete replacement is 6". Figure 6-5 shows an illustration of how

the final removed area of concrete will appear. This type of final configuration will allow membrane loads to be transferred to the new concrete by direct bearing. The surface will be cleaned by using a high pressure air water blast technique to remove all foreign material such as grease. The reinforcing steel will also be cleaned by high pressure air water blasting.

6.3 ADDITIONAL REINFORCEMENT

As an added conservative measure, rock anchors will be used to provide radial forces on the replaced concrete. The radial force will provide for displacement compatibility between the replaced and the new concrete. The radial force from the rock anchors will only be effective if the bond strength between the replaced and the original concrete is not sufficient to carry the load. An illustration of the rock anchor system is shown in Figure 6-6.

6.4 REPAIR OF REINFORCING STEEL, TENDONS AND SHEATHING

Any reinforcing steel, tendons and sheathing in the area where the concrete has been removed by chipping or coring will be repaired in accordance with the following criteria:

(1) Any reinforcing steel which was severed, partially severed or has an indentation greater than or equal to 1/8" will be repaired by lapping or cadwelding an additional piece of #9 reinforcing steel. The preceding requirement will not be inforced if there is enough other reinforcement in the area to satisfy the original design criteria. The lap length will be in accordance with ACI-318-63. Four specimens will be removed (with indentations equal to 1/8" or greater) and tensile tested to verify the acceptability of indentations less than 1/8".

(2) Visible holes in the sheathing will be sealed to prevent concrete leakage during placement.

(3) An inspection window shall be opened in the sheathing for tendon inspection when the following conditions are found:

(a) A hole in the lower half of the sheathing exceeding 3/8" in diameter.

(b) A hole in the upper half of the sheathing exceeding 3/4" in diameter.

(c) A cut sheath where it is apparent that the cutting edge of the coring barrel entered the lower half of the sheathing.

The window shall be at least 2" x 2" in size and sealed by a patch after the inspection.

(4) The original criteria allows 2% of the wires to be damaged during tendon installation and tensioning. One third of this number is allotted to damage due to concrete removal and coring. Two percent of the total number of wires for 165-90 wire dome tendons is 297 wires. Therefore up to 99 wires, damaged by concrete removal and coring may be left in place. If more than 99 wires are found to be damaged then enough tendons shall be repaired so that the 99 wire allotment is not exceeded.

(5) Where the sheathing damage was extensive enough to allow dust, dirt, concrete chips etc. to enter the sheath then the material shall be removed. For any hole greater than 3/4" the tendon shall be examined and the foreign material removed.

(6) All damaged sheathing vent lines shall be repaired so that they will function during regreasing of the dome tendons.

6.5 INSTRUMENTATION

Instrumentation will be provided in the replaced concrete. Instrumentation installed earlier but damaged by concrete removal will be replaced. Strain gages and thermocouples will be installed on both the east and west side of the dome. There will be two lines of gages and thermocouples, a typical line is shown in Figure 6-7. The purpose of the instrumentation is to provide verification that the replaced concrete is carrying a portion of the applied load.

6.6 METHOD OF CONCRETE REPLACEMENT

After all repairs are completed and the surface has been air-water blasted then the surface will be saturated and maintained in that condition for 48 hours prior to concrete placement. At the time of concrete placement the surface will be in a saturated, surface dry condition. A 1/4" to 1/2" thick layer of grout will be applied to the surface immediately before the concrete is placed. The concrete will be placed as illustrated in Figure 6-8. The first lift will be placed and vibrated and allowed to stand approximately two hours. It will then be revibrated before placing the second lift. Other lifts will then be placed in the same manner as the first lift, i.e., placed, vibrated let stand and wait two hours, revibrate and then apply the finish. The curing will be accomplished by a continous flow of water. The concrete will be covered with burlap, cotton matting or a similar material. The water curing will last a minimum of 14 days. When the surface is in a saturated surface dry condition it will be coated with a curing compound.

The previously described method is being used to obtain maximum bond of the replaced to the original concrete and also minimize shrinkage of the replaced concrete.

The aggregate used for the original concrete is no longer available and the replaced concrete will use a new aggregate source. The new aggregate is essentially the same as the old aggregate. Both aggregates are mined from Oolite limestone and previous tests have verified the similarity.

The original concrete used a Type II Cement whereas the replaced concrete will use a low heat of hydration Type II Cement to minimize shrinkage. The concrete placement temperature will be kept as low as practical to also minimize shrinkage.

The concrete will be placed in accordance with specification 5610-C-61 (proprietary).

A consultant on the concrete replacement plan was Mr. Lewis H. Tuthill, retired, formerly of the California Department of Water Resources, Division of Design and Construction.

6.7 POST-TENSIONING SEQUENCE

A new post-tensioning sequence will be used when retensioning the dome tendons. The sequence will be similar to that used on other containments already prestressed. The new sequence will require that the loads be applied more uniformly than for the original tensioning sequence. Prior to retensioning, a set of drawings will be issued showing the detailed sequence.

6.8 PERFORMANCE CRITERIA FOR REPLACED CONCRETE

Test demonstrations will provide evidence of the adequacy of the replaced concrete acting in composite with the originally placed concrete. The forces, applied during tests will be those originally specified and consist of prestressing and prestressing plus 1.15 times design pressure (P) along with changes in environmental conditions which occur during testing.

The demonstrations will show that the completed dome satisfies the original design criteria. The effective prestressing force measured at tendon end anchors, will remain equal or greater than that specified by design. The increase in effective prestress, resulting from containment pressurization to 1.15 P, will be less than 4% of the initial prestressing force as measured by load cells at tendon end anchors. Measured strains will remain within ranges that the resisting materials can withstand as demonstrated by testing. Maximum deformations will remain within a range of values that are small compared to the radius of the dome and that show consistency with the measured strains.

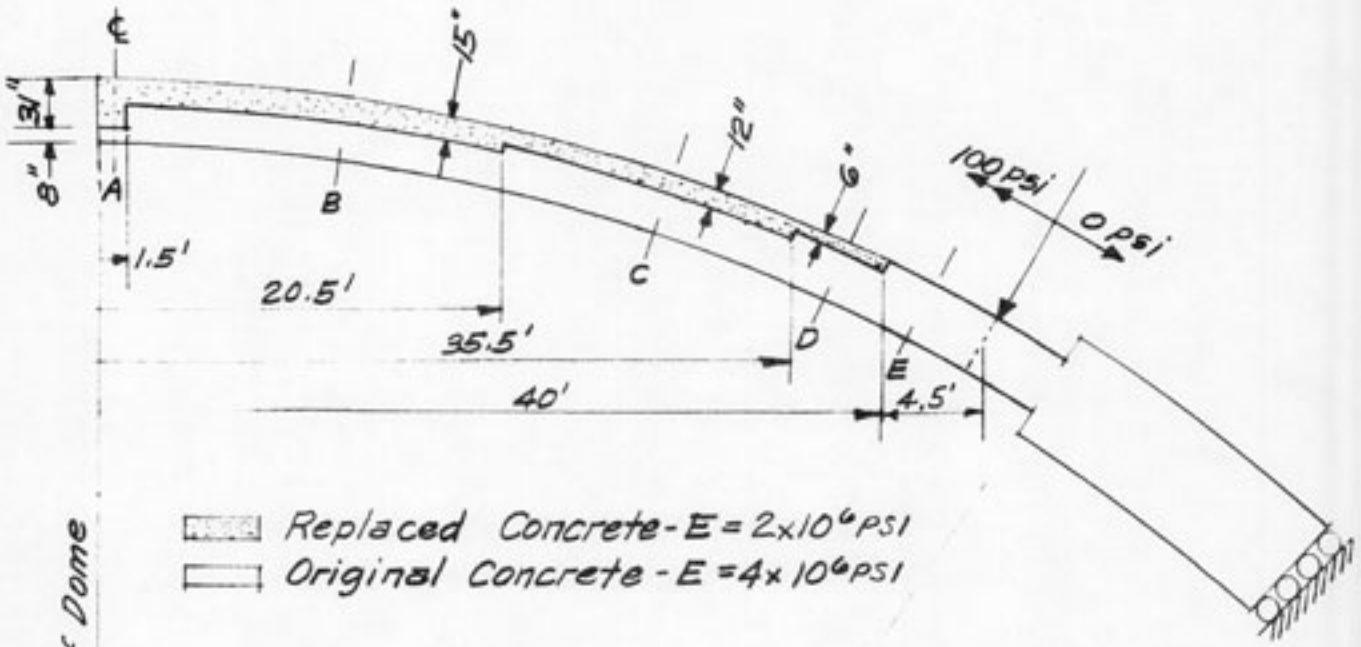

See Figs. 6-2 to 6-4
For Stresses across thickness
at Sections A, B, C, D & E

FIGURE 6-1

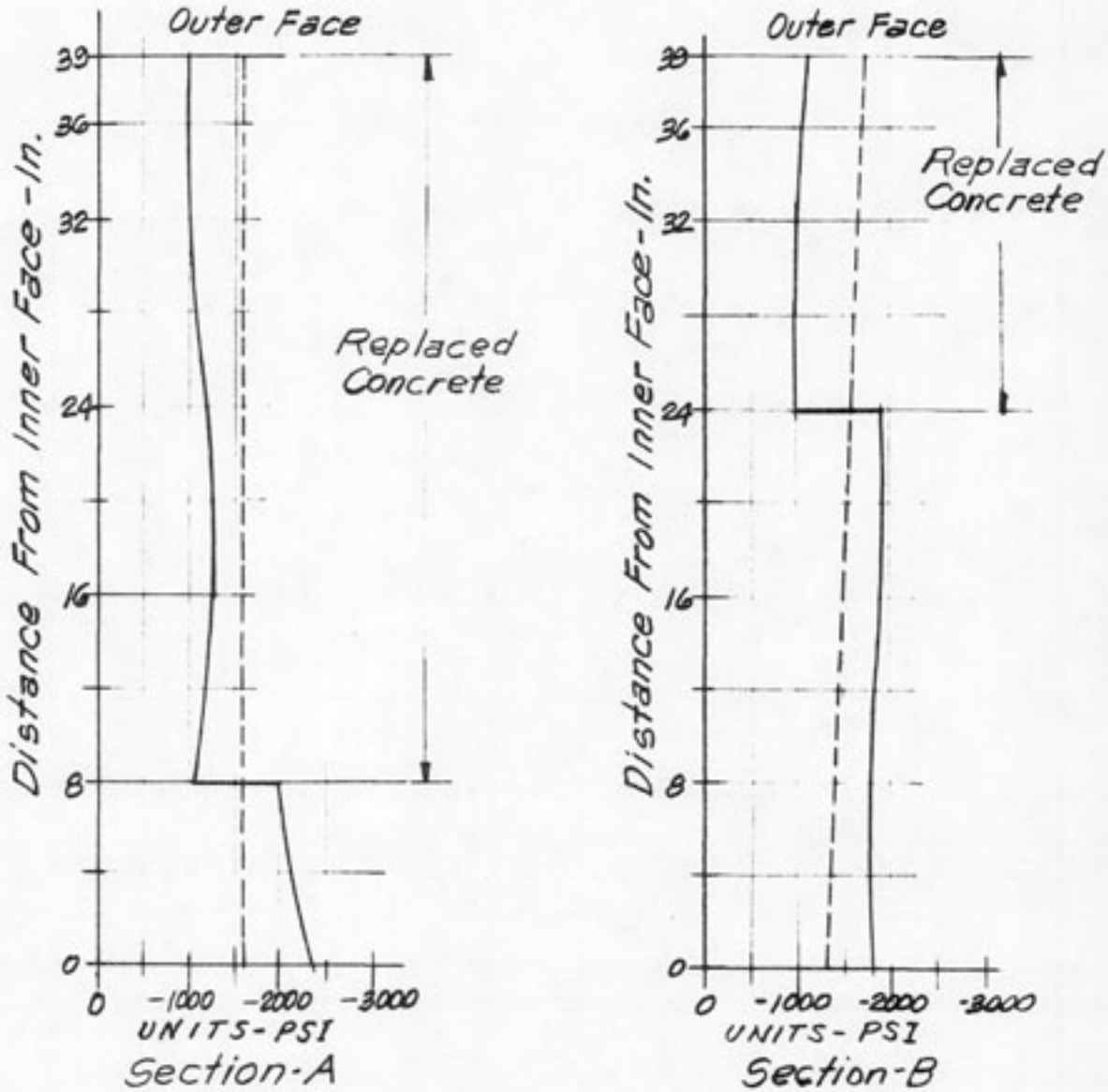

—— "E" of Replaced Concrete = 2×10^6 PSI
"E" of Original Concrete = 4×10^6 PSI

---- "E" of Replaced = "E" of Original Concrete = 4×10^6 PSI

FIGURE 6-2

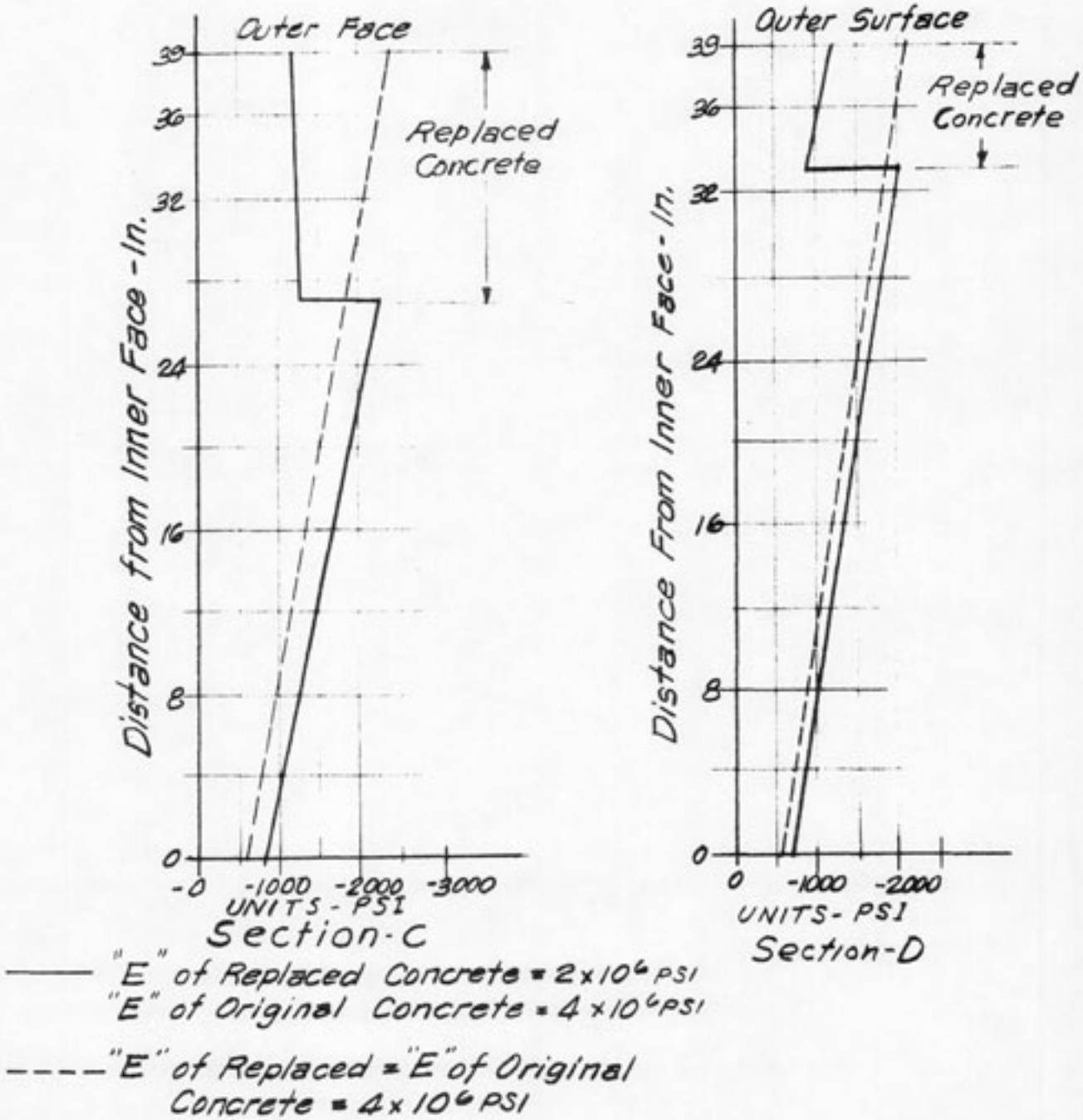
Outer Face
Replaced Concrete
Distance from Inner Face - In.
39
36
32
24
16
8
0
-0
-1000
-2000
-3000
UNITS - PSI
Section-C
Outer Surface
Replaced Concrete
Distance From Inner Face - In.
39
36
32
24
16
8
0
0
-1000
-2000
UNITS - PSI
Section-D
"E" of Replaced Concrete = 2x10⁶ PSI
"E" of Original Concrete = 4x10⁶ PSI
"E" of Replaced = "E" of Original Concrete = 4x10⁶ PSI

FIGURE 6-3

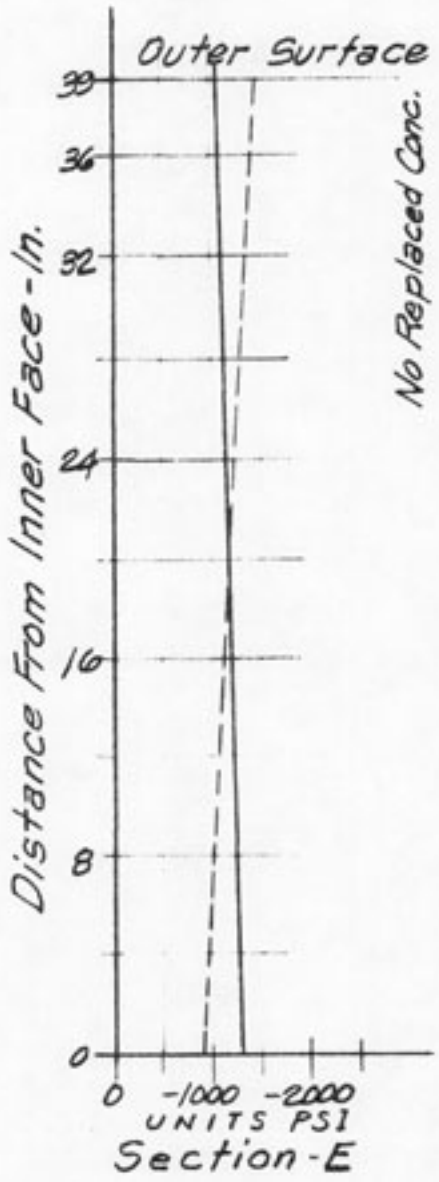

——— "E" of Replaced Concrete = 2×10^6
"E" of Original Concrete = 4×10^6

– – – – "E" of Replaced = "E" of Original Concrete = 4×10^6

FIGURE 6-4

ILLUSTRATION OF CONCRETE REMOVAL AREA

FIGURE 6-5

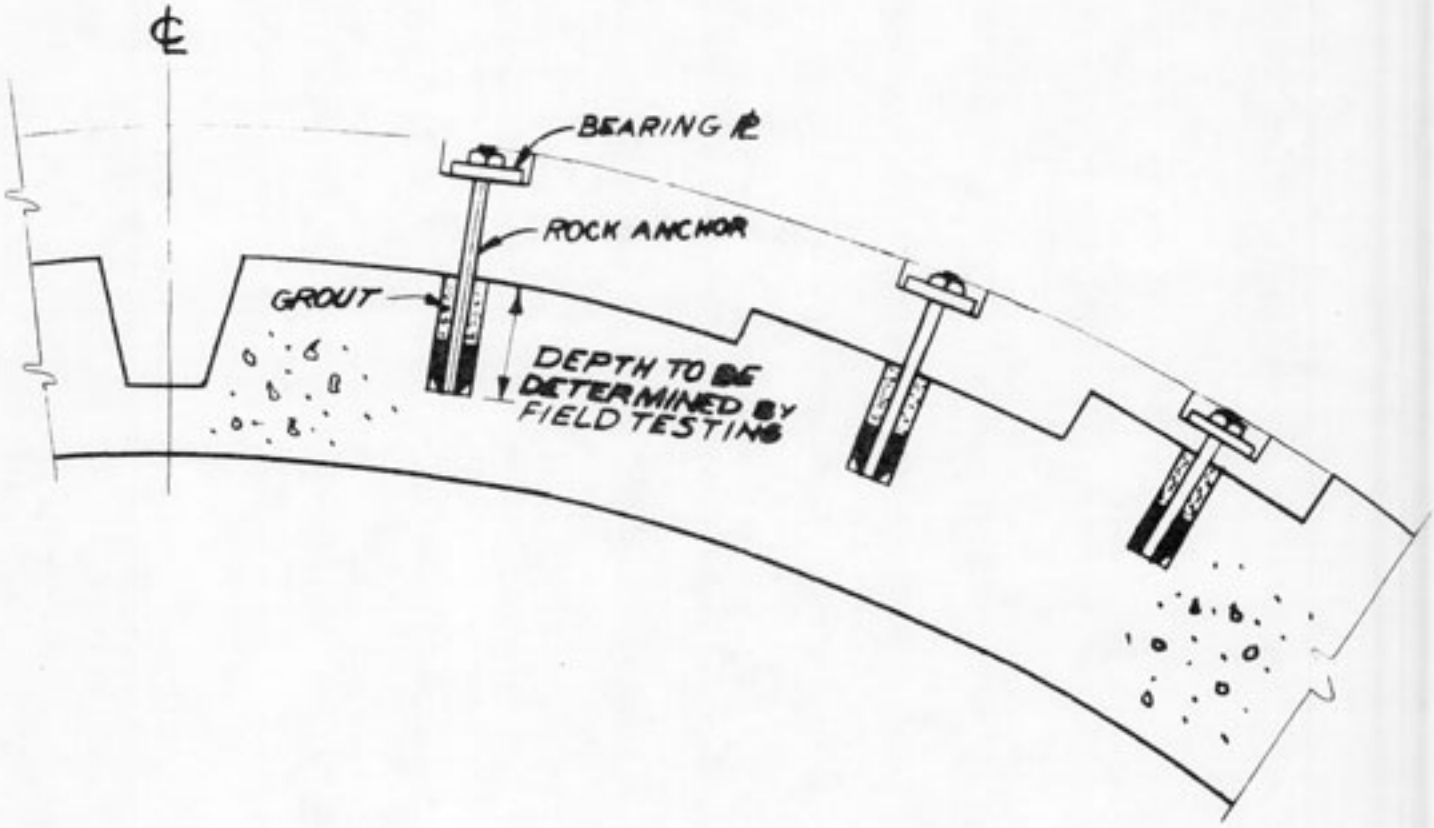

ILLUSTRATION OF
CONCRETE ANCHORS

FIGURE 6-6

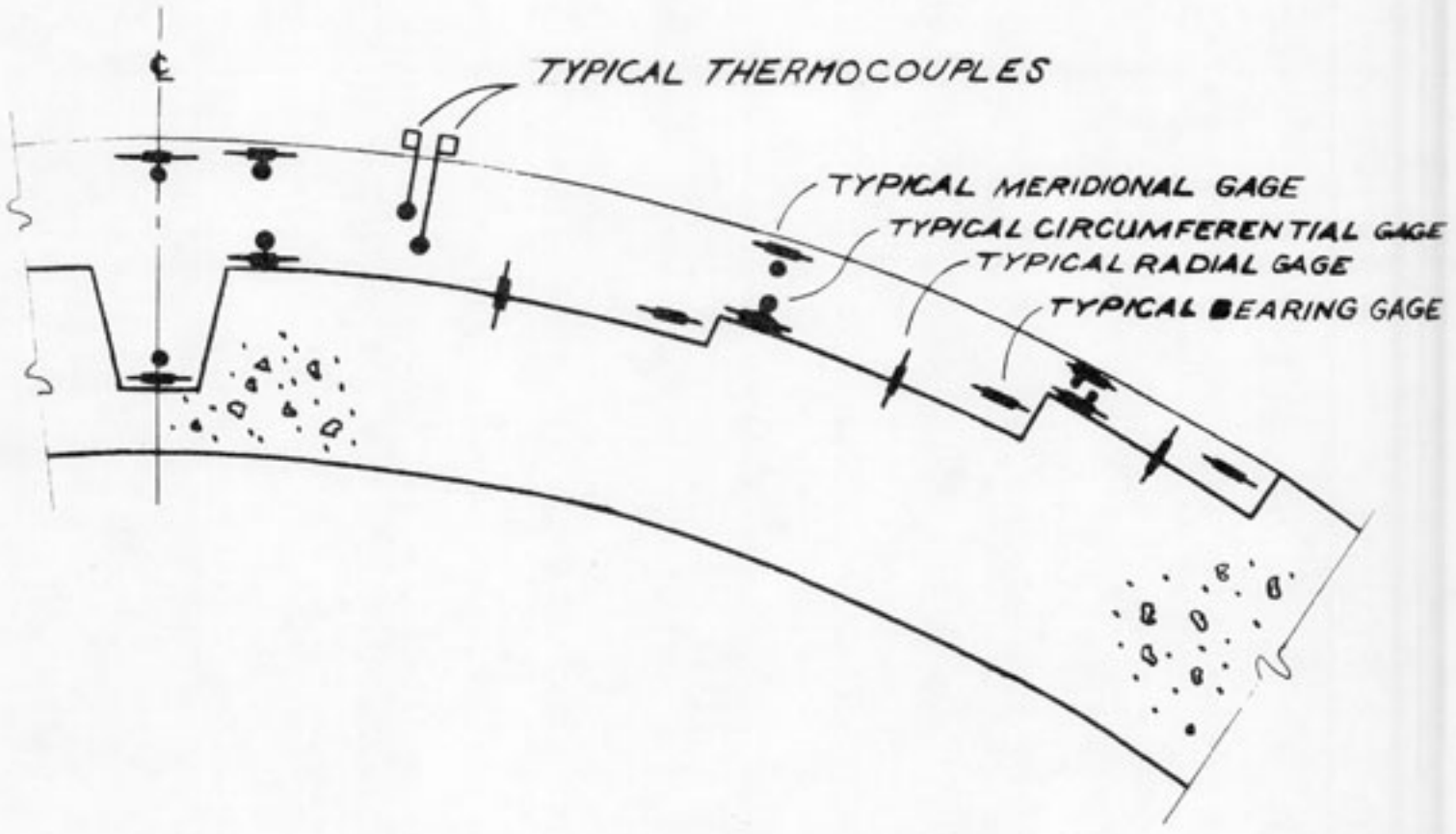

ILLUSTRATION OF TYPICAL
INSTRUMENTATION

FIGURE 6-7

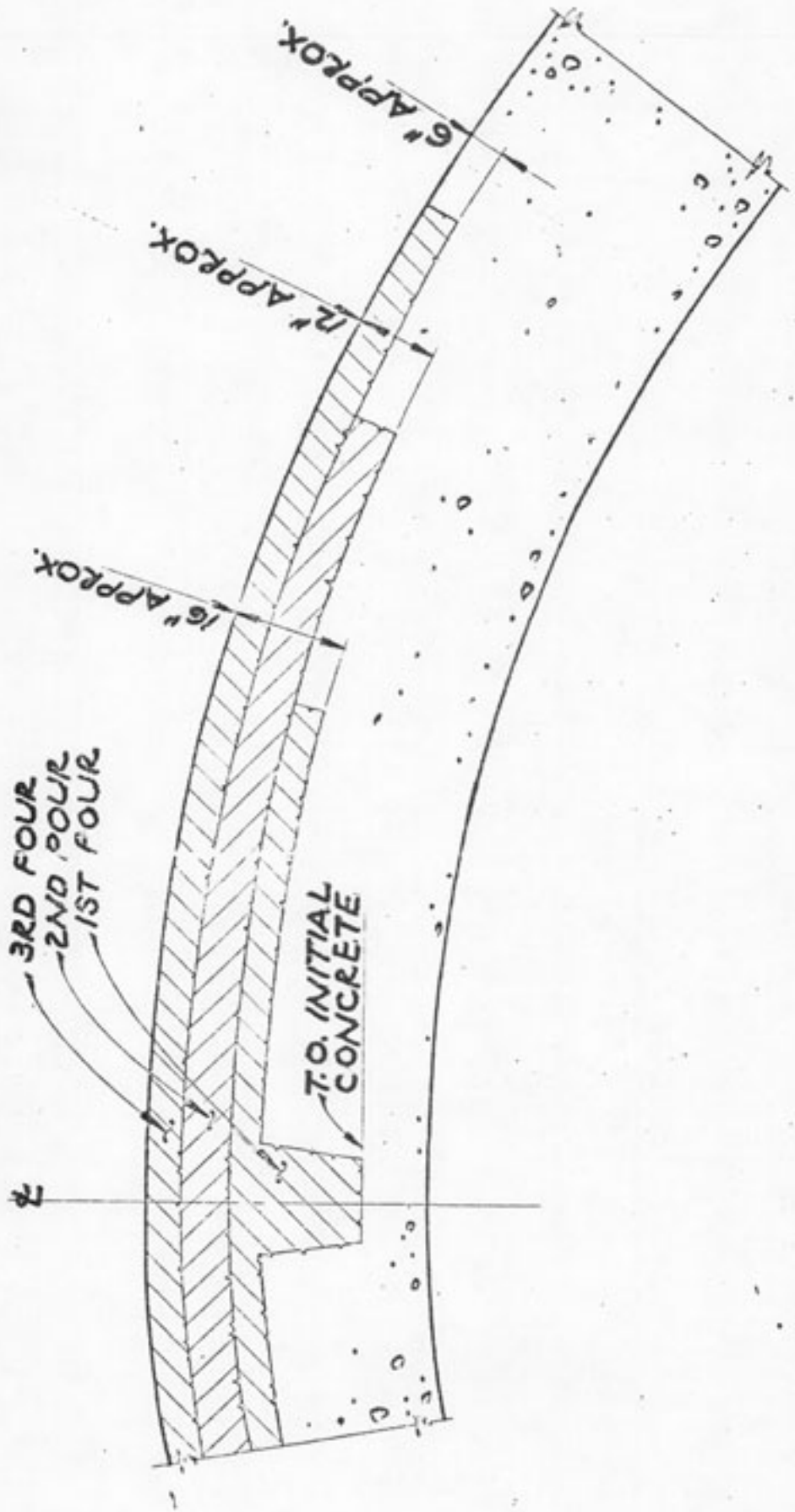

ILLUSTRATION OF CONCRETE REPLACEMENT

FIGURE 6-8

7.0 QUALITY ASSURANCE

The Quality Assurance program described in FSAR Section 1.9.7 will be in effect as usual during the time while dome concrete is being removed and replaced.

Specifications for concrete removal and replacement and specifications covering materials testing will be enforced by site quality control personnel supplemented by engineers from Bechtel's San Francisco and Gaithersburg offices. Quality Assurance Engineers of Bechtel and Florida Power & Light will monitor the overall operation. Written procedures will be in effect, and be enforced by appropriate quality control methods, for the replacement program.

Engineers were present for concrete removal to observe and document "as found" conditions, and to ensure that the steel, sheathing and tendons received proper protection. The engineers will oversee preparations for replacement of the concrete and the placement of new concrete.